BIAS CORRECTION FOR NON-EXTREME AND EXTREME VALUES FOR PRECIPITATION

A THESIS SUBMITTED TO
THE GRADUATE SCHOOL OF NATURAL AND APPLIED SCIENCES
OF
MIDDLE EAST TECHNICAL UNIVERSITY

BY

AHMET KÖRPINAR

IN PARTIAL FULFILLMENT OF THE REQUIREMENTS
FOR
THE DEGREE OF MASTER OF SCIENCE
IN
CIVIL ENGINEERING

APRIL 2023

Approval of the thesis:

BIAS CORRECTION FOR NON-EXTREME AND EXTREME VALUES OF PRECIPITATION

submitted by **AHMET KÖRPINAR** in partial fulfillment of the requirements for the degree of **Master of Science** i**n Civil Engineering, Middle East Technical University** by,

Prof. Dr. Halil Kalıpçılar
Dean, Graduate School of **Natural and Applied Sciences** _____

Prof. Dr. Erdem Canbay
Head of the Department, **Civil Engineering** _____

Prof. Dr. Elçin Kentel
Supervisor, **Civil Engineering, METU** _____

Examining Committee Members:

Prof. Dr. Melih Yanmaz
Civil Engineering, METU _____

Prof. Dr. Elçin Kentel
Civil Engineering, METU _____

Prof. Dr. Ceylan Talu Yozgatlıgil
Statistics, METU _____

Prof. Dr. Yakup Darama
Civil Engineering, Atılım University _____

Assoc. Prof. Dr. Mustafa Tuğrul Yılmaz
Civil Engineering, METU _____

Date: 24.04.2023

I hereby declare that all information in this document has been obtained and presented in accordance with academic rules and ethical conduct. I also declare that, as required by these rules and conduct, I have fully cited and referenced all material and results that are not original to this work.

Name Last name : Ahmet Körpınar

Signature :

ABSTRACT

BIAS CORRECTION FOR NON-EXTREME AND EXTREME VALUES FOR PRECIPITATION

Körpınar, Ahmet
Master of Science, Civil Engineering
Supervisor : Prof. Dr. Elçin Kentel

April 2023, 134 pages

Regional climate models are crucial in climate change impact analysis. Short-term and long-term effects of climate change need to be investigated to plan necessary mitigation measures and to lower the impacts. Regional climate models allow analysis of the effects of climate change in smaller scales such as regions and nations and consequently leads to the development of more effective management strategies. One of the most commonly used products of regional climate models is precipitation predictions. For flood risk analysis, especilly extreme precipitations are crucial. However, raw data obtained from the regional climate model have errors. To obtain reliable predictions, the data should be bias corrected first. The basic principle of bias correction is to reduce the bias in raw data. Bias correction is also region-specific due to climate conditions of the area. In this study, three alternatives for a commonly used bias correction method, the Distribution Based Scaling method, are proposed. Alternatives proposed in this study differ from the original method by division point of data and fitted distributions to extreme part of the data. Performance assesment for these methods are done for 53 meteorological stations located at

different regions of Turkey, and the most effective methods are identified. Performances of alternative methods proposed in this study did not provide significant improvements compared to the original method. Future changes in extreme precipitation according to bias corrected RCM outputs are investigated spatially as well.

Keywords: Daily Precipitation, Bias Correction, Extreme Values, Distribution Based Scaling, Climate Change

ÖZ

UÇ VE UÇ OLMAYAN YAĞIŞ DEĞERLERİ İÇİN YANLILIK DÜZELTMESİ

Körpınar, Ahmet
Yüksek Lisans, İnşaat Mühendisliği
Tez Yöneticisi: Prof. Dr. Elçin Kentel

Nisan 2023, 134 sayfa

İklim değişikliği etkisi analizinde bölgesel iklim modellerinin yeri çok kritiktir. İklim değişikliğinin açığa çıkaracağı sorunların azaltılması ve bu sorunlara karşı önlemler alınabilmesi için kısa ve uzun vadedeki etkilerinin incelenmesi gerekir. Bölgesel iklim modelleri, ülkeler ve bölgeler gibi küçük çaplarda iklim değişikliği etkilerinin analizini mümkün kılar. Dolayısıyla bu etkileri yönetebilmek için daha etkin stratejilerin geliştirilebilmesine öncülük eder. Bölgesel iklim modellerinin en sık kullanılan sonuçlarından biri de yağış tahminidir. Özellikle taşkın risk analizleri için uç yağış değerleri çok önemlidir. Ancak bölgesel iklim modelinden elde edilen işlenmemiş veri yanlılık içerir. Güvenilir tahminler yapabilmek için işlenmemiş verilere öncelikle yanlılık düzeltmesi yapılması gerekir. Bu da gözlemlenen veri ile modelden elde edilen veri arasındaki farkın dikkate alınmasıyla yapılır. Yanlılık düzeltmeleri iklim koşullarından dolayı bölgeden bölgeye değişir. Bu çalışmada Türkiyenin farklı bölgeleri için Dağılım Temelli Ölçeklendirme yöntemine üç alternatif yöntem sunulmuş ve bu yöntemler kullanılarak yanlılık düzeltmesi yapılmıştır. Alternatif yöntemler orjinal yöntemden veriyi bölme noktası ve

kullanılan istatiksel dağılımlar açısından farklıdır. Türkiye'nin farklı bölgelerinden 53 meteoroloji istasyonu için performans değerlendirilmesi yapılmış ve en etkili yöntem belirlenmiştir. Bu çalışmada önerilen alternatif yöntemlerin performansları orjinal yöntemden kayda değer ölçüde iyi değillerdir. Geleceğe yönelik yanlılık düzeltmesi yapılmış yağış tahminlerindeki uç değer değişimleri de mekansal olarak incelenmiştir.

Anahtar Kelimeler: Günlük Yağış, Yanlılık Düzeltme, Uç Değerler, Dağılım Temelli Ölçeklendirme, İklim Değişimi

To the next generations

ACKNOWLEDGMENTS

The first person for my expression of gratitude is the supervisor of this thesis, Prof. Dr. Elçin Kentel. She always reached out and shared her experience in a time of need. She always had time for guidance which let me progress in many ways.

Examining committee members of this thesis, Prof. Melih Yanmaz, Assoc. Prof. Mustafa Tuğrul Yılmaz, Prof. Ceylan Talu Yozgatlıgil, and Prof. Yakup Darama, have contributed to the study with their valuable time, constructive criticism, not once but twice. These feedbacks are much appreciated.

Three fellow colleagues, Ömer Burak Akgün, Murat Yeğin, and Buket Mesta Yoleri, did not hold back themselves for supporting when there is a technical problem. They are very appreciated for their quick responses and solutions they offered.

My mother and father are always tried their best to support me for my entire life. Despite everything, they gave me a chance to pursue my interest in academia. I could not show my gratitude for them enough. The other family I gathered myself during the undergraduate years, Ebrar Sinmez, Seyda Tuğçe Balkan Durhan, Fatma Rabia Fidan, Gözde Merve Türksoy, Etkin Tarlan and Derya Hazar also have continued their academic experience. Experiencing similar hardships with each other and knowing it helped all of us to overcome these hardships. There are two other important mentions, Doruk Karalar and Sinan Abirci. These two offered their support by mental health checks for almost every day and their objective comments when it is needed. And the last honorable mention is Peri Beşarat, as her saying my partner in crime. Her love and enthusiasm make the life more bearable.

This work was funded by TÜBİTAK under grant number 118Y365 and 220N054.

TABLE OF CONTENTS

LIST OF TABLES

TABLES

LIST OF FIGURES

FIGURES

LIST OF ABBREVIATIONS

AIC: Akaike Information Criterion

CDF: Cumulative Distribution Function

CORDEX: Coordinated Regional Climate Downscaling Experiment

DBS: Distribution Based Scaling

GCM: Global Climate Model

GP: Generalized Pareto

LOGN: Lognormal

LS: Linear Scaling

MAE: Mean Absolute Error

MK: Mann-Kendall

MS: Meteorological Station

PBIAS: Percent Bias

QC: Quality Check

QM: Quantile Mapping

RCM: Regional Climate Model

RMSE: Root Mean Square Error

SE: Superensemble

SME: Simple Mean Ensemble

SSE: Sen's Slope Estimator

WCRP: World Climate Research Programme

CHAPTER 1

INTRODUCTION

Climate change is a phenomenon that has various effects on the world we live in. It is changing the conditions of the biosphere gradually. Floods, draughts, and temperature anomalies are the most common expected changes. Changes in different aspects may also occur due to these fundamental changes. Under these circumstances, adapting to new conditions becomes a must to survive. To estimate the changes, climate models are introduced in the past years. These models are called global climate models (GCM) and regional climate models (RCM). They estimate the hydrometeorological parameters like precipitation, temperature, wind pressure, etc. in different scales. Coordinated Regional Climate Downscaling Experiment (CORDEX) has an important role in developing and improving GCMs and RCMs. CORDEX also provides a database containing GCM and RCM outputs for public access with the help of World Climate Research Programme (WCRP).

Although GCM and RCM outputs are useful for climate change analysis, these outputs are biased. The main reasons for these biases are mostly associated with regions of complex terrains like high-altitude or wet, humid regions within the related area, limited spatial resolution, simplified physics, and incomplete knowledge of climate systems (Ayugi et al., 2020). These outputs should be bias corrected before their utilization in any analysis (Casanueva et al., 2016; Teutschbein & Seibert, 2012). To fulfill this need, various bias correction methods have been developed through the years. The main idea behind the bias correction techniques is an application of a transformation procedure to adjust the outputs of RCMs or GCMs according to the observed data (Teutschbein & Seibert, 2012). These methods are ranging from simple scaling techniques to rather more sophisticated quantile

mapping (QM) techniques. QM techniques generally perform better than other bias correction techniques (Ayugi et al., 2020; Enayati et al., 2021; Grillakis et al., 2013; Heo et al., 2019; Douglas Maraun, 2013). QM implements statistical transformations for the post-processing of GCM and RCM outputs (Enayati et al., 2021).

These statistical transformations can be separated into three major groups. They are distribution derived transformations, parametric transformations, and nonparametric transformations. Distribution derived transformations use distribution functions of observed datasets and model outputs. Parametric transformations use linear or nonlinear equations with free parameters to fit to observed dataset and model outputs. Nonparametric transformations use empirical cumulative distribution functions (CDF) or nonparametric regressions of observed datasets and model outputs. However, applying a single transformation to the whole dataset may cause some issues in the bias correction of precipitation. This is due to daily precipitation distributions being typically heavily skewed towards low-intensity values (Yang et al., 2010). Yang et al. (2010) proposed an alternative method called Distribution Based Scaling (DBS). This method tries to overcome the aforementioned problem by dividing the datasets at the 95^{th} percentile and fitting two different gamma distributions for the non-extreme part and extreme part of the datasets. By dividing the dataset, the extreme part of the datasets can be represented after bias correction without the influence of the non-extreme part. DBS has better performance overall due to the ability to consider the extreme parts of the datasets. Although it has better performance, a fixed cut point at the 95^{th} quantile can be considered as a weakness. In flood risk analysis, the most extreme precipitations may cause the most harm. Considering the most extreme precipitation values at the 99^{th} quantile and beyond as extreme part for the bias correction may lead to more accurate extreme value predictions for flood risk analysis.

In this study, the 99^{th} percentile is used as the cut point for the extreme part of the datasets. Another addition introduced in this study is to fit Generalized Pareto (GP) and lognormal (LOGN) distributions to the extreme part of the dataset. LOGN distribution is selected because it is identified as the best fitting distribution to the

extreme part of the observed data. Moreover, GP distribution is selected to assess the efficiency of an extreme value distribution.

The main contribution of this study is that three alternative methods of DBS are developed using different distributions and cut points and their performances with the original DBS method and Linear Scaling method are compared. A wide study area considering 53 MSs is another contribution to the literature. With high number of MSs, the performance of bias corrections, and changes in maximum precipitation values of near, middle, and far future are discussed in a spatial manner as well.

The organization of this study can be summed up in the five following chapters. Chapter 2 consists of the literature review on GCMs, RCMs, and bias correction methods. Chapter 3 consists of details and the development of the proposed methods. Information about the study area and the observed data, and model outputs regarding to study area are presented in Chapter 4. In Chapter 5 the performance assessment statistics of the proposed methods, the discussion of these performance assessment statistics, and expected future changes in precipitation are provided. Finally, highlights of this study and remarks for future studies are given in Chapter 6.

CHAPTER 2

LITERATURE REVIEW

2.1 CORDEX, GCMs, and RCMs

Climate models are developed to predict future climate. Formulations of physical laws are the basis of the climate models with carbon emission scenarios. They can be examined in two major categories which are GCMs and RCMs according to their resolutions. While RCMs have finer resolutions, GCMs let researchers have a general idea on a global scale. The resolution of GCMs is around 1000 km by 1000 km. Thus, GCMs do not provide local or regional predictions. Orographic precipitation, conventional processes, and local scale hydrologic processes are relatively poorly represented by GCMs (Fujihara et al., 2008; Sato et al., 2013). Resolutions of GCMs are not sufficient for precipitation assessment in regions where the topography is particularly complex. Because complex topography is a significant factor for local processes (Lakku & Behera, 2022; Lun et al., 2021; Park et al., 2020; Salathé, 2003; Schmidli et al., 2006; Stefanidis et al., 2020; Sunyer et al., 2015). On the other hand, RCM resolutions are finer than GCMS'. They can have 25 km by 25 km resolutions. These kinds of predictions require more complex mechanics which RCMs have.

To meet the need for estimations in finer resolutions, RCMs are developed with the help of dynamic downscaling (Fujihara et al., 2008). Dynamical downscaling is a method that uses GCMs as boundary conditions to acquire finer resolution models (Kara & Yucel, 2015). However, RCMs have biases due to conceptualizations that are not perfect and/or biases that are already present in GCMs (Casanueva et al., 2016; Fujihara et al., 2008; Teutschbein & Seibert, 2012). The most common biases

are the occurrence of too many wet days with low intensity or incorrect estimation of extreme temperatures, and incorrect seasonal variations of precipitation (Christensen et al., 2008; Ines & Hansen, 2006; Teutschbein & Seibert, 2010).

To help the development of GCMs, RCMs, and downscaling, CORDEX is established worldwide by WCRP. The European branch of CORDEX is called EURO-CORDEX. EURO-CORDEX has a database that contains different RCMs and GCMs. This database is an open access platform to promote the studies on climate change. There is also a list that problems and issues related to different GCMs and RCMs are listed. That list is called Errata Table and it is also accessible from the website of EURO-CORDEX. This list is updated periodically to inform the users about the current situations of GCMs and RCMs. Studies conducted using GCMs and RCMs in Turkey are summarized in Yoleri (2022).

2.2 Bias Correction Methods

There are many different bias correction methods in the literature. They have a range from simple scaling methods to more sophisticated methods like quantile mapping. Most common methods in the literature are compared under the name of comparison method in a number of review articles (Enayati et al., 2021; Ghimire et al., 2019; Gudmundsson et al., 2012; Luo et al., 2018; Mendez et al., 2020; Teutschbein & Seibert, 2012). Bias correction methods that are commonly investigated in the review articles are Linear Scaling, Local Intensity Scaling, Variance Scaling, Power Transformation, Distribution Mapping, Empirical Quantile Mapping, and Delta-change method. Bias correction methods can be examined in two main groups which are scaling methods and statistical transformation methods. Linear Scaling, Local Intensity Scaling, and Variance Scaling are scaling methods. Power Transformation, Distribution Mapping, Empirical Quantile Mapping, and Delta-change methods are statistical transformation methods. These methods are also referred to as Quantile Mapping methods. Several quantile mapping methods have been developed in the past decade with the effort of having a better correction method.

Linear Scaling (LS) is a bias correction method that focuses on correcting the means of model outputs by using correction factors obtained through means of observed data (Lenderink et al., 2007). Correction factors are obtained for each month by using long-term monthly means. Then model outputs are bias corrected by multiplying them with these correction factors. There are several studies that use this method for bias correction of precipitation. Most of these studies focus on the comparison of various methods (Ghimire et al., 2019; Luo et al., 2018; Mendez et al., 2020; Teutschbein & Seibert, 2012). LS can be considered as the simplest bias correction method (Luo et al., 2018). As the cost of its simplicity, it cannot be used in flood risk analysis which use extreme events since correction factors lead to underestimation of extreme events (Haerter et al., 2011).

Local Intensity Scaling is a bias correction method that focuses on correcting the means of model outputs by using correction factors and the wet day threshold (Schmidli et al., 2006). This method is very similar to the LS method. The main difference between the LS and the Local Intensity Scaling methods is that the Local Intensity Scaling method introduces a wet day threshold before calculating the correction factors for each month using long-term monthly means. With the wet day threshold, wet day frequencies are also corrected. The Local Intensity Scaling method corrects both means and wet day frequencies of model outputs. It can be said that the Local Intensity Scaling method is an upgraded version of the LS method. There are many studies in which comparison of the Local Intensity Scaling method with others are provided (Ghimire et al., 2019; Luo et al., 2018; Mendez et al., 2020; Teutschbein & Seibert, 2012).

Variance Scaling is a bias correction method that focuses on correcting the means and variances of model outputs by using correction factors (Chen, Brissette, & Leconte, 2011; Chen, Brissette, Poulin, et al., 2011). This method is very similar to the Local Intensity Scaling method. The main difference between Variance Scaling and Local Intensity Scaling methods is that the Variance Scaling method introduces a step for the correction of variance for model outputs on top of the mean of model outputs. However, Variance Scaling is used for bias correction of temperature only

(Ghimire et al., 2019; Luo et al., 2018; Mendez et al., 2020; Teutschbein & Seibert, 2012).

These three methods are the most common scaling methods in the literature. It can be seen that there is a progression in these methods starting with bias correcting the mean of model outputs, then correcting wet day frequency is added for bias correction of precipitation and correcting the variance of model outputs is added for bias correction of temperature.

The main principle behind the statistical transformation methods, also known as quantile mapping methods, is to fit a distribution or function to observed data and model outputs, then apply the mapping procedure to bias correct the model outputs.

The Power Transformation method is a quantile mapping method that uses parametric transformation functions to use for the mapping procedure (Leander et al., 2008; Leander & Buishand, 2007; Maraun et al., 2010). Generally, a non-linear exponential form is used to allow differences in variances. The most common non-linear forms used in the Power Transformation method, their theoretical background, and the determination of related parameters are explained in Maraun et al. (2010) and Piani et al. (2010). After the parameters are determined, quantile mapping is applied for bias correction.

Distribution Mapping is a very common quantile mapping method. The main idea is to fit a single theoretical distribution to the observed data and model outputs, then using CDFs of the fitted distributions, mapping is conducted (Ines & Hansen, 2006). Several theoretical distributions are used in the literature. Exponential, Gamma, Bernoulli, Lognormal and their combinations like Bernoulli-Gamma, Bernoulli-Exponential, etc. (Block et al., 2009; Boe et al., 2007; Grillakis et al., 2013; Gudmundsson et al., 2012; Heo et al., 2019; Johnson & Sharma, 2011; Sun, 2011).

Empirical Quantile Mapping is another very common quantile mapping method. It can also be referred to as Quantile Mapping. The main idea behind this method is to apply the mapping procedure to empirical CDFs of observed data and model outputs

(Boe et al., 2007). The main difference between Distribution Mapping and Empirical Quantile Mapping methods is that the Empirical Quantile Mapping method is a non-parametric method since it uses empirical CDFs. Studies using this method conclude its performance is very good for historic bias correction (Ayugi et al., 2020; Feigenwinter et al., 2018; Kim et al., 2021; Douglas Maraun, 2013; Piani et al., 2010; Wilcke et al., 2013).

The Delta Change method is another quantile mapping method that focuses on bias correction of future projections. The main idea behind this method is to use anomalies in future projections of model outputs for bias correction of future projections directly (Graham, Andreáasson, et al., 2007). Anomalies between the historic period and projection periods are superimposed to the observed data, generally on a monthly basis. The Delta Change method is used in a number of studies (Bosshard et al., 2011; Graham, Andreáasson, et al., 2007; Graham, Hagemann, et al., 2007; Moore et al., 2008; Olsson et al., 2009).

DBS is another quantile mapping method that has a distinct feature. That feature is that DBS introduces a partition point to the observed data and modeled data at the 95^{th} quantile. Then, call the part lower than the partition point non-extreme part and call the part higher than the partition point extreme part. After the partition, Gamma Distributions are fitted to both non-extreme and extreme parts of the observed and modeled data (Yang et al., 2010). This method is introduced for bias correction of future projections as well, to compete with Delta Change method. The reason for partitioning the data is to bias correct the extremes of the datasets more accurately. Since low intensity data points have high frequencies in precipitation, a single distribution fitted to data is affected by them. By partitioning, high intensity values are not affected by the high frequency and low intensity data points. By doing that, underestimation of the extreme values due to bias correction is avoided (Yang et al., 2010). It is observed that the DBS method worked as intended and improved the bias correction of extreme parts of the datasets in comparison to the Distribution Mapping method (Pastén-Zapata et al., 2020; Rana et al., 2014; Seaby et al., 2013; van Roosmalen et al., 2011).

The current study is conducted within the scope of a TUBITAK project, and the main goal of the project is to carry out flood risk analysis. Since the DBS method outperforms other QM methods due to its distinct feature and bias correction of extreme values it is preferred in this study.

When the thesis studies conducted in METU are checked, it is seen that bias correction is a part of some studies as well. There are also studies that used radar-based data for their bias correction in their studies however, bias correction methods used in radar-based data are not covered in this study. Summary of bias correction parts of other thesis studies can be seen in Table 2.1. Used MS numbers, and applied bias correction methods are the focus of this table.

Table 2.1. Studies Conducted in METU in which Bias Correction is Carried Out

Author	MS Number	Bias Correction Method
(Engin, 2015)	2 stream gauges	LS
(Özkaya, 2017)	13 MS, 18 satellite data	Quantitative Precipitation Estimate
(Yousefi, 2020)	17 radar data	Mean Field Bias, Local Additive Bias, Local Multiplicative Bias
(Çaktu, 2022)	2 MS, 3 stream gauges	Quantile Mapping
(Barkış, 2022)	8 MS	LS
(Ersoy, 2022)	374 MS	LS

In this study, 53 MSs are used with 17 RCMs. RCM outputs are bias corrected with five different methods which are LS, DBS, DBS_99, DBS_99_GP, and DBS_99_LOGN. Latest three of these methods are developed in this study. High number of MSs are also utilized to analyze the results in a spatial manner.

CHAPTER 3

METHODOLOGY

The aim of this study is to correct the biases in the RCM model outputs of precipitation with respect to the observed data using the DBS method and to forecast the changes in extreme parts of the model outputs.

The steps followed in this study can be seen in Figure 3.1. In this study two types of data are used: observations and RCM outputs (from hereafter used interchangeably with model outputs). Observations are obtained from Turkish State Meteorological Services, and RCM outputs are obtained from the CORDEX database (*ESGF-DKRZ - Home | ESGF-CoG*, n.d.). As the second step, statistical analysis of data is carried out. Within the statistical analysis, a quality check (QC) algorithm is applied to the observations at the Meteorological stations (MS). The main reason for applying QC is to evaluate if the MS has sufficient data. Then stationarity check and trend analysis is carried out to understand the general behavior of the precipitation regime in the region. Finally, possible distributions for the extreme part of the observed data (i.e. higher part than the partition point) are determined to develop alternative DBS methods for this study. Six most common distributions and GP distribution are evaluated. The third step is bias correction where LS, DBS, DBS_99_GP, and DBS_99_LOGN methods, which are summarized below, are used to correct the biases in RCM outputs. LS is used as a benchmark in this study. The next step is the performance evaluation of the bias correction methods and selecting the best three RCMs. Finally, forecasting extreme values by using bias corrected model outputs and two different ensembles are done. First ensemble is the Simple Mean Ensemble (SME) which is constructed using 17 RCMs and the second one is the Superensemble (SE) which is constructed using the best performing three RCMs. Ensembles are constructed to overcome the downsides of the single model analysis like increase in uncertanity and variability.

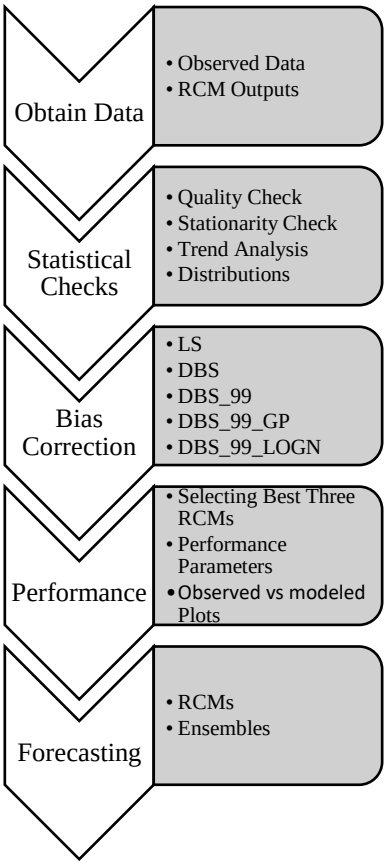

Figure 3.1. Flowchart of the study

The modified DBS methods used in this study are summarized below:

1) DBS_99: In this approach, instead of partitioning the data into two at the 95th percentile, data is divided into two at the 99th percentile. Gamma distributions are fitted to both parts.
2) DBS_99_GP: In this approach similar to DBS_99, partitioning is done at the 99th percentile but instead of fitting Gamma distribution to both parts, GP distribution is used for the extreme part and gamma distribution is fitted to the non-extreme part.

3) DBS_99_LOGN: In this approach similar to DBS_99, partitioning is done at the 99th percentile but instead of fitting gamma distribution to both parts, LOGN distribution is used for the extreme part and gamma distribution is fitted to the non-extreme part.

3.1 Statistical Checks

3.1.1 Quality Check

In this study, daily precipitation data of 53 MSs from Turkey are used. Study area covers the southern and south-eastern regions of Turkey. Dataset is obtained from Turkish State Meteorological Services and consists of the period between 1976 and 2010. Initially, 521 MSs are identified in the study area however, QC is applied before starting to analysis. MSs having no data after 2010 are removed due to inability to represent the situation of the last decade. Steps of the QC are explained below:

1. Months with more than 10 days of missing daily precipitation observation are marked as unreliable months and removed from the dataset.
2. Seasons with more than 1 month of missing data are marked as unreliable seasons and removed from the dataset.
3. Years with more than 1 season of missing data are marked as unreliable years and removed from the dataset.
4. Years with all zero entries are marked as unreliable years and removed from the dataset.

After the QC, MSs with minimum 35 years of reliable data are selected to be used in the analysis. 53 MSs having daily precipitation from 1976 to 2010 in the study area passed the QC and used in this study.

3.1.2 Stationarity Check

Stationarity Check is done for all observed data and uncorrected model outputs. For the stationarity check, two most common stationarity tests are used. They are the Augmented Dickey-Fuller (ADF) test and the Kwiatkowski-Phillips-Schmidt-Shin (KPSS) test (Moravej, 2016). These two tests are considered as complimentary to each other due to the difference of their null hypothesis (Kwiatkowski et al., 1992). The null hypothesis of the ADF test is that the series has a unit root while the null hypothesis of the KPSS test is that the series has no unit root. Since the null hypothesis of these two tests are opposites of each other, comparing the results of these two tests give more accurate indication of the stationarity of the series (Kwiatkowski et al., 1992).

3.1.2.1 The ADF Test

The ADF test is a unit root test. The null hypothesis of the test is that the series has a unit root which means the series is non-stationary while the alternative hypothesis is that the series has no unit root which means the series is stationary. Main principle of this test is to eliminate autocorrelation in the data by adding lagged values of dependent variable to the existing variable while allowing for higher-order serial correction in time series. Linear regression model with both a constant and a linear trend used for the ADF test is shown below (Dickey, 2014):

$$\Delta y_t = \mu + \gamma t + \delta y_{t-1} + \sum_{i=1}^{\rho} \beta_i \, \Delta y_{t-i} + \varepsilon_t \tag{1}$$

where Δy_t is $y_t - y_{t-1}$, y_{t-i} is the difference of y_t at lag i, δ is the coefficient of observed data at time $t-1$, μ is the intercept constant also called as drift, γ is the coefficient on a time trend, ρ is the lag order of autoregressive process, β_i is

autoregressive coefficient, t and i are the time indices, and ε_t is a sequence of independent random variables with a mean of zero and variance of $\sigma^2 = 0$ at time t.

The ADF statistic is calculated according to the model given in Equation (1) is (Dickey, 2014):

$$ADF = \frac{\hat{\delta}}{SE(\hat{\delta})} \tag{2}$$

where $\hat{\delta}$ is the expected value of δ for observed data and $SE(\hat{\delta})$ is the standard error for $\hat{\delta}$.

3.1.2.2 The KPSS Test

The KPSS test also uses a linear regression model for the decision of the stationarity. The null hypothesis is that the series is stationary while the alternative hypothesis is that the series is non-stationary. Linear regression model used for KPSS test is (Kwiatkowski et al., 1992):

$$Y_t = r_t + \beta_t + \varepsilon_t \qquad t = 1, \dots, T \tag{3}$$

$$r_t = r_{t-1} + u_t \qquad u_t \sim N(0, \sigma_u^2) \tag{4}$$

where Y_t is the time series, r_t is the random walk, β_t is the deterministic trend, ε_t is stationary error term, t is the time index, T is the number of observations, and u_t is the independent and identically distributed random variable.

The KPSS statistic is calculated according to the model given in Equation (3) is (Kwiatkowski et al., 1992):

$$KPSS = \frac{1}{T^2} \sum_{t=1}^{T} \frac{\hat{s}_t^2}{\hat{\sigma}_\infty^2} \tag{5}$$

$$\hat{s}_t = \sum_{j=1}^{t} \varepsilon_j \tag{6}$$

$$\hat{\sigma}_\infty^2 = \lim_{T\to\infty} var(\sum_{t=1}^{T} r_t) \tag{7}$$

where T is the sample size and $\hat{\sigma}^2$ is a consistent estimate of the variance of $\hat{u}_t$.

3.1.3 Trend Analysis

For trend analysis, Mann Kendall (MK) test and Sen's Slope Estimator (SSE) are used. Slope values obtained from SSE are treated as trends. By using MK test it is checked whether these trends are significant or not.

MK test checks whether a significant monotonic trend is present in the data. Its null hypothesis is that there is no monotonic trend in data while its alternative hypothesis is that there is a monotonic trend in data. Formula of test statistic is as follows (Mann, 1945):

$$S = \sum_{i=1}^{n-1} \sum_{j=i+1}^{n} sign\left(x_j - x_i\right) \tag{8}$$

where n is the number of observations, x_i and x_j are the sequential data values ($j > i$), and $sign\ (x_j - x_i)$ is the function given in Equation (9).

$$sign\ (x_j - x_i) \begin{cases} +1 \ \ if\ \left(x_j - x_i\right) > 0 \\ 0 \ \ if\ (x_j - x_i) = 0 \\ -1 \ \ if\ (x_j - x_i) < 0 \end{cases} \tag{9}$$

Then Z which depends on variance of S is calculated.

$$var(S) = \frac{n(n-1)(2n+5) - \sum_{p=1}^{q} t_p(t_p-1)(2t_p+5)}{18} \tag{10}$$

$$Z\begin{cases}\dfrac{S-1}{\sqrt{var(S)}} & if\ S>0\\ 0 & if\ S=0\\ \dfrac{S+1}{\sqrt{var(S)}} & if\ S<0\end{cases} \tag{11}$$

where, q is the tied group's number and t_p is the value of the overall data of p^{th} tied group ($p = 1, 2, 3, \ldots, n$).

SSE is used to obtain the magnitude of the trend in data. It is a nonparametric procedure for the estimation of the slopes of time series. Formula used for SSE is (Sen, 1968):

$$\beta = Median\left(\frac{x_j - x_i}{j - i}\right) \quad for\ 1 \le i < j \le n \tag{12}$$

where β is the estimated slope, x_j and x_i are data values at times j and i, respectively, and n is the number of time periods. Positive slopes indicate increasing trend while negative slopes indicate decreasing slope.

3.1.4 Identification of the Best Fitting Distribution for the Extreme Part

Six commonly used distributions are checked for their goodness of fit and compared with gamma distribution for the extreme part of the observed data. These distributions are normal, uniform, exponential, logistic, lognormal, and Weibull distributions. In addition to these six distributions a commonly used extreme value distribution, the generalized Pareto distribution is also checked. Best fitting distribution among these seven distributions to the extreme part of the observed data is identified. Akaike Information Criterion (AIC) is used for comparing the distributions and determining which distribution is more suitable. AIC for gamma distribution is calculated as well for comparison. AIC is calculated by the following formula (Akaike, 1974):

$$AIC = 2K - \log L \tag{13}$$

where K is the number of independently adjusted parameters and L is the maximum likelihood. Lower AIC value means better goodness of fit. As a result of this analysis, lognormal distribution is identified as the best fitting distribution to the extreme part of the observed data. This result lead to development of DBS_99_LOGN Method as explained in Section 3.5.5.

3.2 Bias Correction Methods

3.2.1 The LS Method

As a benchmark, one of the rather simpler scaling methods is used for the bias correction of the model outputs. The method used as a benchmark is the LS method. LS method focuses on correcting the means of model outputs by correction factors obtained through means of observed data. In total, 12 correction factors are calculated for each month of the year. The correction factor for each month is the ratio of the long-term mean of observed data of the related month to the long-term mean of model outputs. Then, model outputs are bias corrected by multiplying them with these correction factors. The formula used for the LS method is (Lenderink et al., 2007):

$$P_{COR} = P_{RCM} \left[\frac{\overline{P_{OBS,i}}}{\overline{P_{RCM,i}}}\right] \tag{14}$$

where P_{COR} is corrected data, P_{RCM} is model outputs, $\overline{P_{OBS,i}}$ is long term mean of observed data of month i, $\overline{P_{RCM,i}}$ is long term mean of model outputs of month i where $1 \leq i \leq 12$.

3.2.2 The DBS Method

In DBS, the data is divided into two parts at the 95th percentile. Because distribution of daily precipitation data is heavily skewed towards low intensities, distribution parameters are highly influenced by values with high frequency (Haylock et al.,

2006). By partitioning the data, extreme values may be represented without the influence of values with low intensity and high frequency. The parts composed of the data below the 95th percentile and over the 95th percentile can be referred to as the non-extreme part and the extreme part, respectively. Moreover, threshold for the wet day is introduced to the data to eliminate the drizzling effect (i.e., very small precipitation values generated by climate models). All the observed data with lower than the selected threshold value is replaced by zero. After partitioning, gamma distributions are fitted to the non-extreme and extreme parts. Gamma distribution has two-parameters, scale (α) and shape (β) parameters. Its CDF, $F(z)$ is formulated as follows (Wilks, 1995):

$$F(z) = \frac{\gamma(\beta, \frac{z}{\alpha})}{\Gamma(\beta)} \tag{15}$$

where z is the modeled variable, $\Gamma(i)$ is Gamma function and $\gamma(i, a)$ is the lower incomplete Gamma function. Details of Gamma function and lower incomplete Gamma function are as follows (Arfken, 1985):

$$\Gamma(i) = (i-1)! \tag{16}$$

where i is any positive number.

$$\gamma(i, a) = \int_0^a t^{i-1} e^{-t} dt \tag{17}$$

where i and a are any positive numbers, and t is the integration variable.

Then mapping procedure is used to bias correct each datapoint in the non-extreme part and the extreme part with Equations (18) and (19), respectively:

$$P_{CNE} = F_{ONE}^{-1}(F_{MNE}(P_{MNE})) \tag{18}$$

$$P_{CE} = F_{OE}^{-1}(F_{ME}(P_{ME})) \tag{19}$$

where P_{CNE} is the corrected non-extreme data, F_{ONE}^{-1} is the inverse CDF of the observed non-extreme data, F_{MNE} is the CDF of modeled non-extreme data, P_{MNE} is the modeled non-extreme data, P_{CE} is the corrected extreme data, F_{OE}^{-1} is the inverse

CDF of the observed extreme data, F_{ME} is the CDF of the modeled extreme data, and P_{ME} is the modeled extreme data.

The steps followed for the DBS method are listed below:

1. Determine a threshold for wet days for the observed data, $Th_{Observed}$.
2. Replace all the observed data lower than the threshold with zero.
3. Find the corresponding quantile of the threshold value for the observed data, $QTh_{Observed}$.
4. Find the value corresponding to $QTh_{Observed}$ for the model outputs (data to be bias corrected). Call it the threshold for the model outputs, Th_{Model}.
5. Replace all model outputs lower than Th_{Model} with zero.
6. Divide the observed data and model outputs into two parts at their 95th quantiles.
7. Fit gamma distribution to non-extreme parts of the observed data and the model outputs.
8. Fit gamma distribution to extreme parts of the observed data and the model outputs.
9. Apply the mapping procedure to correct bias.
10. Check the performance of bias correction using performance statistics.

Without the wet day threshold, drizzling effect may have a negative impact on bias correction (Teutschbein & Seibert, 2012). Quantile values may change, and the partition of the datasets may be affected. So, the wet day threshold is introduced to avoid these problems. The most commonly used threshold values are 0.1 mm/day or 1 mm/day (Teutschbein & Seibert, 2012; Yang et al., 2010). In this study, 1 mm/day is used as $Th_{Observed}$.

Steps 1 and 2 are used to correct the observed data with respect to the wet day threshold. Steps 3 and 4 are used to correct the model outputs with respect to the wet day threshold. First, Th_{Model} is calculated as follows:

$$Th_{Model} = F_{RCM}^{-1}(F_{OBS}(Th_{Observed})) \quad (20)$$

where F_{RCM}^{-1} is the inverse of CDF of model outputs and F_{OBS} is the CDF of observed data. By using Equation (13) the $Th_{Model}$is calculated and the model outputs below Th_{Model} are replaced by zero in Step 5.

In Step 6, after both observed data and model outputs are corrected for the wet day threshold, they are partitioned into extreme and non-extreme parts at their 95th quantiles. In Steps 7 and 8, gamma distributions are fitted to both parts of the observed data and model outputs using the Maximum Likelihood Estimation (MLE). Thus, a total of 4 gamma distributions are fitted.

Step 9 consists of the mapping procedure which uses CDFs of the observed data and model outputs to obtain bias correct the model outputs. Bias corrected model outputs, P_{COR} is obtained using the following equation (Yang et al., 2010):

$$P_{COR} = F_{OBS}^{-1}(F_{RCM}(P_{RCM})) \tag{21}$$

where P_{RCM} is the model outputs, F_{RCM} is the CDF of the model outputs, F_{OBS}^{-1} is the inverse CDF of the observed data. The graphical representation of this mapping procedure is shown in Figure 3.2.

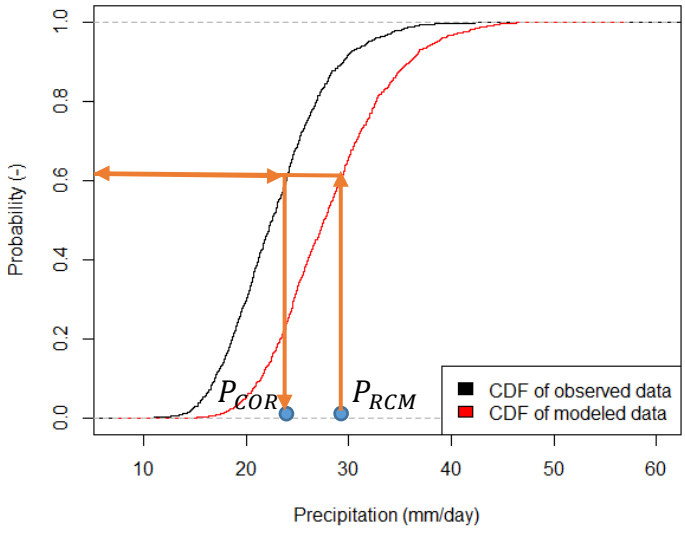

Figure 3.2. Mapping Procedure

3.2.3 DBS_99 Method

Using a 95th percentile for the partition of data and fitting gamma distributions to both parts may not be optimal for the bias correction of the most extreme parts. In this approach, instead of partitioning the data into two at the 95th percentile, data is divided into two at the 99th percentile. Similar to DBS method, gamma distributions are fitted to both parts. Thus, all the steps other than Step 6 of DBS are the same for this method. In Step 6 instead of using 95th percentiles, 99th percentiles are used. The steps followed for the DBS_BM method are listed below:

1. Determine a threshold for wet days for the observed data, $Th_{Observed}$.
2. Replace all the observed data lower than the threshold with zero.
3. Find the corresponding quantile of the threshold value for the observed data, $QTh_{Observed}$.
4. Find the value corresponding to $QTh_{Observed}$ for the model outputs (data to be bias corrected). Call it the threshold for the model outputs, Th_{Model}.
5. Replace all model outputs lower than Th_{Model} with zero.
6. Divide the observed data and model outputs into two parts at their 99th quantiles.
7. Fit gamma distribution to non-extreme parts of the observed data and the model outputs.
8. Fit gamma distribution to extreme parts of the observed data and the model outputs.
9. Apply the mapping procedure to correct bias.
10. Check the performance of bias correction using performance statistics.

3.2.4 DBS_99_GP Method

It is thought that using distributions related to extreme values (e.g., Gumbel, generalized extreme value, generalized Pareto) may be more representative for the extreme part of the data (Katz, 2013; Cooley, 2013) and GP distribution is used

instead of gamma distribution for the extreme part. CDF of GP distribution, $F(z)$ is formulated as follows (Jenkinson, 1955):

$$F(z) = 1 - \left[1 + \xi\left(\frac{z-\mu}{\sigma}\right)\right]^{-1/\xi} \quad (22)$$

where z is the selected variable for modeling, μ is location parameter, σ is scale parameter, and ξ is shape parameter.

In this approach similar to DBS_99, partitioning is done at 99th percentile, but instead of fitting gamma distribution to both parts, GP distribution is used for the extreme part while gamma distribution is fitted to the non-extreme part. Thus, the only difference from DBS_99 is in Step 8, where GP distribution is fitted to extreme part of both observed data and model outputs.

1. Determine a threshold for wet days for the observed data, $Th_{Observed}$.
2. Replace all the observed data lower than the threshold with zero.
3. Find the corresponding quantile of the threshold value for the observed data, $QTh_{Observed}$.
4. Find the value corresponding to $QTh_{Observed}$ for the model outputs (data to be bias corrected). Call it the threshold for the model outputs, Th_{Model}.
5. Replace all model outputs lower than Th_{Model} with zero.
6. Divide the observed data and model outputs into two parts at their 99th quantiles.
7. Fit gamma distribution to non-extreme parts of the observed data and the model outputs.
8. Fit GP distribution to extreme parts of the observed data and the model outputs.
9. Apply the mapping procedure to correct bias.
10. Check the performance of bias correction using performance statistics.

3.2.5 DBS_99LOGN Method

In this approach similar to DBS_99, partitioning is done at 99th percentile, but instead of fitting gamma distribution to both parts, LOGN distribution is used for the extreme part while gamma distribution is fitted to the non-extreme part. CDF of LOGN distribution, $F(z)$ is formulated as follows (Forbes et al., 2010):

$$F(z) = \Phi\left(\frac{(lnx) - \mu}{\sigma}\right) \tag{23}$$

where z is the selected variable for modeling, μ is location parameter, σ is scale parameter, and Φ is the CDF of the standard normal distribution. Thus, the only difference from DBS_99 is in Step 8, where LOGN distribution is fitted to extreme part of both observed data and model outputs.

1. Determine a threshold for wet days for the observed data, $Th_{Observed}$.
2. Replace all the observed data lower than the threshold with zero.
3. Find the corresponding quantile of the threshold value for the observed data, $QTh_{Observed}$.
4. Find the value corresponding to $QTh_{Observed}$ for the model outputs (data to be bias corrected). Call it the threshold for the model outputs, Th_{Model}.
5. Replace all model outputs lower than Th_{Model} with zero.
6. Divide the observed data and model outputs into two parts at their 99th quantiles.
7. Fit gamma distribution to non-extreme parts of the observed data and the model outputs.
8. Fit LOGN distribution to extreme parts of the observed data and the model outputs.
9. Apply the mapping procedure to correct bias.
10. Check the performance of bias correction using performance statistics.

3.3 Performance Evaluation

3.3.1 Performance Statistics

In this study, performances of different bias correction methods are evaluated using the following three statistics; the mean absolute error (MAE), the root mean square error (RMSE) and the percent bias (PBIAS):

$$MAE = \frac{1}{n}\sum|P_{OBS} - P_{COR}| \tag{24}$$

$$RMSE = \sqrt{\frac{1}{n}\sum(P_{OBS} - P_{COR})^2} \tag{25}$$

$$PBIAS = \frac{\sum(P_{OBS} - P_{COR})}{\sum P_{OBS}} \times 100 \tag{26}$$

where n is the number of datapoints. These statistics are also calculated for model outputs (i.e., in Equations (24), (25) and (26) P_{RCM} is used instead of P_{COR}) to evaluate the improvement due to bias correction. Since RMSE is sensitive to outliers, its value will be much higher than the value of MAE if a model has a few large outliers. By checking both MAE and RMSE and comparing them provides the information about outliers in errors (Hodson, 2022).

3.3.2 Selecting the Best Performing Bias Correction Method

A scoring system based on PBIAS values is developed to select the best performing bias correction method. For each MS, the following steps are conducted:

1. Methods are sorted according to their PBIAS values from the lowest to the highest for each RCM (i.e., the best performing model placed at the top).

2. Since five methods are compared, scores are assigned to each method from 5 to 1 so that the best performing method gets 5 points and the worst performing method gets 1 point.
3. Total score for each method is calculated for each MS.
4. The mean of total scores is obtained for each method.

At the end of this procedure each method has a score that represents the performance of that method for all MSs.

3.4 Forecasting

Two different ensemble approaches are used to generate model outputs in this study in addition to the RCM outputs. These approaches are SME and SE. SME and SE approaches are similar to each other. Main difference between them is the weight assigned to each RCM (Mesta Yoleri, 2022). While SME gives equal weight to each RCM, SE gives weights to RCM based on Multiple Linear Regression (MLR). While constructing ENS2, basic assumptions for linear regression are not checked and this situation is a limitation of the current study. These ensembles are calculated for each MS. They are refered to as ENS1 and ENS2 from now on, for SME and SE, respectively. In this study, ENS1 and ENS2 are calculated with the bias corrected RCM outputs, using all the RCM models and the best performing three RCM outputs, respectively.

Following formula is used for ENS1 (Cane & Milelli, 2010):

$$ENS1 = \overline{P_{OBS}} + \frac{1}{M}\sum_{j=1}^{M}\left(P_{RCM,j} - \overline{P_{RCM,J}}\right) \tag{27}$$

where $\overline{P_{OBS}}$ is the mean of observed series, $j = 1,2,\dots,M$ is the number of RCM, $M = 17$ in this study (all 17 RCMs are used for ensembling in $ENS1$), $P_{RCM,j}$ is the model outputs of RCM number j , and $\overline{P_{RCM,J}}$ is the mean of model outputs of RCM number j.

Following formula is used for ENS2 (Cane & Milelli, 2010):

$$ENS2 = \overline{P_{OBS}} + \sum_{j=1}^{N} a_j \left(P_{RCM,j} - \overline{P_{RCM,J}}\right) \tag{28}$$

where $\overline{P_{OBS}}$ is the mean of observed series, $j = 1,2,\dots,N$ is the number of RCM, $N = 3$ in this study (3 best RCMs are used for ensembling in $ENS2$), a_j is the weight of RCM number j, $P_{RCM,j}$ is the model outputs of RCM number j , and $\overline{P_{RCM,J}}$ is the mean of model outputs of RCM number j.

By using the best three bias-corrected RCMs and ensembles constructed in this study, changes in mean extreme precipitations are calculated for projection periods. The projection period is seperated into three parts as near, middle, and far future which cover the periods 2011-2040, 2041-2070, 2071-2100, respectively. Sample sizes of the time series used for ensembling for future periods range between 10800 and 10957 (i.e., 360×30 to 365.25×30). Means of the extreme parts are calculated for the observed data, bias corrected model outputs (correction is carried out using the best performing method), and ensembles. Partition point for the extreme part is is selected as the partition point of the best performing method. Percent change in the mean of extreme parts and whole datasets are calculated by the following formula:

$$Percent\ Change = \frac{\overline{P_P} - \overline{P_O}}{\overline{P_O}} * 100 \tag{29}$$

where $\overline{P_P}$ is the mean of the projection period (three periods used in this study are near, middle, and far future), $\overline{P_O}$ is the mean of the observed period.

CHAPTER 4

CASE STUDY AND RCMS

4.1 Study Area

Selected 53 MSs are located at different elevations and varying climate zones according to Köppen Climatic Zones (Beck et al., 2018). Effects of elevation, proximity to sea and climate zones are investigated in the analysis as well. Locations of MSs are labeled as white circles and given with Köppen Climatic Zones in Figure 4.1 and characteristics of MSs can be seen in Table 4.1.

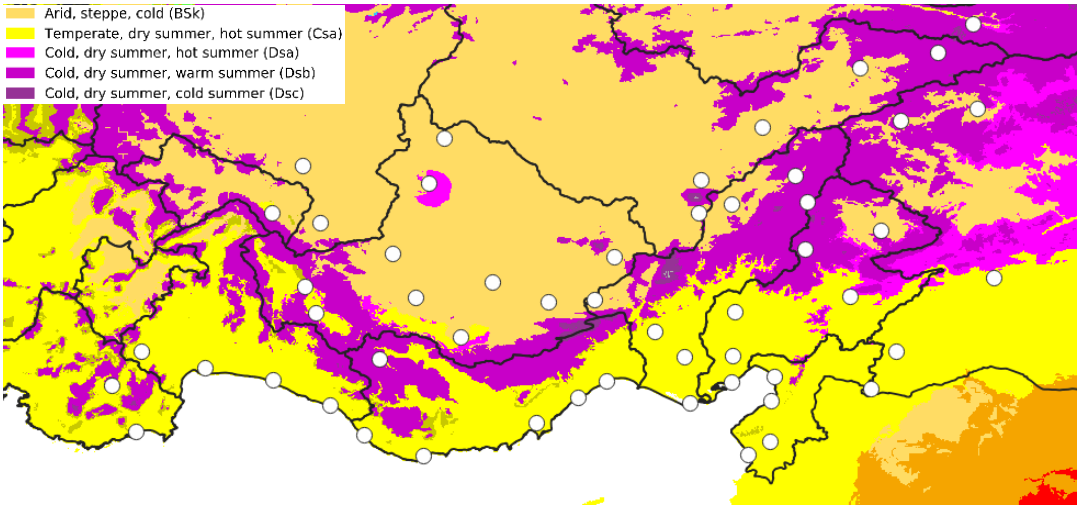

Figure 4.1. Köppen Climatic Zones (Beck et al., 2018) and Locations of MSs in the Study Area

As it can be seen in Figure 4.1, five different climates are observed in the study area. Legend on Figure 4.1 shows the typical climatic conditions regarding the colors associated with codes given by them (Beck et al., 2018). BSk refers to cold semi-arid climate, Csa refers to hot-summer Mediterranean climate, Dsa refers to

Mediterranean-influenced hot-summer humid continental climate, Dsb refers to Mediterranean-influenced warm-summer humid continental climate, and Dsc refers to Mediterranean-influenced subarctic climate. MSs on the shoreline are influenced by Csa. As the distance to sea increases MSs are more influenced by colder continental climates like Dsa, Dsb, Dsc. Twenty-seven of the MSs are in the Csa zone and 19 of the MSs are in the BSk zone which makes 87% of all the MSs.

Table 4.1. Characteristics of 53 MSs

MS #	MS ID	Latitude	Longitude	Elevation (m)	Dist. to Sea (km)	Climate Type
1	17090	39.744	37.002	1294	149	BSk
2	17162	39.185	36.081	1182	231	BSk
3	17191	38.651	32.922	973	247	Dsa
4	17196	38.687	35.500	1094	223	BSk
5	17239	38.369	31.430	1002	171	Csa
6	17242	37.678	31.746	1141	103	Dsa
7	17244	37.984	32.574	1031	166	BSk
8	17246	37.193	33.220	1018	113	BSk
9	17248	37.526	34.049	1046	96	BSk
10	17250	37.959	34.680	1211	127	BSk
11	17255	37.576	36.915	572	85	Csa
12	17261	37.059	37.351	854	44	Csa
13	17262	36.709	37.112	640	4	Csa
14	17265	37.755	38.278	672	94	Csa
15	17300	36.906	30.799	64	6	Csa
16	17310	36.551	31.980	6	0	Csa
17	17320	36.069	32.865	2	0	Csa
18	17330	36.382	33.937	10	9	Csa
19	17340	36.781	34.603	7	0	Csa
20	17351	37.004	35.344	23	38	Csa
21	17370	36.592	36.158	4	0	Csa
22	17372	36.205	36.151	104	33	Csa
23	17375	36.302	30.146	2	0	Csa
24	17684	40.162	38.075	1164	86	Dsb
25	17716	39.893	37.747	1338	122	Dsb

Table 4.1. (continued)

26	17734	39.362	38.114	1121	175	BSk
27	17754	39.079	33.066	1005	272	BSk
28	17762	39.243	37.389	1521	202	BSk
29	17798	38.821	31.726	1148	257	BSk
30	17802	38.725	36.390	1542	202	BSk
31	17832	38.276	31.894	1036	170	BSk
32	17836	38.374	35.480	1204	167	BSk
33	17837	38.452	35.791	1402	171	BSk
34	17840	38.478	36.504	1599	178	Dsb
35	17866	38.024	36.482	1344	129	Dsb
36	17870	38.204	37.198	1137	177	BSk
37	17898	37.427	31.849	1129	83	Csa
38	17900	37.566	32.790	1014	134	BSk
39	17902	37.715	33.526	996	141	BSk
40	17906	37.548	34.487	1453	84	BSk
41	17908	37.434	35.819	112	58	Csa
42	17926	37.057	30.191	1017	44	Csa
43	17928	36.989	32.456	1552	63	Dsb
44	17936	37.251	35.063	240	55	Csa
45	17952	36.737	29.912	1095	61	Csa
46	17954	36.790	31.441	38	4	Csa
47	17958	36.627	34.338	7	0	Csa
48	17960	37.015	35.796	30	19	Csa
49	17962	36.824	36.198	29	2	Csa
50	17974	36.272	32.305	21	2	Csa
51	17979	36.769	35.790	34	0	Csa
52	17981	36.568	35.389	22	1	Csa
53	17986	36.081	35.949	4	0	Csa

4.2 RCMs

RCMs used in this study are obtained from EURO-CORDEX published through ESGF (*ESGF-DKRZ - Home | ESGF-CoG*, n.d.). Step by step guide for obtaining the data can be accessed at https://cordex.org/data-access/esgf/. There is a publicly published table for the known issues about the RCMs within CORDEX. It is called Errata Table and can be accessed at https://euro-cordex.net/078730/index.php.en. Errata Table is used for the selection of RCMs in this study. When the most recent version of Errata Table is inspected, which is dated to 30.01.2021, 17 RCMs are selected from the table labeled as with no known issues or solved issues. List of RCMs used in this study can be seen in Table 4.2. RCP 8.5 scenario is used for the study.

Table 4.2. RCMs used in this study

Model ID	Driving GCM	RCM
RCM1	CNRM-CM5	CCLM4-8-17
RCM2	CNRM-CM5	ALADIN63
RCM3	CNRM-CM5	RCA4
RCM4	EC-EARTH	HIRHAM5
RCM5	EC-EARTH	CCLM4-8-17
RCM6	EC-EARTH	RACMOE22E
RCM7	EC-EARTH	RCA4
RCM8	CM5A-MR	WRF331F
RCM9	CM5A-MR	WRF381P
RCM10	CM5A-MR	RCA4
RCM11	HadGEM2-ES	CCLM4-8-17
RCM12	HadGEM2-ES	RACMOE22E
RCM13	HadGEM2-ES	RCA4
RCM14	MPI-ESM-LR	CCLM4-8-17
RCM15	MPI-ESM-LR	REMO2009(r1i1p1)
RCM16	MPI-ESM-LR	REMO2009(r2i1p1)
RCM17	NoRESM1-M	HIRHAM5

CHAPTER 5

RESULTS AND DISCUSSIONS

As shown in Figure 3.1, precipitation time series of RCM outputs are bias corrected with LS, DBS, DBS_99, DBS_99_GP, and DBS_99_LOGN methods. Within the scope of this study R programming language is used for all checks, analysis and bias correction procedures with the help of 3 packages. The first one is the "openxlsx" package (Walker & Braglia, 2018). It is used for importing observed data and model outputs from excel files. The second one is the "extRemes" package (Gilleland, 2022). It is used for fitting GP distributions into extreme parts for DBS_99_GP method. The third one is the "tseries" package used for stationarity and trend analyis. The rest of the analysis are carried out by the base package of R. Summary of the use of the packages can be seen in Table 5.1.

Table 5.1. Packages Used in this Study

Package	Used Step
openxlsx	For transferring data from excel files to the R environment
tseries	For stationarity check and trend analysis
extRemes	For fitting the GP distribution
Base R	The rest of the analysis

The study area has 53 MSs and 17 RCMs are used in this study. Bias correction is done for each RCM dataset at the closest grid to each MS. In total 4505 (i.e., 53x17 times 5 different bias correction methods) different bias corrected time series are generated. MAE, RMSE and PBIAS are used to compare the performances of five different bias correction approaches used in this study. These performance statistics are calculated for uncorrected version of model outputs as well.

RCM data are divided into two parts as historic period and projection period. 1976-2010 period is used as the historic period and 2011-2100 period is used as the projection period.

Although historic period for RCM outputs are provided up to 2005, to utilize the full time range of observed data (i.e., 1976-2010), projected RCM outputs from 2006 to 2010 are used as the historic period in this study. As stated in the Guidance for EURO-CORDEX (Benestad et al., 2017), historic period of RCM outputs are generated with observed climate datasets, known historical changes in greenhouse gas concentrations, solar radiation, etc. while future period of RCM outputs are initialized with conditions of historic period and forced with different RCP scenarios. Outputs generated with these two types of approaches are combined to obtain the historic model outputs in the current study. This fact should be recognized while making inferences about the outcomes.

Observed values in the historic period are used for parameter estimation for distribution fitting. These parameters are used for the bias correction of the projection period as well. The most of the MSs in Turkey are converted to automatic stations starting 2000s (Yılmaz & Darende, 2021). However, it is stated by Yilmaz and Darende (2021) that some of the manual and automatic entries are not consistent with each other.

In Section 5.1, results of statistical checks are given. In Section 5.2, CDFs of extreme parts of the data corrected by DBS, DBS_99, DBS_99_GP, and DBS_99_LOGN methods are given and discussed. In Section 5.3, performance statistics of LS, DBS, DBS_99, DBS_99_GP, and DBS_99_LOGN methods are compared and best performing method is determined. Observed vs modeled plots are also checked for comparing the results of bias correction methods. In Section 5.4 estimated changes in extreme precipitation by the best method and ensembles for projection period are presented.

5.1 Results of Statistical Checks

5.1.1 Stationarity Check

ADF test results and KPSS test results are obtained for observed data and all model outputs. If both tests conclude as stationary then the time series is represented by S, if both tests conclude as non-stationary then the time series is represented by NS. Otherwise, the time series is represented by IN meaning inconsistent results from the tests. Based on this analysis most of the observed data and model outputs are identified as S. The results are given in Appendix A.

5.1.2 Trend Analysis

Results of SSE and MK test are obtained for observed data and model outputs for 95% confidence interval. Trend values from SSE for all RCMs are given in Table 5.2. Green cells mean significant positive trend while red cells mean significant negative trend. Uncolored cells are without significant trend. As it can be seen in Table 5.2, observed data at most of the MSs have significant trends. Twenty-nine out of 53 MSs show significant negative trend. However, not all of the RCMs have significant trends. RCM3, RCM 7, RCM 8, RCM 10, RCM 11, RCM 13, RCM16, and RCM 17 have no significant trend for almost all MS locations. Significant trends in observed data and model outputs tend to be negative for most of the time. However, there are some significant positive trends as well. Results show only MS 24, MS 29, and MS 33 have significant positive trend for observed data. RCM 5, and RCM 9 shows significant positive trends for most of the MS locations as well. Remaining RCMs tend to have a significant negative trend.

Table 5.2. SSE and MK Test Results for All RCMs

M	O	1	2	3	4	5	6	7	8	9	10	11	12	13	14	15	16	17
1	0.00	0.01	0.01	0.00	0.00	0.03	0.01	0.00	0.01	0.02	0.00	0.01	0.01	0.01	0.02	0.01	0.01	0.00
2	0.02	0.01	0.01	0.01	0.01	0.01	0.01	0.01	0.01	0.02	0.01	0.01	0.01	0.01	0.03	0.01	0.00	0.00
3	0.02	0.02	0.01	0.00	0.04	0.05	0.02	0.01	0.00	0.03	0.00	0.01	0.03	0.00	0.04	0.01	0.01	0.00
4	0.03	0.01	0.01	0.01	0.04	0.01	0.02	0.01	0.01	0.02	0.01	0.01	0.01	0.01	0.04	0.01	0.01	0.00
5	0.03	0.03	0.01	0.01	0.04	0.03	0.01	0.01	0.00	0.02	0.00	0.01	0.01	0.00	0.03	0.01	0.01	0.00
6	0.00	0.02	0.01	0.01	0.06	0.01	0.00	0.01	0.00	0.02	0.00	0.01	0.01	0.00	0.04	0.02	0.01	0.00
7	0.01	0.02	0.01	0.01	0.06	0.03	0.00	0.01	0.00	0.01	0.00	0.01	0.02	0.00	0.03	0.02	0.01	0.00
8	0.02	0.03	0.01	0.02	0.04	0.03	0.01	0.01	0.00	0.01	0.01	0.01	0.02	0.00	0.04	0.02	0.00	0.01
9	0.00	0.02	0.02	0.01	0.07	0.01	0.03	0.00	0.01	0.02	0.01	0.01	0.01	0.00	0.04	0.02	0.00	0.01
10	0.01	0.02	0.02	0.01	0.06	0.02	0.02	0.00	0.01	0.02	0.00	0.01	0.01	0.00	0.03	0.01	0.00	0.00
11	0.03	0.01	0.01	0.02	0.08	0.07	0.01	0.00	0.01	0.01	0.00	0.01	0.02	0.00	0.04	0.03	0.00	0.01
12	0.03	0.02	0.01	0.00	0.09	0.10	0.01	0.01	0.01	0.01	0.00	0.01	0.01	0.01	0.04	0.03	0.01	0.00
13	0.03	0.02	0.01	0.00	0.08	0.11	0.02	0.01	0.01	0.01	0.00	0.01	0.01	0.01	0.04	0.02	0.01	0.01
14	0.02	0.01	0.00	0.01	0.13	0.07	0.03	0.01	0.01	0.02	0.00	0.01	0.01	0.00	0.04	0.03	0.00	0.01
15	0.03	0.02	0.01	0.00	0.13	0.09	0.01	0.02	0.01	0.01	0.00	0.01	0.01	0.00	0.04	0.03	0.01	0.01
16	0.02	0.02	0.00	0.01	0.09	0.09	0.02	0.01	0.00	0.00	0.01	0.01	0.01	0.00	0.03	0.02	0.01	0.01
17	0.02	0.02	0.01	0.02	0.08	0.10	0.03	0.01	0.00	0.00	0.01	0.00	0.01	0.01	0.04	0.02	0.01	0.00
18	0.02	0.02	0.01	0.03	0.06	0.06	0.03	0.01	0.00	0.00	0.01	0.01	0.01	0.01	0.04	0.02	0.01	0.01
19	0.01	0.02	0.00	0.02	0.03	0.09	0.05	0.01	0.00	0.01	0.00	0.00	0.01	0.01	0.04	0.02	0.00	0.01
20	0.03	0.02	0.00	0.02	0.04	0.11	0.05	0.00	0.01	0.02	0.01	0.00	0.02	0.01	0.05	0.02	0.00	0.00
21	0.01	0.02	0.01	0.01	0.00	0.10	0.07	0.01	0.01	0.02	0.01	0.01	0.00	0.00	0.04	0.01	0.00	0.00
22	0.01	0.02	0.01	0.01	0.02	0.08	0.06	0.02	0.02	0.01	0.00	0.01	0.01	0.00	0.05	0.02	0.01	0.02
23	0.01	0.03	0.00	0.00	0.07	0.07	0.04	0.02	0.00	0.00	0.00	0.02	0.01	0.01	0.04	0.02	0.01	0.01
24	0.02	0.01	0.01	0.01	0.02	0.01	0.00	0.01	0.01	0.02	0.01	0.01	0.00	0.00	0.02	0.00	0.00	0.01
25	0.00	0.01	0.02	0.01	0.01	0.01	0.01	0.01	0.01	0.02	0.01	0.01	0.01	0.00	0.02	0.00	0.00	0.00
26	0.02	0.01	0.01	0.01	0.01	0.00	0.02	0.00	0.01	0.02	0.01	0.01	0.01	0.01	0.03	0.01	0.00	0.00
27	0.03	0.01	0.01	0.01	0.05	0.05	0.01	0.01	0.01	0.02	0.00	0.01	0.03	0.00	0.04	0.01	0.00	0.00
28	0.01	0.01	0.01	0.01	0.01	0.01	0.00	0.01	0.01	0.03	0.00	0.01	0.01	0.00	0.03	0.01	0.00	0.01
29	0.04	0.02	0.01	0.01	0.04	0.04	0.01	0.00	0.00	0.02	0.00	0.00	0.02	0.00	0.03	0.02	0.01	0.00
30	0.00	0.01	0.02	0.01	0.02	0.01	0.01	0.00	0.01	0.03	0.01	0.01	0.01	0.00	0.03	0.01	0.00	0.00
31	0.00	0.02	0.01	0.01	0.04	0.01	0.00	0.01	0.00	0.02	0.00	0.01	0.01	0.00	0.03	0.02	0.01	0.00
32	0.00	0.01	0.02	0.01	0.05	0.01	0.01	0.00	0.01	0.03	0.00	0.02	0.01	0.00	0.03	0.02	0.00	0.00
33	0.02	0.01	0.02	0.01	0.01	0.01	0.01	0.00	0.01	0.03	0.00	0.01	0.01	0.00	0.04	0.01	0.00	0.00
34	0.00	0.01	0.02	0.01	0.02	0.01	0.01	0.01	0.01	0.03	0.01	0.01	0.01	0.00	0.03	0.02	0.00	0.00
35	0.03	0.02	0.02	0.01	0.04	0.02	0.00	0.01	0.01	0.03	0.01	0.01	0.01	0.01	0.04	0.02	0.00	0.01
36	0.03	0.01	0.02	0.01	0.06	0.04	0.00	0.01	0.01	0.02	0.00	0.01	0.02	0.00	0.03	0.02	0.00	0.00
37	0.01	0.03	0.01	0.01	0.04	0.01	0.01	0.01	0.00	0.01	0.00	0.01	0.01	0.00	0.03	0.02	0.01	0.00
38	0.01	0.02	0.02	0.01	0.06	0.05	0.01	0.02	0.00	0.02	0.01	0.01	0.02	0.00	0.04	0.02	0.01	0.00
39	0.01	0.02	0.01	0.01	0.06	0.06	0.00	0.01	0.00	0.02	0.00	0.01	0.02	0.00	0.04	0.01	0.01	0.01
40	0.02	0.02	0.02	0.02	0.06	0.00	0.03	0.00	0.01	0.02	0.00	0.01	0.01	0.00	0.04	0.02	0.00	0.01
41	0.02	0.01	0.00	0.01	0.06	0.06	0.01	0.00	0.02	0.03	0.00	0.01	0.01	0.01	0.04	0.02	0.00	0.00
42	0.00	0.02	0.01	0.01	0.08	0.01	0.00	0.02	0.00	0.02	0.00	0.01	0.02	0.01	0.04	0.02	0.01	0.00
43	0.03	0.03	0.02	0.01	0.05	0.01	0.01	0.01	0.01	0.02	0.00	0.01	0.01	0.00	0.03	0.01	0.01	0.01
44	0.02	0.01	0.00	0.02	0.06	0.03	0.00	0.00	0.01	0.02	0.01	0.01	0.01	0.00	0.05	0.02	0.00	0.00
45	0.00	0.03	0.01	0.01	0.03	0.02	0.02	0.02	0.00	0.02	0.00	0.02	0.02	0.01	0.04	0.02	0.01	0.01
46	0.02	0.02	0.01	0.01	0.12	0.08	0.01	0.01	0.00	0.00	0.01	0.00	0.01	0.00	0.03	0.02	0.01	0.01
47	0.02	0.02	0.00	0.03	0.03	0.10	0.06	0.01	0.00	0.01	0.01	0.00	0.01	0.01	0.04	0.02	0.01	0.01
48	0.02	0.02	0.01	0.01	0.04	0.11	0.05	0.00	0.01	0.02	0.00	0.00	0.01	0.01	0.05	0.02	0.00	0.00
49	0.01	0.02	0.01	0.01	0.01	0.09	0.05	0.01	0.01	0.02	0.01	0.01	0.00	0.01	0.04	0.01	0.00	0.00
50	0.01	0.02	0.00	0.01	0.08	0.10	0.02	0.01	0.01	0.00	0.01	0.00	0.01	0.01	0.03	0.02	0.01	0.01
51	0.01	0.02	0.00	0.01	0.05	0.13	0.05	0.00	0.01	0.03	0.00	0.00	0.01	0.00	0.04	0.02	0.00	0.01
52	0.03	0.02	0.01	0.01	0.02	0.14	0.07	0.01	0.01	0.02	0.00	0.00	0.01	0.00	0.04	0.02	0.01	0.00
53	0.01	0.02	0.00	0.01	0.00	0.10	0.06	0.01	0.01	0.01	0.01	0.01	0.00	0.01	0.04	0.01	0.00	0.01

M represents MS number, O represents observed series, and numbers from 1 to 17 represent RCM numbers. Red means negative and green means positive trends.

5.1.3 Determination of Best Fitting Distributions

Seven most commonly used distributions and the GP distribution are fitted to extreme part of the observed data (i.e., with a partition point of 99th quantile) and compared using AIC for each MS. AIC values are given in Table 5.3. In Table 5.3, Nor., Uni., Exp., Log., Logn. means normal distribution, uniform distribution, exponential distribution, logistic distribution, and lognormal distribution, respectively. Lowest AIC value for each MS is marked as bold. As can be seen in Table 5.3, the lowest AIC values are generally obtained for the lognormal distribution. Thus, DBS_99_LOGN method is developed and evaluated as an alternative bias correction method. AIC values for GP distribution are also checked and given in Table 5.3.

Table 5.3. AIC Values for Alternative Distributions

MS #	Nor.	Uni.	Exp.	Log.	Logn.	Weibull	Gamma	GP
1	827	937	1061	795	**776***	847	791	819
2	887	921	1063	860	**826**	890	843	876
3	813	879	1021	796	**769**	823	781	805
4	855	911	1065	831	**804**	866	818	847
5	958	964	1152	953	**922**	962	932	951
6	1020	1080	1170	990	**954**	1017	973	1013
7	912	989	1063	874	**842**	910	861	904
8	856	973	1067	836	**811**	868	823	851
9	892	986	1036	848	**815**	888	836	885
10	814	899	995	784	**757**	821	773	802
11	951	1079	1213	926	**909**	977	921	939
12	926	959	1163	918	**893**	938	902	920
13	929	960	1135	916	**887**	937	899	919
14	954	992	1223	940	**919**	973	929	947
15	1322	1308	1457	1321	**1282**	1314	1292	1318
16	1245	1289	1380	1219	**1178**	1238	1197	1238
17	1129	1192	1339	1117	**1090**	1138	1101	1121
18	1147	1204	1250	1109	**1064**	1129	1087	1135
19	1149	1276	1261	1114	**1070**	1135	1091	1140
20	1143	1163	1270	1126	**1083**	1133	1099	1138

Table 5.3. (continued)

21	1133	1246	1233	1085	**1043**	1115	1067	1126
22	1333	1529	1361	1249	**1191**	1281	1228	1328
23	1233	1345	1355	1185	**1146**	1222	1170	1227
24	812	853	1045	800	**775**	825	785	806
25	855	1004	1085	825	**805**	876	818	848
26	826	869	1038	803	**778**	838	792	815
27	888	1069	1040	838	**808**	891	828	879
28	836	874	1035	820	**790**	844	803	827
29	920	987	1084	903	**871**	921	884	916
30	838	890	1032	805	**779**	847	796	825
31	959	1115	1126	914	**887**	964	906	951
32	878	955	1055	860	**825**	880	840	868
33	816	843	1045	807	**781**	827	791	805
34	926	1040	1115	898	**870**	934	885	911
35	971	1045	1182	948	**920**	983	935	961
36	843	846	1061	836	**807**	851	817	838
37	1058	1077	1261	1037	**1008**	1066	1022	1049
38	840	884	1035	828	**797**	846	809	829
39	888	950	1039	867	**833**	886	847	875
40	890	973	1036	853	**817**	887	838	881
41	1148	1223	1280	1117	**1078**	1140	1097	1140
42	1030	1164	1130	985	**942**	1012	965	1017
43	923	935	1191	922	**900**	936	907	910
44	1204	1346	1329	1167	**1129**	1195	1148	1191
45	906	916	1164	903	**880**	919	887	898
46	1195	1274	1384	1172	**1143**	1201	1157	1189
47	1124	1235	1247	1090	**1051**	1114	1070	1112
48	1095	1208	1267	1059	**1029**	1100	1048	1084
49	1076	1095	1294	1066	**1037**	1085	1048	1068
50	1077	1111	1295	1071	**1041**	1085	1051	1068
51	1146	1240	1310	1120	**1087**	1147	1103	1134
52	1185	1280	1299	1146	**1105**	1172	1127	1177
53	1187	1344	1292	1135	**1095**	1171	1119	1178
*bold values are the lowest for each MS.								

5.2 Results of Bias Correction Methods

5.2.1 The DBS Method Results

CDFs of the bias corrected extreme parts by DBS for 9 MSs are given in Figure 5.1. Red line in the plots represent the CDF of extreme part of the observed data. Light gray shadow is the range of CDFs of the uncorrected model outputs (i.e., 17 uncorrected RCM outputs) and dark gray shadow is the range of CDFs of the corrected model outputs. Reamining CDFs are given in Appendix B.

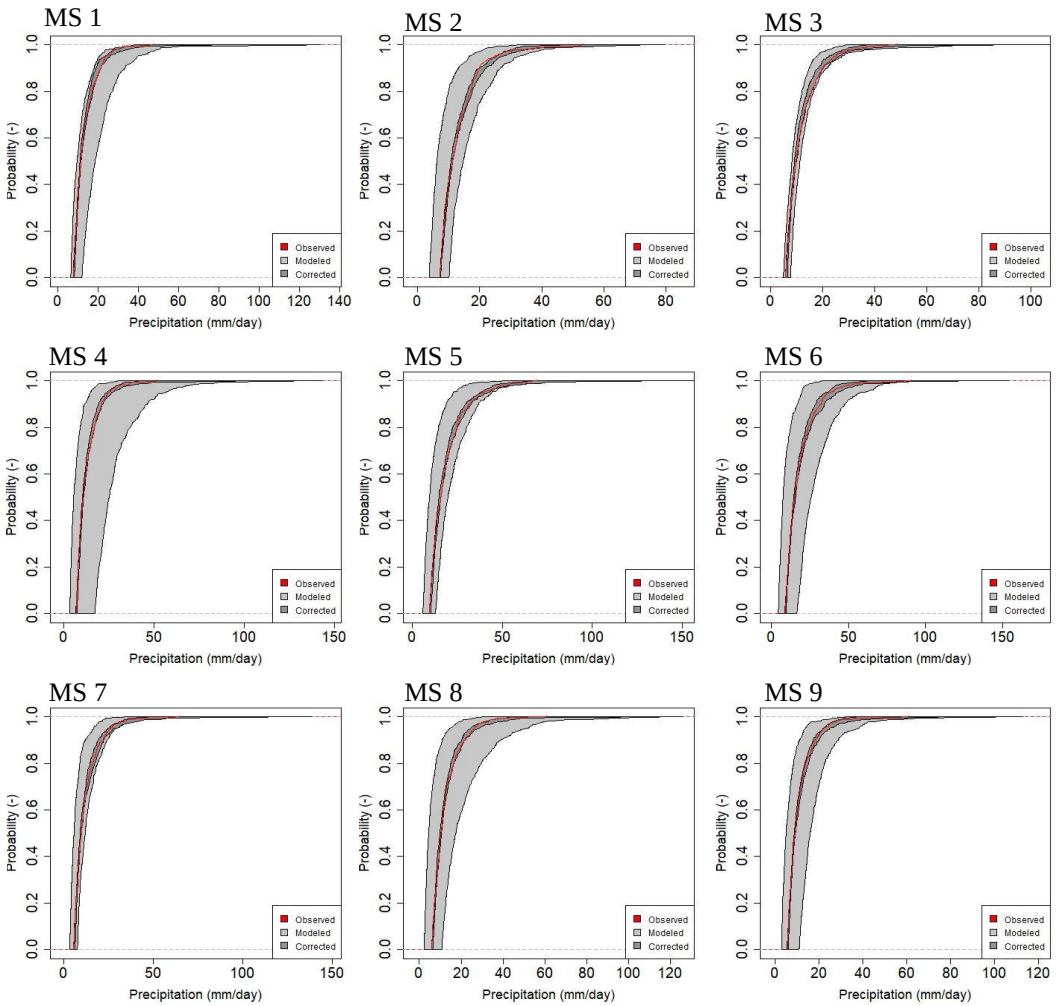

Figure 5.1. CDF of the extreme part of selected MSs (DBS)

It is expected that dark gray shadow has a narrower range than light gray shadow and dark gray shadow is in the vicinity of the red line. As it can be seen in Figure 5.1, expected results are aciheved. It can be said that gamma distribution works well for bias correction of the extreme part of model outputs.

5.2.2 The DBS_99 Method Results

CDFs of the bias corrected extreme parts by the DBS_99 method of 9 MSs are given in Figure 5.2. Reamining CDFs are given in Appendix B.

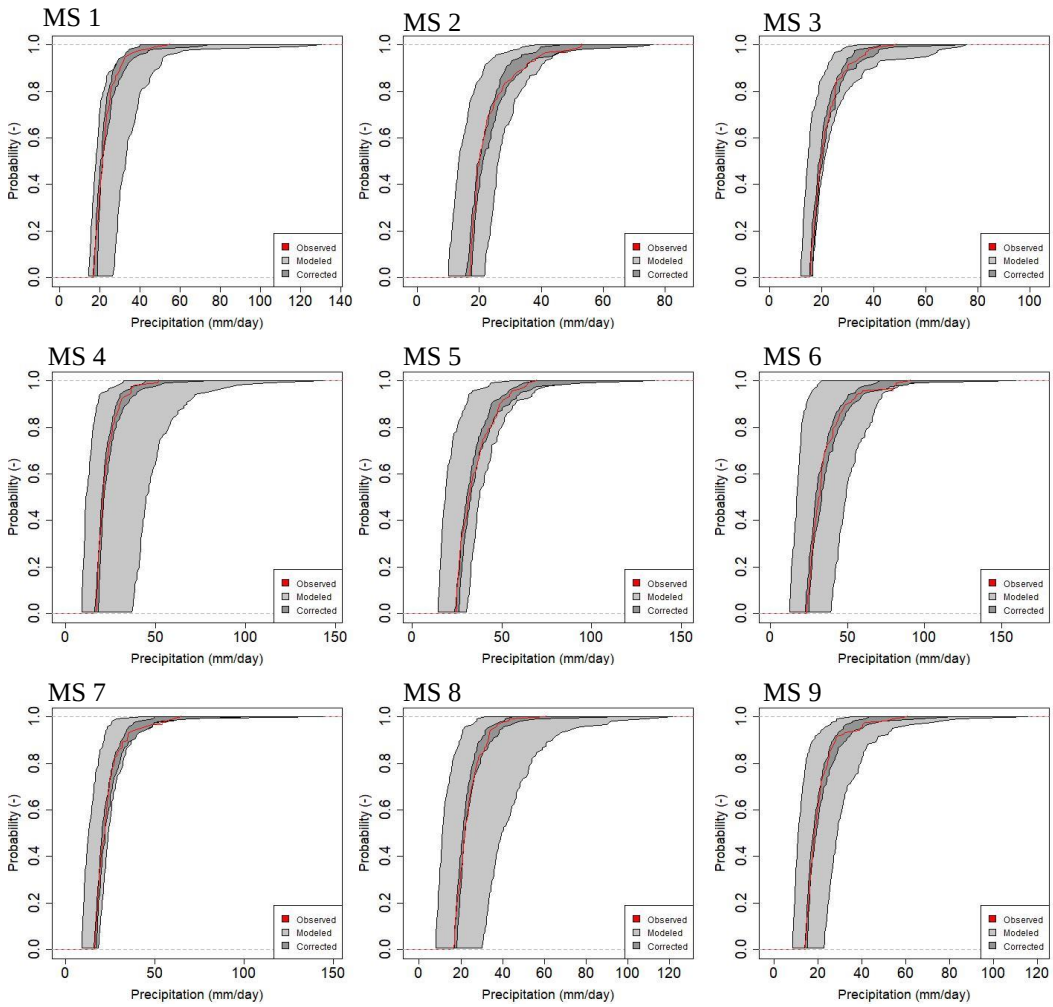

Figure 5.2. CDF of the extreme part of selected MSs (DBS_99)

As it can be seen in Figure 5.2, expected outcome is obtained with this method as well. Dark gray shadow is narrower than the light gray shadow and it is in the vicinity of the red line. Comparing with the CDFs with Figure 5.1, it can be said that ranges of both uncorrected and corrected model outputs increased with the change of partition point. In other words, DBS_99 does not perform as good as DBS.

5.2.3 The DBS_99_GP Method Results

CDFs of the bias corrected extreme parts by the DBS_99_GP method of 9 MSs are given in Figure 5.3. Reamining CDFs are given in Appendix B.

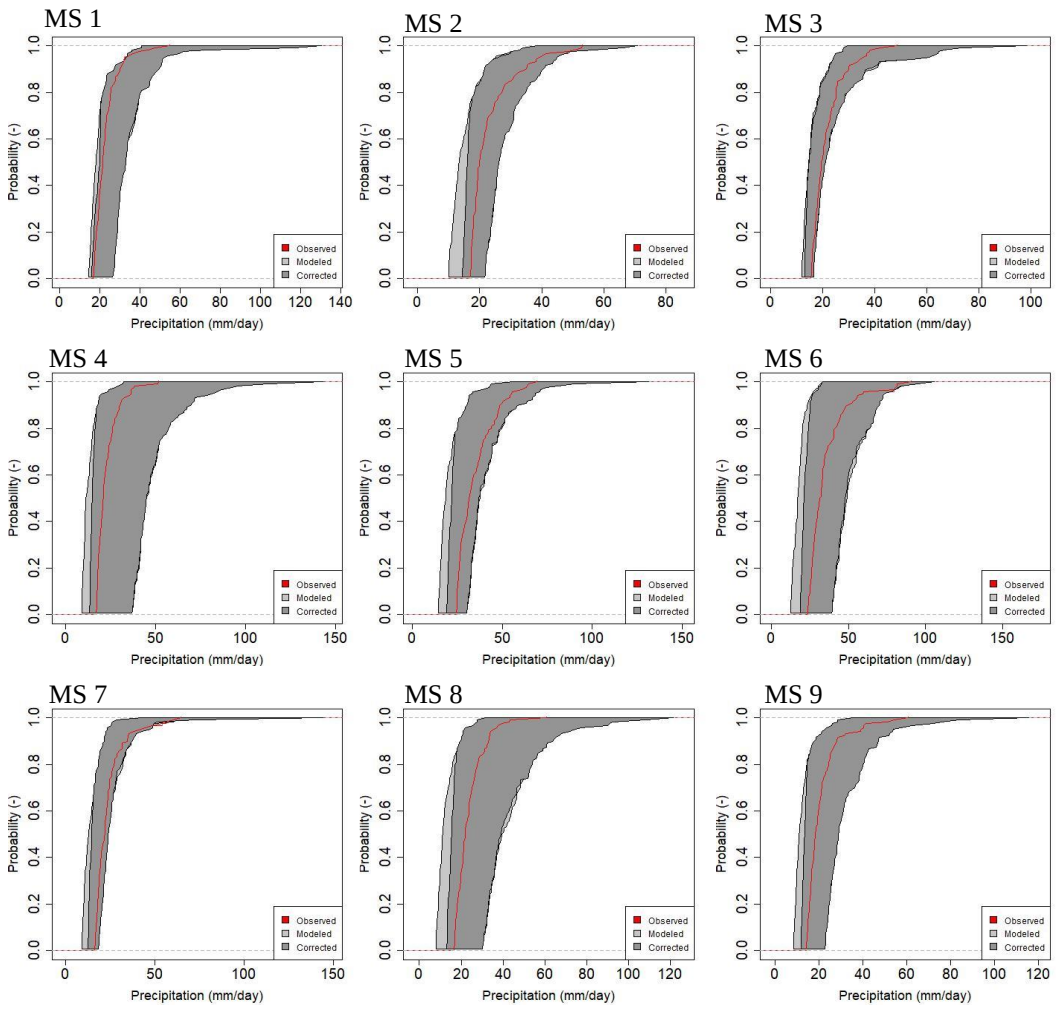

Figure 5.3. CDF of the extreme part of selected MSs (DBS_99_GP)

In Figure 5.3, the light gray shadow can barely be seen which means that corrected and uncorrected range of CDFs with DBS_99_GP method is very similar, unlike DBS and DBS_99 methods. In other words, the performance of DBS_99_GP is not as good as DBS or DBS_99. The reason for this may be the fact that sample size is very important when extreme value distributions such as generalized extreme value (GEV) and GP are used (Butler, Heffernan, Tawn, & Flather, 2007; Butler, Heffernan, Tawn, Flather, et al., 2007; Coles, 2001; Davison, 2005).

In this study, 99^{th} quantile is used as the partitioning point for the extreme part of the data set. This led to a sample size of 127 in our study. In the literature, the GP distribution is identified to be suitable for the Peak Over Threshold (POT) approach (Coles, 2001; Davison, 2005). Hosking & Wallis (2016) stated that sample sizes between 200 and 500 gave better performance with MLE when GP distribution is used. Thus, sample size is identified as one of the reasons for the poor performance of DBS_99_GP method.

It is also clearly seen that for most of the MSs the range of observed data is much smaller than the bias corrected range. For example, the red line for the MS 8, starts around 20 mm/day and ends around 60 mm/day while, the start of the dark gray shadow is between 20 mm/day and 30 mm/day, and the end of the dark gray shadow is between 30 mm/day and 120 mm/day. Due to use of GP distribution, the range of data is uncorrectly widened. These results indicate that GP is not a suitable distribution to be used in bias correction, especially when the length of time series is limited (i.e. observation period is short).

5.2.4 The DBS_99_LOGN Method Results

CDFs of the bias corrected extreme parts by the DBS_99 method of 9 MSs are given in Figure 5.4. Reamining CDFs are given in Appendix B.

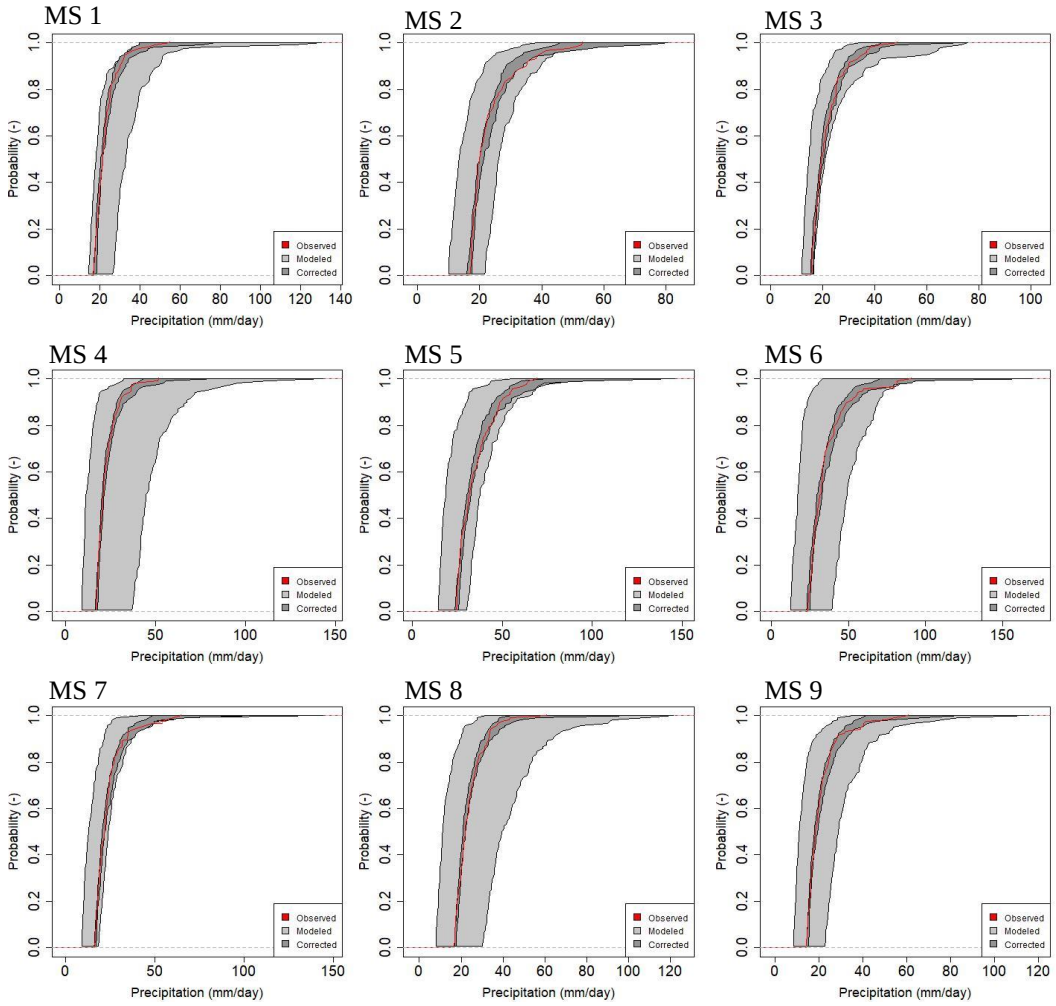

Figure 5.4. CDF of the extreme part of selected MSs (DBS_99_LOGN)

As it can be seen in Figure 5.4, the dark gray shadow is narrower than the light gray shadow and it is in the vicinity of the red line. Comparing with the CDFs with Figure 5.2, it can be said that ranges of both uncorrected and corrected model outputs are very similar. It can be said that the performances of the DBS method with LOGN distribution and gamma distribution are similarly.

5.3 Performance Evaluation

5.3.1 Selecting The Best Three RCMs

Mean performance statistics (means of 53 stations) for uncorrected version of model outputs are given in Table 5.4. Box plots of PBIAS, RMSE and MAE are given in Figure 5.5, Figure 5.6, and Figure 5.7, respectively.

Table 5.4. Mean Performance Statistics for RCMs

RCM #	PBIAS (%)	RMSE (mm/day)	MAE (mm/day)
1	-55.08	8.39	3.43
2	-50.47	8.41	3.39
3	**8.77***	7.11	2.64
4	21.43	7.31	2.55
5	**-1.90**	7.53	2.79
6	14.34	7.03	2.60
7	22.15	6.98	2.49
8	-29.52	7.87	3.15
9	-43.00	7.60	3.23
10	33.91	6.61	2.32
11	-33.03	8.70	3.38
12	-16.99	8.02	3.19
13	**3.16**	7.69	2.87
14	-25.41	8.02	3.09
15	-26.20	9.49	3.38
16	-28.18	9.79	3.41
17	19.41	7.46	2.58
Average	-10.98	7.88	2.97
*Bold values are the smallest three values.			

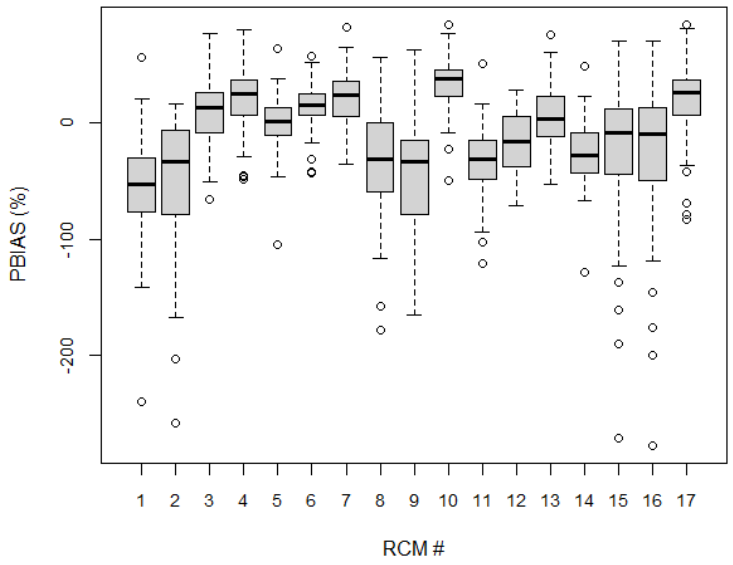

Figure 5.5. PBIAS of the RCMs for all 53 MSs

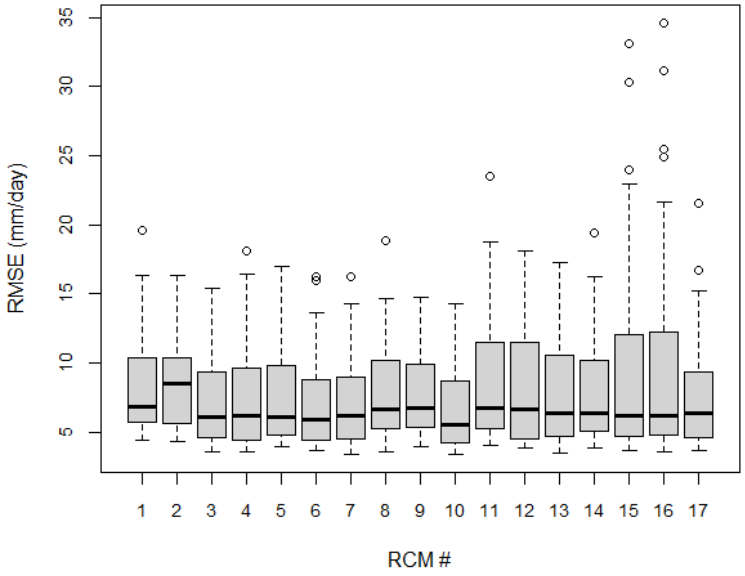

Figure 5.6. RMSE of the RCMs for all 53 MSs

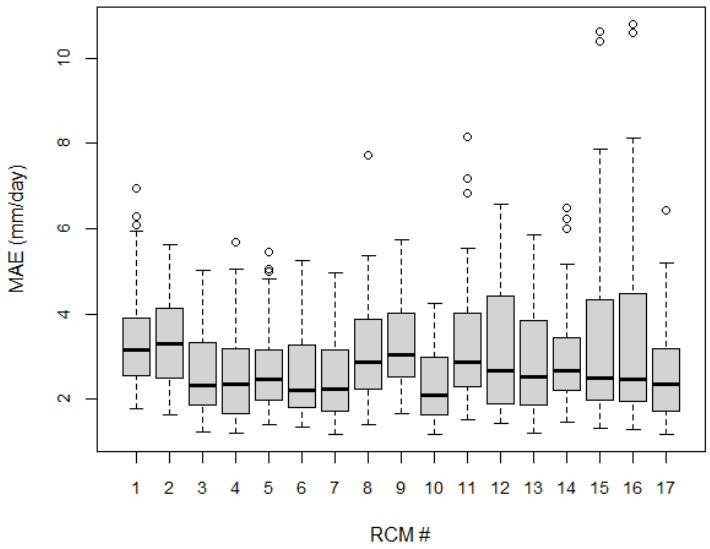

Figure 5.7. MAE of the RCMs for 53 MSs

Since our goal is to correct biases, the best performing three RCMs are selected to be analyzed in more detail. The more the PBIAS value is close to zero, the better the performance. The smallest absolute PBIAS values are marked in bold in Table 5.4. RCM 3, RCM 5, and RCM 13 have less than 10% mean PBIAS values so they are chosen as the best performing three RCMs. They will be referred to as the best-three RCMs from hereafter. The reason for choosing the best-three RCMs is to investigate the improvement by bias correction methods in more detail. Considering the average PBIAS, RMSE, and MAE values given in Table 5.4, the best-three RCMs have better than average performances in terms of RMSE and MAE as well.

5.3.2 Performance Parameters

PBIAS is used to determine the best method for each MS. PBIAS values are given for best-three RCMs for each MS in Table 5.5. M represents the MS number, U represents the uncorrected, LS represents corrected by LS method, D1 represents corrected by DBS method, D2 represents corrected by DBS_99, D3 represents corrected by DBS_99_GP, and D4 represents corrected by DBS_99_LOGN in Table 5.5. Best PBIAS values are marked with green excluding the LS method. RMSE and MAE values are given in Appendix C.

Table 5.5. Comparison of PBIAS values

	RCM3						RCM5						RCM13					
M	U	LS	D1	D2	D3	D4	U	LS	D1	D2	D3	D4	U	LS	D1	D2	D3	D4
1	-51	0.0	-1.3	-3.0	-7.8	-3.0	-19	0.0	-0.8	-1.9	-2.6	-1.9	-39	0.0	0.2	-0.6	-6.7	-0.6
2	29	0.0	-0.2	0.8	5.9	0.8	-1	0.0	-0.9	-2.0	0.6	-2.0	33	0.0	0.0	2.5	5.5	2.4
3	-38	0.0	-1.0	-3.8	-6.6	-3.8	5	0.0	0.1	-1.0	2.0	-1.0	-27	0.0	0.3	-1.7	-5.9	-1.7
4	38	0.0	-0.7	0.3	7.0	0.3	-17	0.0	-1.1	-2.6	-1.0	-2.6	44	0.0	1.0	2.1	8.8	2.1
5	11	0.0	-1.3	-3.4	2.3	-3.4	6	0.0	-0.7	-2.9	3.2	-2.9	10	0.0	-0.5	-1.7	2.0	-1.8
6	14	0.0	-1.1	-2.8	3.2	-2.8	10	0.0	-0.9	-2.6	4.1	-2.7	8	0.0	-0.5	-1.1	3.4	-1.1
7	0	0.0	-0.9	-2.4	1.7	-2.4	1	0.0	-0.3	-1.9	2.8	-1.9	4	0.0	-0.7	-3.0	2.1	-3.1
8	33	0.0	0.6	-0.5	6.9	-0.6	2	0.0	0.2	-1.4	1.6	-1.5	30	0.0	0.2	-0.8	7.4	-0.8
9	30	0.0	0.1	-0.1	5.9	-0.1	-46	0.0	-0.8	-2.2	-6.4	-2.2	36	0.0	0.1	1.0	9.5	1.1
10	-39	0.0	-1.1	-2.9	-7.4	-2.9	-40	0.0	-0.7	-3.4	-5.1	-3.4	-28	0.0	-0.7	-1.2	-6.0	-1.1
11	26	0.0	0.9	2.2	4.4	2.2	16	0.0	0.2	0.3	3.3	0.3	10	0.0	2.1	3.8	-0.4	3.8
12	-19	0.0	-1.8	-2.8	-2.6	-2.8	12	0.0	0.1	0.9	1.9	0.9	-46	0.0	-1.3	-2.4	-6.6	-2.4
13	-25	0.0	-0.8	-1.8	-5.0	-1.8	3	0.0	0.1	0.7	2.2	0.6	-42	0.0	0.4	-0.8	-7.1	-0.8
14	-1	0.0	-0.3	0.9	-3.0	0.9	-29	0.0	0.0	0.1	-7.4	0.1	-42	0.0	0.3	1.0	-13.2	1.0
15	16	0.0	-1.3	-3.8	11.6	-3.9	-2	0.0	-1.4	-4.0	6.1	-4.0	3	0.0	0.1	-2.5	7.2	-2.5
16	18	0.0	-0.9	-1.1	6.0	-1.1	14	0.0	0.3	0.5	3.4	0.3	-1	0.0	-1.0	-1.7	3.2	-1.7
17	53	0.0	1.0	2.6	14.2	2.6	21	0.0	1.5	2.5	1.7	2.2	37	0.0	0.9	2.1	9.9	2.1
18	26	0.0	0.2	1.4	8.4	1.6	2	0.0	-1.0	-1.8	1.5	-1.8	18	0.0	0.2	1.3	4.8	1.3
19	42	0.0	0.7	2.2	10.6	2.2	6	0.0	-0.4	0.0	1.0	0.0	28	0.0	0.5	2.9	6.4	2.9
20	-26	0.0	-1.5	-3.9	0.0	-3.9	12	0.0	-0.6	-1.2	4.7	-1.5	-40	0.0	-0.8	-3.1	-5.8	-3.1
21	14	0.0	0.1	0.0	4.8	0.1	36	0.0	0.7	1.4	9.7	1.5	3	0.0	0.6	0.4	3.0	0.4
22	77	0.0	0.8	4.0	20.5	4.3	64	0.0	1.9	4.3	18.4	4.6	76	0.0	1.1	3.2	20.4	3.6
23	13	0.0	-1.0	-1.2	2.6	-1.0	-7	0.0	-0.8	-1.1	-5.8	-1.1	-4	0.0	-2.0	-2.6	-2.5	-2.5
24	-13	0.0	-0.1	-0.9	-2.2	-0.9	-34	0.0	-1.1	-3.0	-4.5	-3.0	-8	0.0	0.9	1.2	-2.6	1.2
25	22	0.0	0.6	1.9	3.8	1.8	-8	0.0	-0.4	-2.1	-0.7	-2.1	26	0.0	1.9	4.0	3.4	4.0
26	29	0.0	0.3	1.7	5.5	1.7	-25	0.0	-0.6	-1.0	-3.8	-1.0	26	0.0	1.5	2.7	3.8	2.7
27	-20	0.0	-1.5	-3.2	-3.2	-3.2	14	0.0	-0.3	-0.1	3.4	-0.1	-12	0.0	-0.6	-0.7	-3.5	-0.6
28	-4	0.0	-1.5	-0.6	0.3	-0.7	-8	0.0	-0.2	-0.2	1.6	-0.2	0	0.0	0.4	2.2	1.2	2.2
29	-17	0.0	-2.3	-4.4	-0.6	-4.5	18	0.0	-0.6	-0.4	6.7	-0.4	-3	0.0	-1.2	-2.6	1.3	-2.7
30	-4	0.0	-0.6	-1.0	-0.6	-1.0	-38	0.0	-0.9	-2.7	-4.7	-2.7	4	0.0	1.2	1.4	1.4	1.4
31	24	0.0	-1.6	-2.7	6.0	-2.7	-7	0.0	-1.2	-2.5	1.9	-2.5	23	0.0	-1.0	-2.0	6.3	-2.0
32	-66	0.0	-1.4	-1.0	-14.2	-1.1	-41	0.0	-1.5	-2.6	-6.2	-2.6	-53	0.0	-0.4	1.5	-14.5	1.5
33	16	0.0	-0.2	-0.2	2.9	-0.2	-10	0.0	-0.3	-1.6	0.7	-1.7	21	0.0	1.3	1.9	4.1	1.9
34	13	0.0	0.2	-0.2	3.7	-0.2	-9	0.0	-0.1	-1.7	0.5	-1.7	15	0.0	0.7	0.1	4.3	0.1
35	-31	0.0	-0.9	-2.6	-3.7	-2.6	-15	0.0	-0.5	-1.1	-2.3	-1.1	-44	0.0	-0.3	-2.1	-5.6	-2.1

Table 5.5. (continued)

36	-20	0.0	-0.7	-1.3	-4.2	-1.3	-18	0.0	-1.4	-1.2	-3.8	-1.2	-21	0.0	-0.4	-0.2	-3.9	-0.2
37	56	0.0	-1.6	-2.0	11.2	-2.0	36	0.0	-1.2	-1.8	8.7	-1.8	50	0.0	-1.5	-1.1	11.1	-1.2
38	-29	0.0	-1.0	-4.0	-6.6	-4.0	11	0.0	-0.4	-1.3	4.1	-1.4	-26	0.0	-1.0	-3.4	-4.4	-3.4
39	-8	0.0	-0.5	-1.3	1.8	-1.3	-6	0.0	-0.4	-1.5	2.3	-1.7	-2	0.0	-0.4	-1.2	2.3	-1.1
40	-7	0.0	-0.6	-0.9	-1.1	-0.9	-105	0.0	-0.7	-2.5	-16.1	-2.5	6	0.0	0.8	1.4	1.8	1.5
41	6	0.0	-0.6	0.1	2.3	0.2	1	0.0	-0.7	-1.2	0.6	-1.3	-4	0.0	0.4	1.5	-2.1	1.6
42	4	0.0	-1.7	-2.9	1.9	-2.9	-33	0.0	-1.5	-3.3	-2.6	-3.3	3	0.0	-0.7	-1.2	-0.2	-1.2
43	42	0.0	-1.7	-1.9	7.1	-2.0	2	0.0	-1.5	-2.7	1.4	-2.7	35	0.0	-2.0	-3.1	6.2	-3.1
44	10	0.0	-1.5	-3.0	1.4	-3.0	-11	0.0	-0.8	-2.0	-1.8	-2.1	0	0.0	-0.8	-1.3	-1.5	-1.3
45	67	0.0	0.5	1.3	17.7	1.3	-5	0.0	-0.7	-1.3	-0.6	-1.3	61	0.0	0.4	2.0	16.2	2.0
46	9	0.0	-1.1	-1.5	2.7	-1.4	15	0.0	-0.6	-1.5	2.8	-1.5	-7	0.0	-0.6	-1.1	1.5	-1.1
47	36	0.0	0.4	2.0	9.9	2.0	14	0.0	-0.2	0.1	2.3	-0.1	17	0.0	0.5	2.1	3.8	2.1
48	12	0.0	-1.3	-3.1	5.0	-3.1	22	0.0	-0.5	-1.8	5.8	-1.8	-2	0.0	-0.7	-2.3	2.7	-2.2
49	40	0.0	0.2	1.6	8.2	1.6	28	0.0	0.3	0.9	4.7	0.8	32	0.0	1.0	2.6	6.6	2.6
50	4	0.0	-0.7	-0.5	1.6	-0.4	3	0.0	0.3	2.1	-1.6	2.1	-15	0.0	0.7	0.6	-1.6	0.6
51	17	0.0	-1.8	-3.6	6.3	-3.6	13	0.0	-0.3	-0.4	1.6	-0.6	-12	0.0	-1.4	-3.7	-0.1	-3.7
52	16	0.0	-1.3	-3.4	7.0	-3.2	38	0.0	-0.2	0.1	11.3	0.1	-21	0.0	-1.1	-3.3	-0.8	-3.2
53	15	0.0	-0.8	-1.7	4.8	-1.6	8	0.0	-0.3	-0.6	2.9	-0.5	8	0.0	-0.6	-1.3	4.2	-1.2

M represents the MS number, U represents the uncorrected, LS represents corrected by LS method, D1 represents corrected by DBS method, D2 represents corrected by DBS_99, D3 represents corrected by DBS_99_GP, and D4 represents corrected by DBS_99_LOGN. Best PBIAS values are marked with green excluding LS.

All bias correction methods used in this study improved the performance parameters compared to those for the uncorrected series. Unfortunately, the methods proposed in this study rarely worked better than the original DBS method. As can be seen in Table 5.5, DBS_99 DBS_99_GP and DBS_99_LOGN performed best only for a few of the MSs. For the rest of the MSs, DBS method performed the best.

According to the results it can be said that changing the partition point from 95th quantile to 99th quantile did not cause an improvement. The purpose of changing it from 95th quantile to 99th quantile was to represent extreme part more efficiently. However, it also reduced the sample size for distribution fitting. It is seen that tradeoff between the sample size and the representation of extreme part of the data is not favorable.

To select the best performing bias correction method, steps described in Chapter 3.3.2 are followed and the results are given in Table 5.6.

Table 5.6. Scores of Bias Correction Methods

Method	Score
LS	84
DBS	64
DBS_99	41
DBS_99_GP	26
DBS_99_LOGN	40

As it can be seen in Table 5.5, PBIAS values corrected by LS method are almost zero and this leads to LS having the highest score when only PBIAS is considered as the performance criteria. Since LS method focuses on correcting means of model outputs, it is an expected result. However, correcting only means of model outputs may lead to underestimation or overestimation of extreme values as can be seen in Figure 5.8. QM methods are suggested to overcome this deficiency (Ghimire et al., 2019; Luo et al., 2018; Mendez et al., 2020; Teutschbein & Seibert, 2012). Thus, DBS is identified as the best performing method in this study.

5.3.3 Observed versus Corrected and Uncorrected Model Outputs

Observed versus bias corrected and uncorrected model outputs are plotted for best three RCMs. Observed vs modeled plots of RCM 3 for the first 8 MSs are given in Figure 5.8. Purple points represent the uncorrected model outputs. Results corrected by DBS, DBS_99, DBS_99_GP, DBS_99_LOGN are represented with the colors black, red, blue, and green, respectively. An identity line is also introduced to the plots to make interpretation easier. Plots of RCM 3 for the remaining MSs, plots of RCM 5 and RCM 13 for all MSs are given in Appendix D.

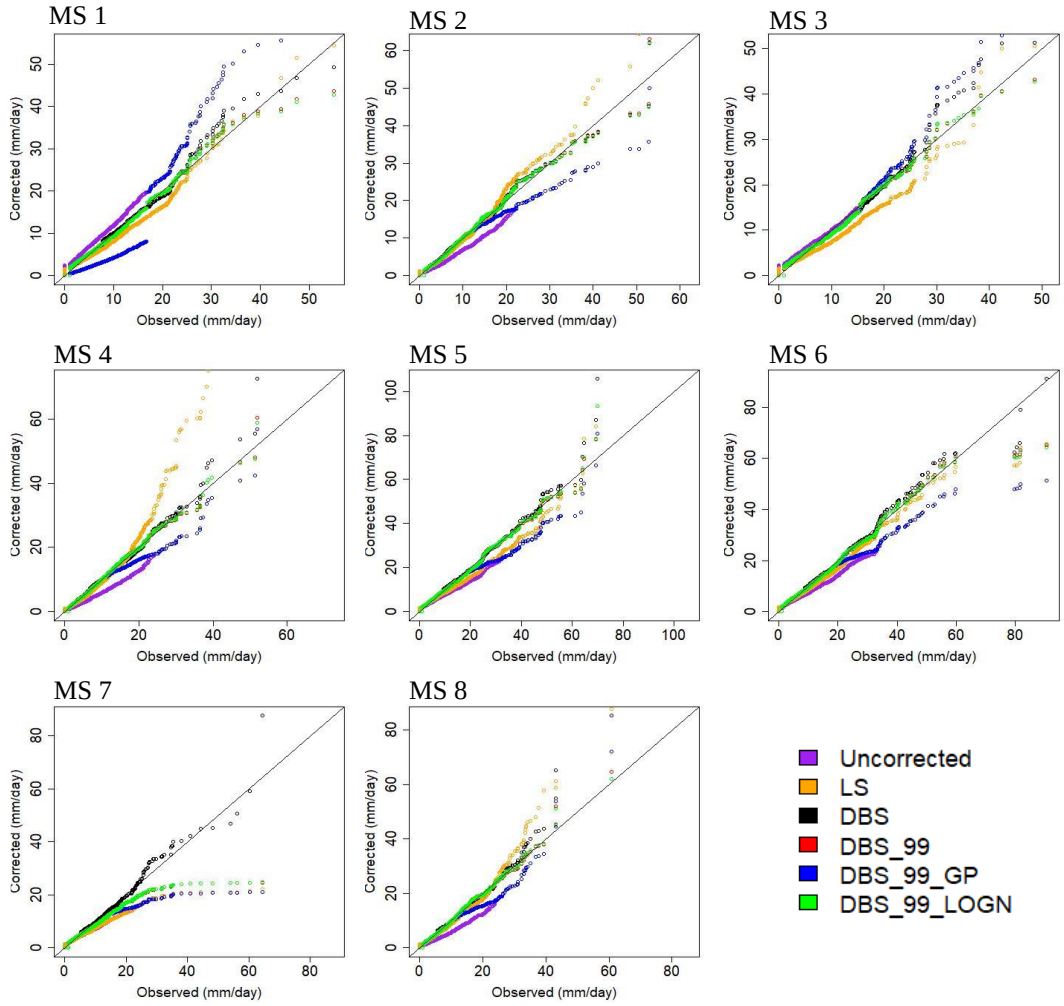

Figure 5.8. Observed versus bias-corrected and uncorrected modeled plots of RCM 3 for MS1 to MS8

Points getting closer to the identity line means the bias correction method corrected the model outputs better. As it can be seen in Figure 5.8, the closest points to the identity line are mostly black which means bias correction with DBS worked better than the other methods. On the other hand, DBS_99_GP method resulted in points further away from the identity line. There is always either a considerable underestimation or overestimation with the DBS_99_GP method (i.e., the furthest points to the identity line are blue points most of the time). LS tends to underestimate or overestimate especially for the extreme values as well. Observed versus bias

corrected and uncorrected model outputs also show that DBS is the best performing method which is consistent with the results presented in Chapter 5.3.2.

5.4 Forecasting

Projection period for this study is selected as 2011-2100 and forecasting is done for this period. This period is separated to three parts as 2011-2040, 2041-2070, and 2071-2100 to represent near, middle, and far future, respectively. Percentage changes in mean extreme precipitations comparing the historic period are calculated for these periods. Bias corrected outputs of the best three RCMs with DBS method and outputs of ensembles constructed for this study (i.e., ENS1 and ENS2) are used for the calculation of changes in mean extreme precipitations. Since the DBS method is selected as the best performing method, 95^{th} quantile is used as the partition point to obtain the mean extreme precipitations.

Box plots of the whole daily precipitation time series for the first 9 MSs for near future are prepared and given in Figure 5.9. However, since the goal of this study is to analyze extreme values, the box plots box plots for the extreme parts of the best three RCMs and ensembles are prepared for the near, middle, and far future for all MSs. Uncorrected RCM outputs are also included in these plots for comparison. Box plots of the extreme parts of first 9 MSs are given in Figure 5.10, Figure 5.11, and Figure 5.12 for the near, mid, and far future, respectively. The rest of the box plots are given in Appendix E.

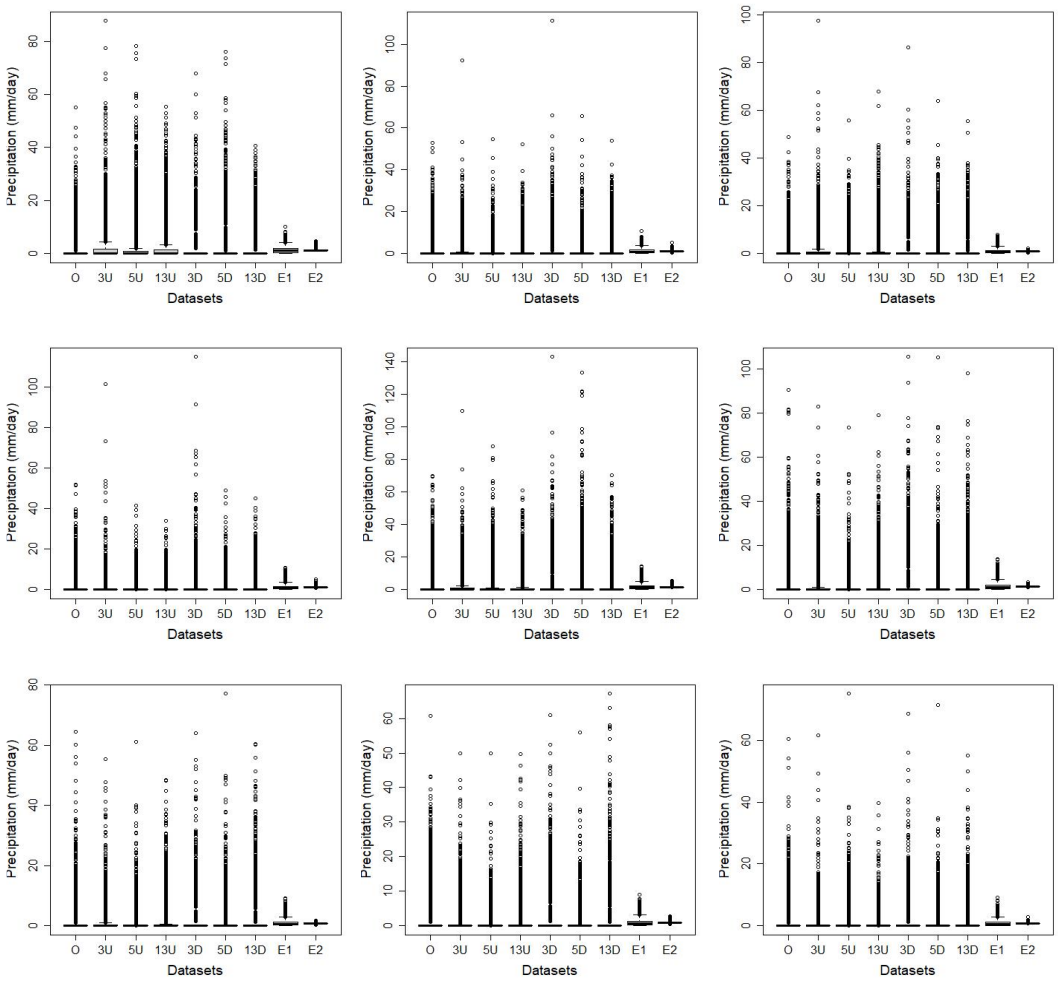

Figure 5.9. Box Plots of Whole Datasets (2011-2040).

In Figures 5.9 to 5.12, O, 3U, 5U, 13U, 3D, 5D, 13D, E1, and E2 are observed data, uncorrected RCM 3 outputs, uncorrected RCM 5 outputs, uncorrected RCM 13 outputs, RCM 3 outputs corrected by DBS method, RCM 5 outputs corrected by DBS method, RCM 13 outputs corrected by DBS method, ENS1, and ENS2, respectively. Since the whole time series contain high number of zero values, their means are very low. This situation leads box plots to perceive most of the non-zero values as outliers as can be seen in Figure 5.9. Similar situation if valid for the near, middle, and far future for all the MSs.

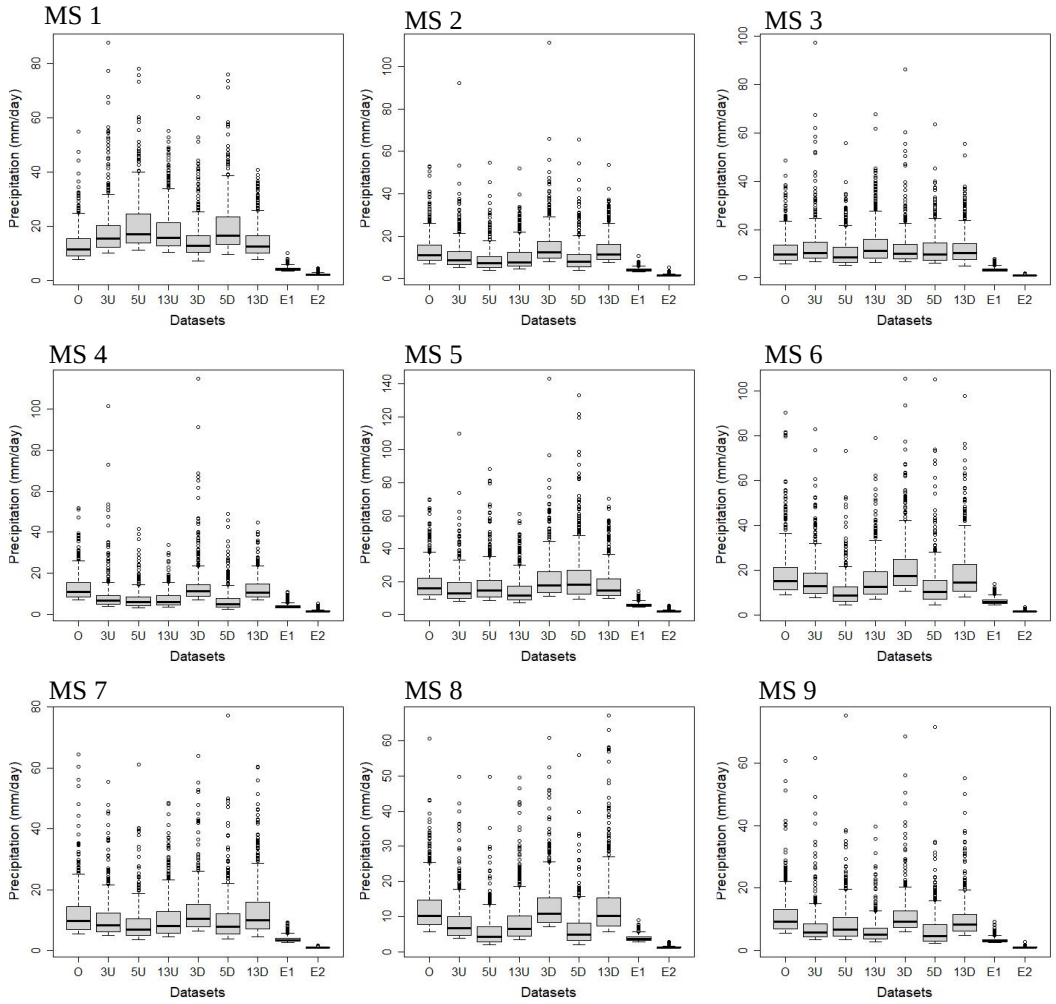

Figure 5.10. Box Plots of Extreme Parts (2011-2040).

Here O, 3U, 5U, 13U, 3D, 5D, 13D, E1, and E2 are observed data, uncorrected RCM 3 outputs, uncorrected RCM 5 outputs, uncorrected RCM 13 outputs, RCM 3 outputs corrected by DBS method, RCM 5 outputs corrected by DBS method, RCM 13 outputs corrected by DBS method, ENS1, and ENS2, respectively.

Basic statistical properties of extreme parts of the aforementioned time series can be seen in Figure 5.10. Slight increases and decreases in the mean values compared to the observed data can be seen for the near future. However, the most striking fact in Figure 5.10 are the results of ensembles. It can be seen that both ensembles have very low mean values and very small ranges compared to the other datasets. For example, the ranges of the extreme parts of RCM 3, RCM 5, and RCM 13 for MS1 for the near future are 8 – 68 mm/day, 10 – 76 mm/day, and 8 – 41 mm/day, respectively. On the other hand, the ranges of ENS1 and ENS2 for MS1 for the near future are 4 – 10 mm/day and 2 – 5 mm/day, respectively. As it can be seen, there is a drastic decrease in the range of ensembles compared to the best three RCMs. This drastic decrease in the ranges of data which is valid for the rest of the MSs as well, leads to almost 100% decrease in the mean extreme precipitation forecasts of the future periods. Thus, it is concluded that ensembles using SME and SE approaches results in poor extreme precipitation forecasts due to incorrect reduction in the range of data. Same problem can be observed in the box plots for middle and far future as well as shown in Figure 5.11 and Figure 5.12, respectively.

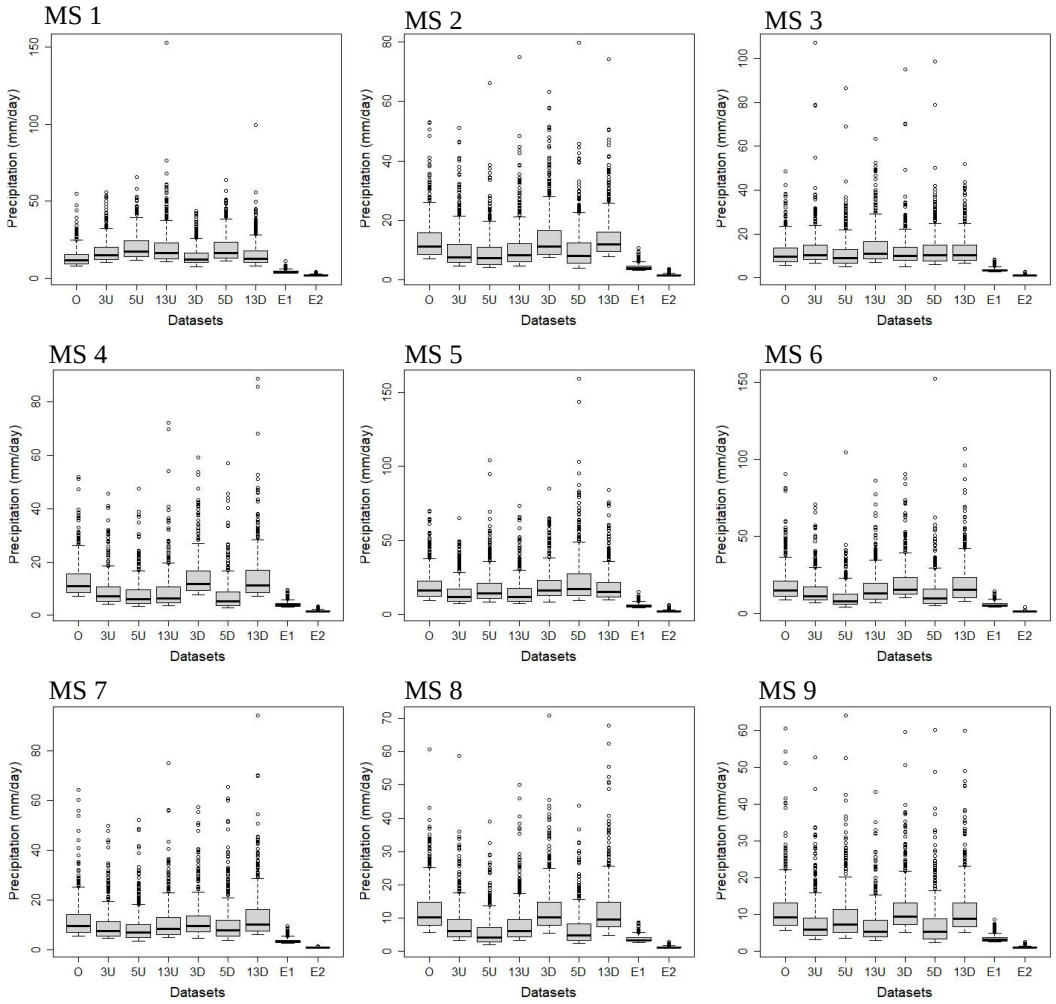

Figure 5.11. Box Plots of Extreme Parts (2041-2070).

Here O, 3U, 5U, 13U, 3D, 5D, 13D, E1, and E2 are observed data, uncorrected RCM 3 outputs, uncorrected RCM 5 outputs, uncorrected RCM 13 outputs, RCM 3 outputs corrected by DBS method, RCM 5 outputs corrected by DBS method, RCM 13 outputs corrected by DBS method, ENS1, and ENS2, respectively.

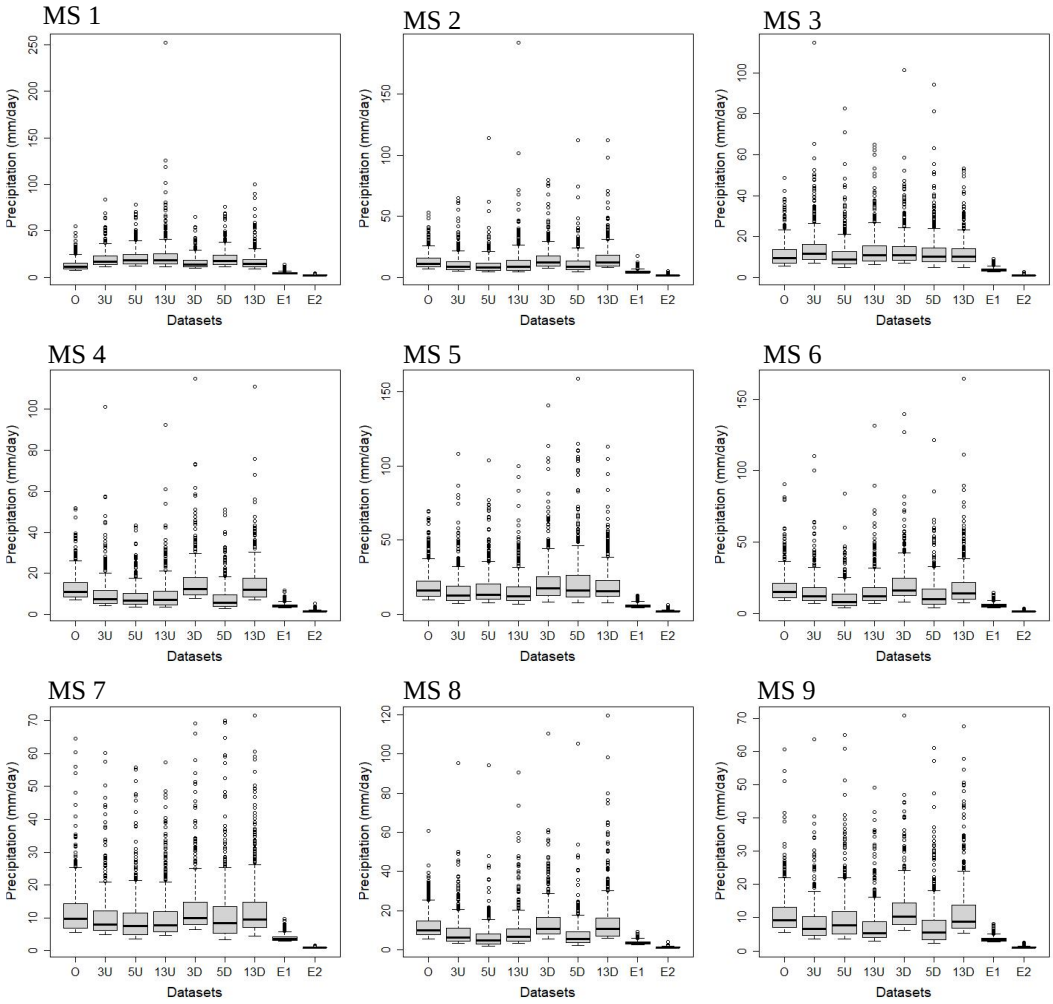

Figure 5.12. Box Plots of Extreme Parts (2071-2100).

Here O, 3U, 5U, 13U, 3D, 5D, 13D, E1, and E2 are observed data, uncorrected RCM 3 outputs, uncorrected RCM 5 outputs, uncorrected RCM 13 outputs, RCM 3 outputs corrected by DBS method, RCM 5 outputs corrected by DBS method, RCM 13 outputs corrected by DBS method, ENS1, and ENS2, respectively.

To discuss the changes in mean extreme precipitation spatially, maps with a color scale of -100% (represented with red) to 100% (represented with green) are given in Figure 5.13 to Figure 5.27 for near, middle, and far future. The summary of the

results is given in Table 5.7. To see the changes between near, middle, and far future, percentage changes for RCM 3, RCM 5, and RCM 13 are given in Table 5.8 as well. Color code used in Table 5.8 shows whether the change compared to the previous period is increasing or decreasing. For example, if the mean extreme precipitation of 2071-2100 period is less than the mean extreme precipitation of 2041-2070 period, then the cell containing the value for 2071-2100 period is red.

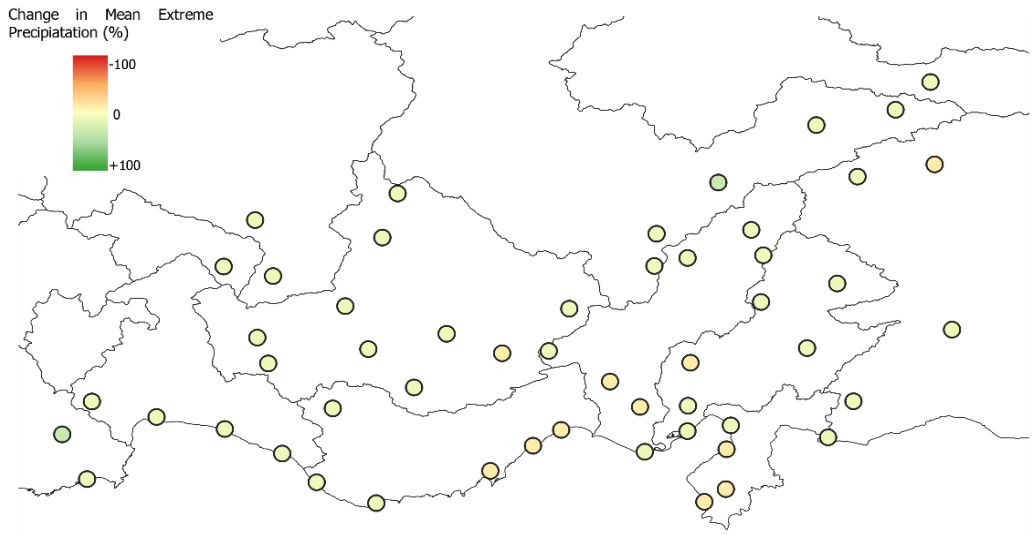

Figure 5.13. Percent Change in Mean Extreme Precipitation for RCM 3 (2011-2040)

There are some slight increases and decreases with RCM 3 in near future as it can be seen in Figure 5.13. It can be said that decreases are mostly cumulated in the middle section of the shoreline. The rest of the MSs show slight increases. As the distance to sea increases, MSs that have increasing trend are more frequent. Decreases in the study area are up to 12% while increases are up to 22%. On the average 5% increase is expected according to RCM 3 in the study area in the near future. In total, 11 MSs will suffer a decrease while 42 MSs will have an increase in the near future in the mean extreme precipitation (i.e., 2011-2040).

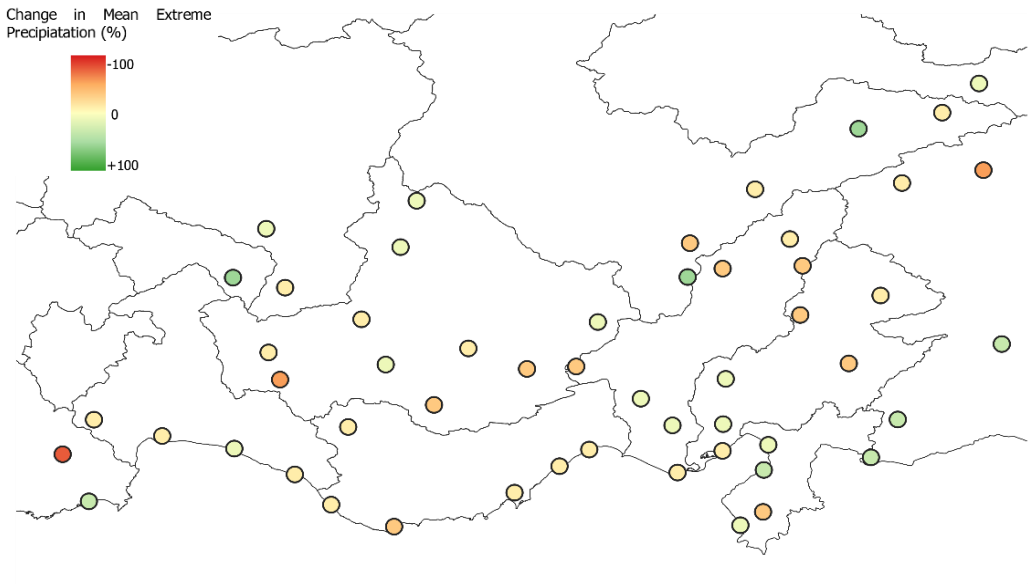

Figure 5.14. Percent Change in Mean Extreme Precipitation for RCM 5 (2011-2040)

As can be seen in Figure 5.14, there is more variety in terms of increase or decrease when RCM 5 outputs are used for near future. It can be said that decreases are mostly encountered on the shoreline. Most of the MSs on the shoreline are expected to experience a decrease in the mean extreme precipitation. Some MSs located in the north-east of the study area are expected to experience a decrease as well. Up to 78% decrease in the mean extreme precipitation is expected to happen in the study area while increases up to 48% are forecasted. On the average 5% decrease is expected according to RCM 5 outputs in the study area in the near future. In total 32 MSs will suffer a decrease while 21 MSs will have an increase in near future in mean extreme precipitation.

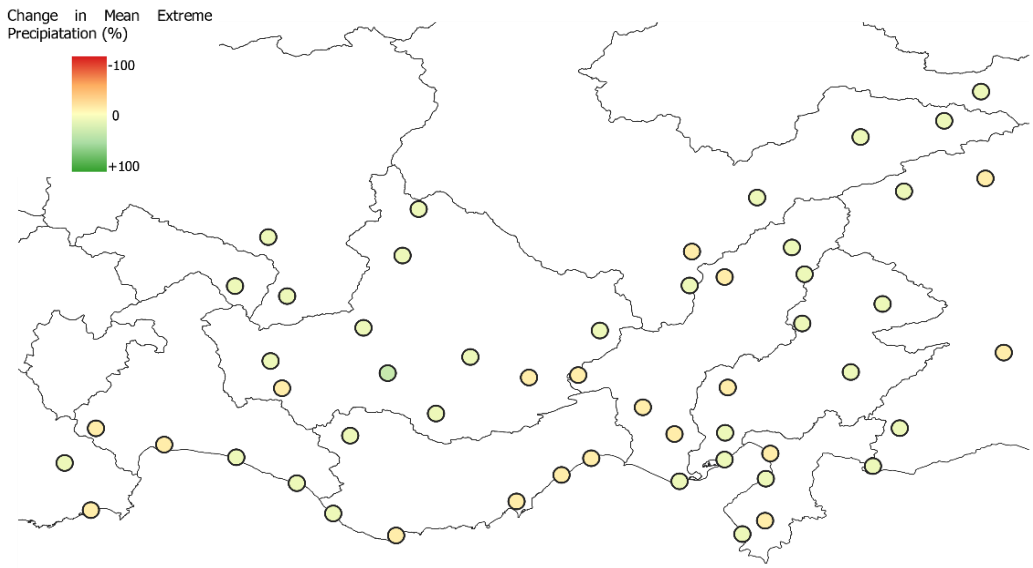

Figure 5.15. Percent Change in Mean Extreme Precipitation for RCM 13 (2011-2040)

The results with RCM 13 are similar to those of RCM 3 for the near future as it can be seen in Figure 5.15. There are some slight increases and decreases within the study area. It can be said that decreases are mostly cumulated in the middle section and the west part of the shoreline. The rest of the MSs show slight increases, mostly. As the distance to sea increases, MSs that have increase are more frequent. Decrease in the mean extreme precipitation in the study area is up to 16% while increase is up to 21%. On the average 3% increase in the mean extreme precipitation is expected according to RCM 13 outputs in the study area in near future. In total 19 MSs are forecasted to experience a decrease while 34 MSs will have an increase in the near future.

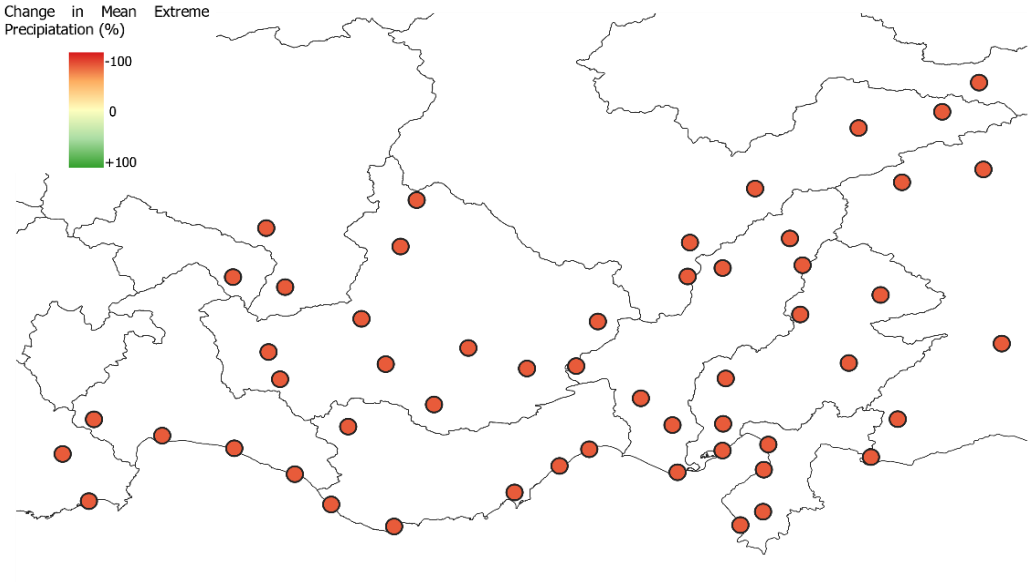

Figure 5.16. Percent Change in Mean Extreme Precipitation for ENS1 (2011-2040)

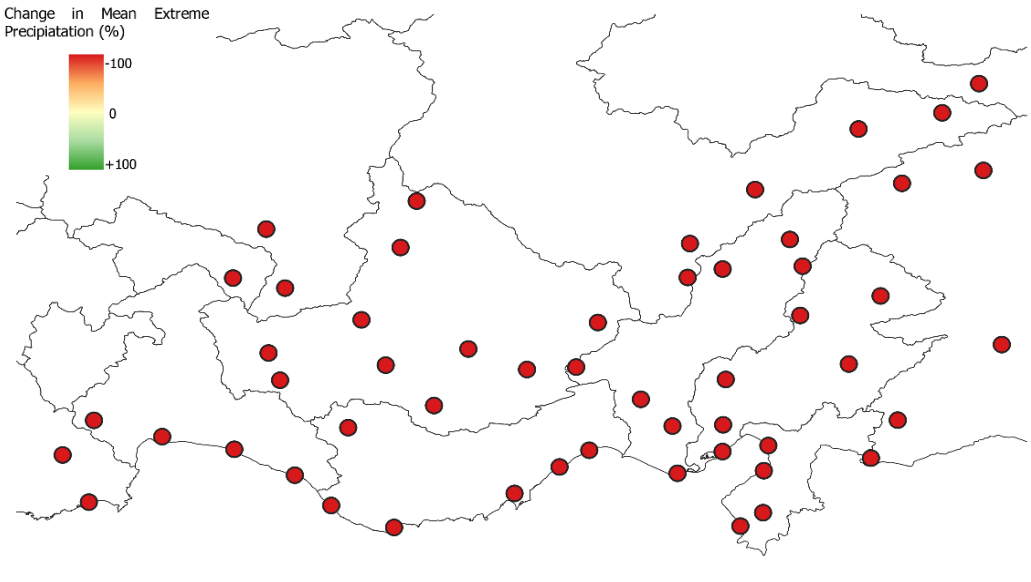

Figure 5.17. Percent Change in Mean Extreme Precipitation for ENS2 (2011-2040)

ENS1 and ENS2 results are given in Figure 5.16 and Figure 5.17, respectively. Both ensembles show significant decreases reaching almost 100%. Decrease in ranges of the data obtained through ensembles (see Figure 5.10) led to underestimation of the extreme parts.

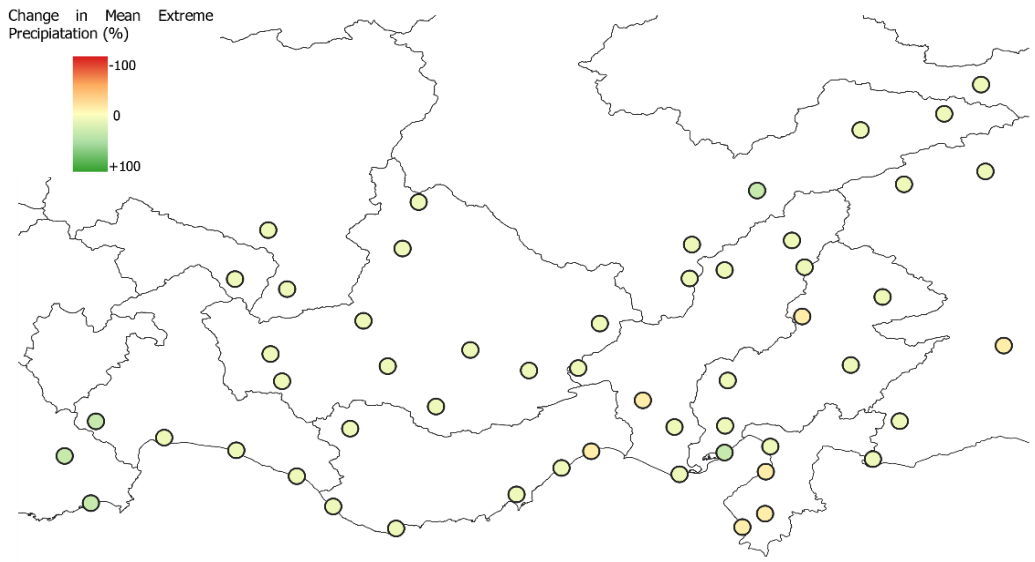

Figure 5.18. Percent Change in Mean Extreme Precipitation for RCM 3 (2041-2070)

There are some slight increases and decreases with RCM 3 for the middle future as it can be seen in Figure 5.18. It can be said that decreases are mostly cumulated in the middle section of the shoreline. The rest of the MSs show slight increases. As the distance to sea increases, MSs that have increasing trends get more frequent. Decreases in the study area are up to 12% while increases are up to 22%. On the average 6% increase is expected according to RCM 3 in the study area for the middle future. In total, 7 MSs are forecasted to experience a decrease while 46 MSs will have an increase in the middle future (i.e., 2041-2070) compared to the historic period.

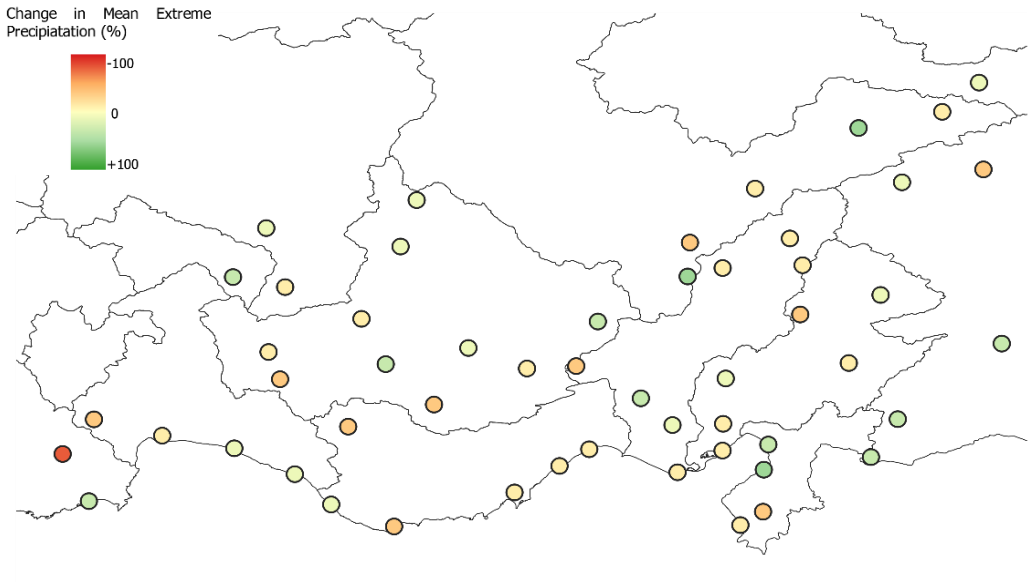

Figure 5.19. Percent Change in Mean Extreme Precipitation for RCM 5 (2041-2070)

As can be seen in Figure 5.19, the increases and decreases are more pronounced for RCM 5 for the middle future. It can be said that decreases are mostly encountered on the shoreline. Most of the MSs on the shoreline are expected to experience a decrease. Some decreases are also present in the north-east of the study area. Decreases in the study area are up to 80% while increases are up to 55%. On the average, 1% decrease is expected according to RCM 5 in the study area for middle future. In total, 29 MSs are forecasted to experience a decrease while 24 MSs are expected to have an increase in the middle future.

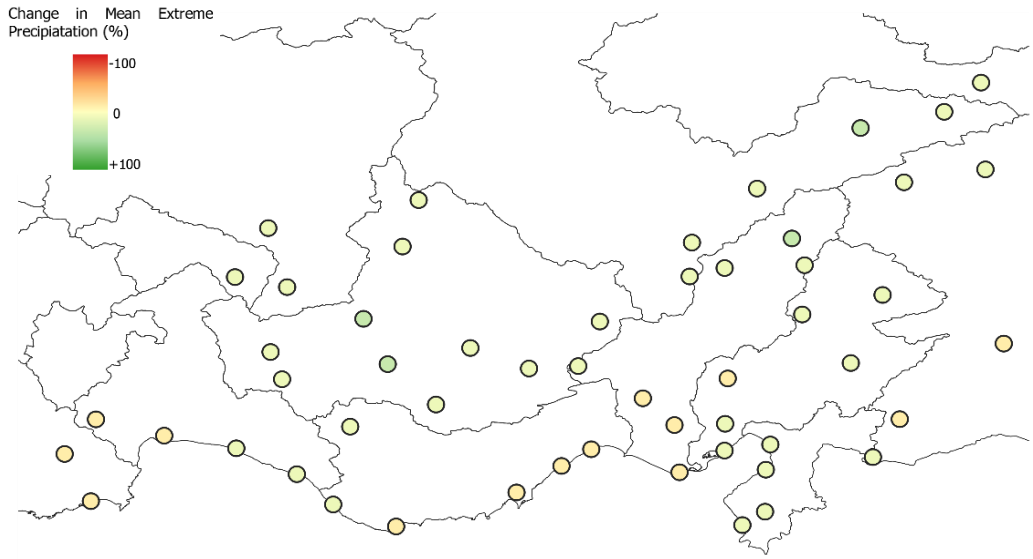

Figure 5.20. Percent Change in Mean Extreme Precipitation for RCM 13 (2041-2070)

The results with RCM 13 mostly show slight increases and decreases for the middle future as can be seen in Figure 5.20. It can be said that decreases are mostly cumulated in the middle section and west part of the shoreline. The rest of the MSs generally show slight increases. Decreases in the study area are up to 13% while increases are up to 24%. On the average 7% increase in the mean extreme precipitation is expected according to RCM 13 in the study area for the middle future. In total 14 MSs are expected to have ta decrease while 39 MSs will have an increase for the middle future.

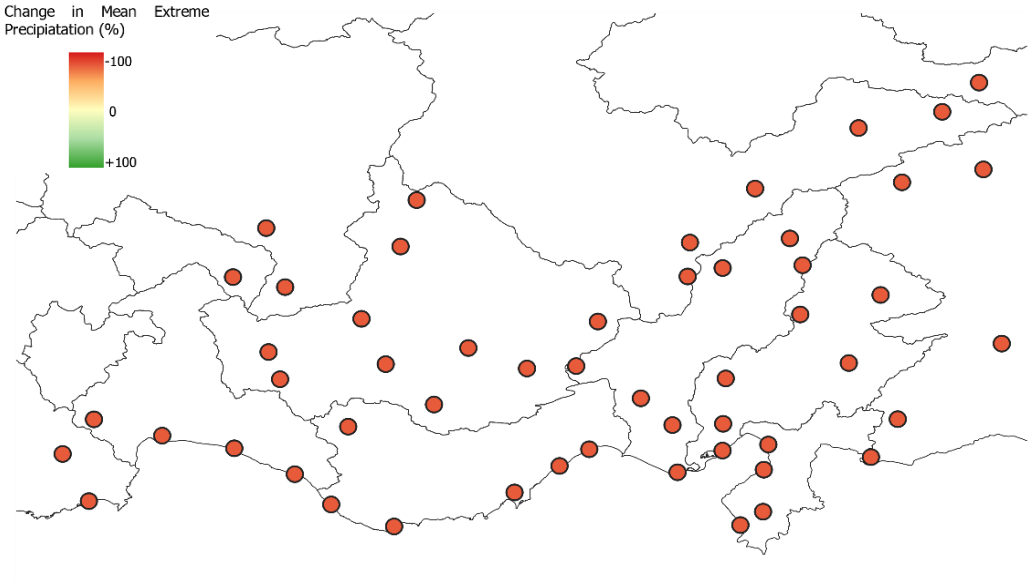

Figure 5.21. Percent Change in Mean Extreme Precipitation for ENS1 (2041-2070)

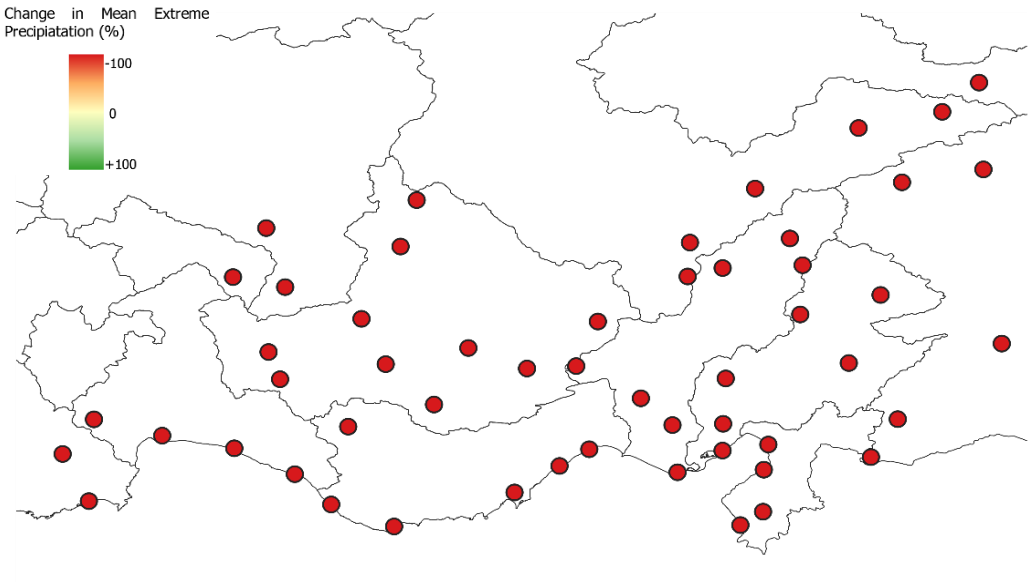

Figure 5.22. Percent Change in Mean Extreme Precipitation for ENS2 (2041-2070)

Problem with ensembles is also present for the middle future as it can be seen in Figure 5.21 and Figure 5.22. Both ensembles show almost 100% decrease in the whole study area.

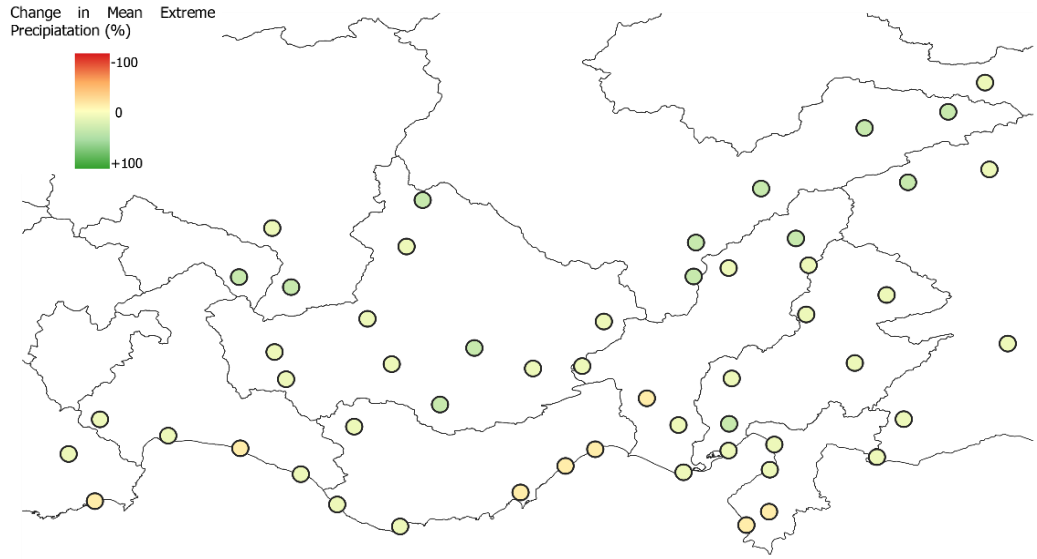

Figure 5.23. Percent Change in Mean Extreme Precipitation for RCM 3 (2071-2100)

There are some slight increases and decreases predicted with RCM 3 for the far future as can be seen in Figure 5.23. While up to 8% decrease is predicted, the increase is expected to reach 33%. On the average 14% increase is expected according to RCM 3 in the study are for the far future. In total 8 MSs are forecasted to experience a decrease while 45 MSs will have an increase for the far future (i.e., 2071-2100) compared to the historic period.

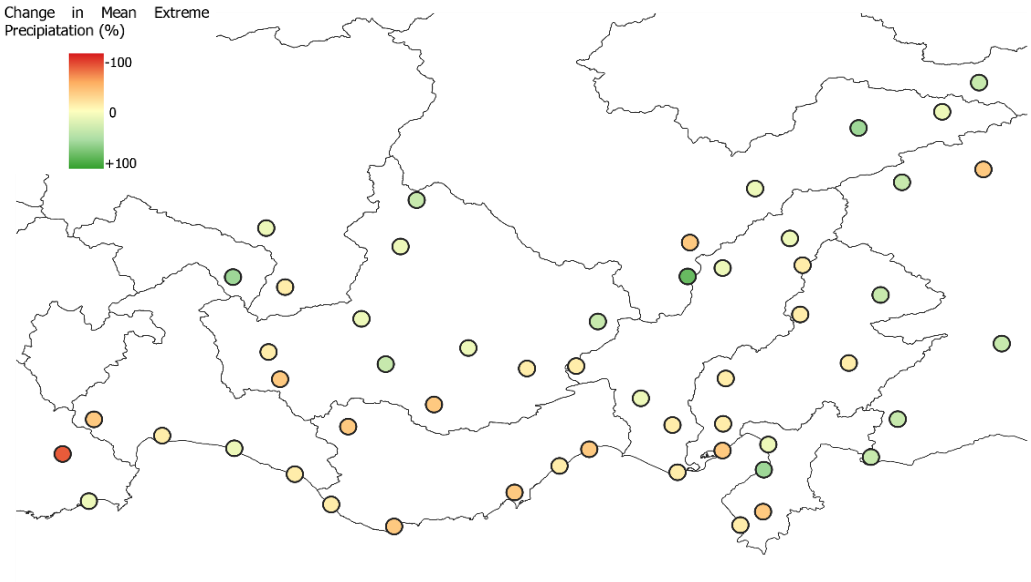

Figure 5.24. Percent Change in Mean Extreme Precipitation for RCM 5 (2071-2100)

As can be seen in Figure 5.24, considerable increases and decreases are predicted with RCM 5 for the far future. It can be said that decreases are mostly encountered on the shoreline and near the shoreline. Most of the MSs on the shoreline are expected to experience a decrease. MSs that are far from the shoreline show increasing trends most of the time. Decreases in the study area are up to 78% while increases are up to 80%. On average 1% increase is expected according to RCM 5 in the study area in the far future. In total 28 MSs forecasted to experience ta decrease while 25 MSs will have an increase in the far future.

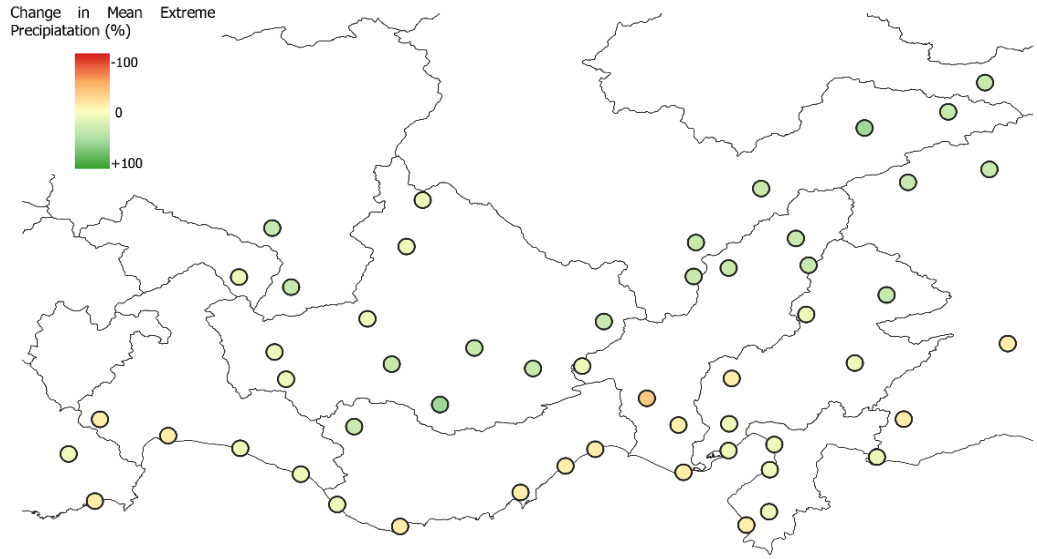

Figure 5.25. Percent Change in Mean Extreme Precipitation for RCM 13 (2071-2100)

The results with RCM 13 shows mostly slight increases and decreases for the future (see Figure 5.25). Decreases in the study area are up to 21% while increases are up to 41%. On the average 13% increase is expected according to RCM 13 in the study area for the far future. In total 14 MSs are forecasted to experience a decrease while 39 MSs will have an increase in far future.

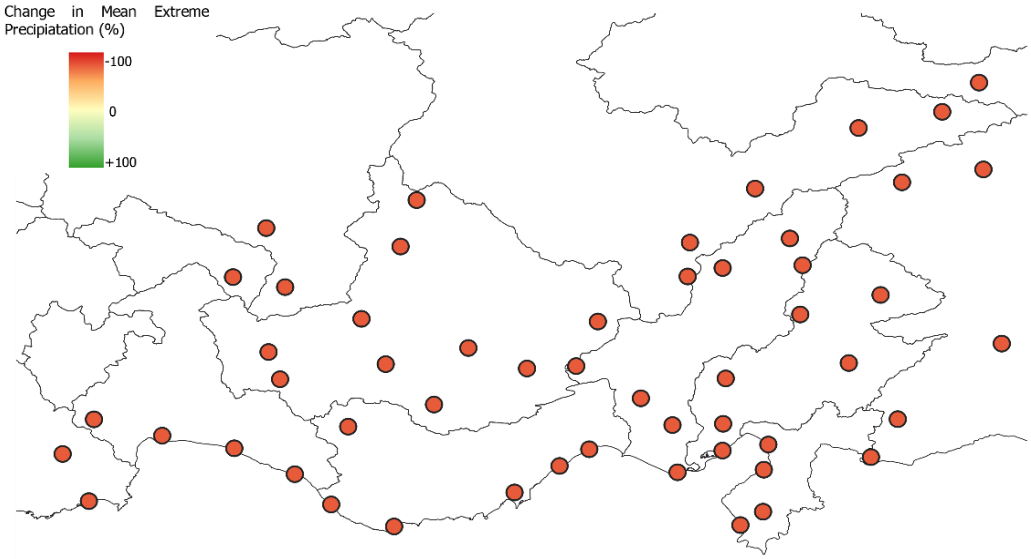

Figure 5.26. Percent Change in Mean Extreme Precipitation for ENS1 (2071-2100)

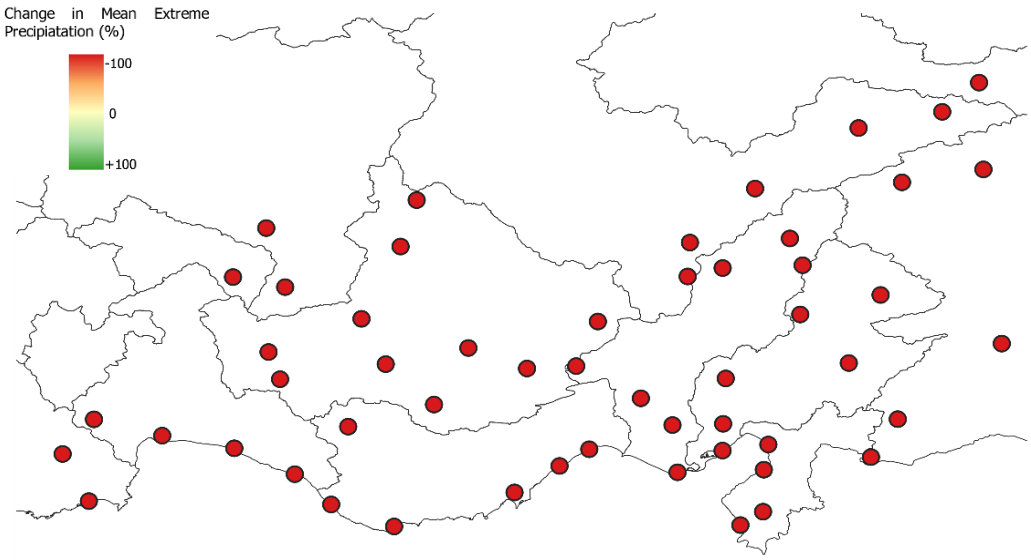

Figure 5.27. Percent Change in Mean Extreme Precipitation for ENS2 (2071-2100)

Problem with ensembles is also present for the far future as can be seen in Figure 5.26 and Figure 5.27. Both ensembles show almost 100% decrease in the whole study area.

Changes according to maps shown in Figure 5.13 to Figure 5.27 are summarized in Table 5.7 where Min. shows the biggest decrease, max. shows the biggest increase, avg. shows the average change in the whole study area, # of dec. shows the number of MSs that experiences a decrease, and # of inc. shows the number of MSs that have an increase. It can be said that RCM 3 and RCM 13 give similar results. They tend to have smaller changes compared to RCM 5 for all three periods. Ensembles show almost constant drastic decreases for all MSs for all three periods. Since there is no increase with ensemble results, max. values are given as NA. The average change in the mean extreme precipitation for the whole study area tend to increase with time for all three RCMs. The number of MSs that are forecasted to experience a decrease in the mean extreme precipitation tend to decrease with time for all three RCMs. Thus, it can be concluded that the mean extreme precipitation in the study area is expected to increase.

Table 5.7. Basic Statistics of Changes in Projection Period

		2011-2040	2041-2070	2071-2100
RCM3	min.	-12	-12	-8
	max.	17	22	33
	avg.	3	6	14
	# of dec.	17	7	8
	# of inc.	36	46	45
RCM5	min.	-78	-80	-78
	max.	48	55	80
	avg.	-5	0	1
	# of dec.	32	29	28
	# of inc.	21	24	25
RCM13	min.	-16	-13	-21
	max.	21	24	41
	avg.	4	7	13
	# of dec.	19	14	14
	# of inc.	34	39	39
ENS1	min.	-79	-78	-79
	max.	NA	NA	NA
	avg.	-76	-76	-75
	# of dec.	53	53	53
	# of inc.	0	0	0
ENS2	min.	-95	-95	-95
	max.	NA	NA	NA
	avg.	-91	-91	-90
	# of dec.	53	53	53
	# of inc.	0	0	0

Min. represents the biggest decrease, max. represents the biggest increase, avg. represents the average change in study area, # of dec. represents the number of MSs that suffer a decrease, and # of inc. represents the number of MSs that have an increase.

To compare the changes in the mean values of extreme precipitation series and whole series with near, middle, and far future for each MS, Table 5.8 and Table 5.9 are constructed. In these tables, N is the near future (i.e., 2011-2040), M is the middle future (i.e., 2041-2070), and F is the far future (i.e., 2071-2100). Green cells show an increase, while red cells show a decrease compared to the previous period. In Table 5.8, RCM 3 shows that slight increases are expected for most of the MSs for the near future (i.e., 2011-2040 period). For the middle future (i.e., 2041-2070 period), half of the MSs will have smaller mean extreme precipitations compared to the near future. For the far future (i.e., 2071-2100 period), only 9 MSs will have smaller mean extreme precipitations compared to the middle future. RCM 5 shows that most of the MSs will experience decreases in the mean extreme precipitations. Fifteen MSs will have decreases in the middle future compared to the near future. RCM 13 shows that the most of MSs will have increases. RCM 3 and RCM 13 tend to have similar results for the projection period while RCM 5 tends to stand against them. RCM 5 shows a decrease, when RCM 3 and RCM 13 show an increase, most of the time. RCM 5 also shows more drastic changes compared to RCM 3 and RCM 13 when maximum increase and decrease for each RCM are considered. However, at the end of the projection periods all three RCMs agree on the fact that most of the MSs will experience increased mean extreme precipitation. As it can be seen in Table 5.8, there are some oscillations in trends for some MSs (i.e., increase followed by decrease followed by increase or vise versa). When the locations of these MSs are checked, it is seen that these MSs are on the shoreline or near to the shoreline, most of the time. The reason for these oscillations may be the effect of urbanization. Shoreline and its vicinity are commonly experience high degree of urbanization which may result in the MSs in this zone to stay very close to the buildings. This may cause incorrect readings at these stations.

Table 5.8. Percent Changes in Mean Extreme Precipitation for the Projection Period

	RCM 3			RCM 5			RCM 13			ENS1			ENS2		
M	**N**	**M**	**F**	**N**	**M**	**F**	**N**	**M**	**F**	**N**	**M**	**F**	**N**	**M**	**F**
1	14	-9	18	48	-2	7	5	16	17	-76	3	8	-87	-4	5
2	21	1	6	-12	6	10	5	8	20	-76	3	11	-91	1	4
3	11	-7	14	6	7	5	8	1	1	-77	-1	9	-94	2	1
4	16	-4	11	-33	9	7	-6	27	5	-76	1	6	-91	-1	7
5	19	-7	14	43	-2	12	2	1	10	-77	0	-1	-91	-1	3
6	17	-5	7	-20	9	5	8	11	-4	-76	-3	4	-95	2	2
7	3	-3	8	-10	7	13	19	3	-5	-78	0	8	-95	1	3
8	4	2	18	-37	3	20	20	-8	27	-77	-2	6	-93	1	10
9	-2	7	7	-24	11	13	-8	16	19	-78	2	2	-94	3	4
10	12	-8	15	3	20	5	7	9	8	-77	-2	11	-93	1	4
11	1	1	10	-23	5	14	2	-1	2	-73	-7	2	-87	0	9
12	1	1	5	21	2	4	4	-7	0	-73	-8	1	-88	1	4
13	0	2	6	28	-1	1	15	-11	2	-74	-9	-1	-89	1	6
14	2	-7	8	36	3	-12	-4	-6	-1	-73	-9	1	-88	-3	0
15	9	8	-5	-1	-8	-10	-8	7	-7	-77	-3	-3	-90	5	-1
16	4	0	2	-2	14	-18	14	-2	4	-75	1	5	-87	-1	4
17	4	0	2	-22	-1	-13	-5	3	-5	-73	-9	1	-88	0	3
18	-2	5	-4	-8	-1	-14	-9	-3	6	-76	-9	2	-91	2	1
19	-3	-2	2	-17	16	-22	-2	0	-12	-75	-2	1	-93	1	-2
20	-5	15	8	7	-6	-12	0	0	0	-77	-1	4	-93	5	2
21	-11	4	8	29	13	-4	5	-4	0	-75	-5	-2	-91	5	1
22	-10	-2	4	-20	-4	-1	-3	12	-5	-73	-10	0	-90	-2	2
23	7	13	-20	34	-5	-15	-5	-8	0	-75	-7	-6	-89	4	-11
24	9	-2	8	1	7	18	2	5	26	-76	0	15	-91	1	6
25	11	-4	17	-8	5	21	7	6	22	-75	-1	15	-89	-2	12
26	-6	13	12	-51	24	23	-4	13	13	-77	7	9	-91	8	7
27	16	-5	14	14	3	3	9	0	1	-76	0	7	-92	-1	4
28	5	5	20	-10	14	18	3	15	18	-76	4	14	-90	6	11
29	15	-1	4	3	10	4	12	0	11	-77	2	3	-94	1	1
30	5	2	22	-17	11	21	4	17	11	-76	5	10	-92	1	11
31	13	0	10	-17	7	6	13	-2	9	-77	2	1	-95	1	2
32	14	-6	14	43	9	16	2	10	9	-76	0	11	-88	2	11
33	8	-6	15	-27	13	22	0	8	12	-77	6	12	-92	-2	10
34	3	-3	15	-27	15	16	5	13	13	-75	3	8	-91	-1	9
35	1	-4	21	-33	10	15	0	6	10	-74	-2	4	-90	1	10
36	2	0	14	-13	16	20	13	-1	9	-75	0	3	-90	9	13
37	6	-1	0	-42	7	6	-1	8	6	-75	-7	1	-91	1	0
38	3	-1	2	15	10	1	21	2	2	-78	3	-1	-91	5	-1
39	3	3	15	-13	20	5	13	5	17	-79	12	3	-92	3	8
40	6	6	3	-34	7	14	-16	32	3	-77	-2	9	-93	3	5

Table 5.8. (continued)

41	-2	3	16	20	-13	-7	-1	-4	-3	-76	-4	9	-91	1	9
42	12	10	-7	-9	-15	4	-2	2	-2	-78	1	-7	-94	5	-3
43	1	5	-1	-20	-4	3	12	-1	10	-76	-3	3	-92	1	3
44	-2	-7	4	13	8	-16	-1	-9	-12	-76	-4	-1	-92	1	-4
45	22	0	-2	-78	-11	11	2	-6	9	-74	-7	-4	-89	-1	0
46	5	-3	-3	10	3	-12	6	4	6	-75	-3	-1	-87	-2	-1
47	-3	5	-3	-11	11	-13	-3	3	-12	-76	-2	-1	-92	2	-1
48	0	10	13	2	-4	-12	12	-4	2	-77	2	2	-92	3	4
49	2	2	2	19	5	-13	-3	11	3	-74	-2	-8	-91	1	-2
50	6	-4	16	0	8	-15	7	-2	5	-73	-4	4	-89	-1	7
51	7	13	-1	-14	1	-12	7	-6	6	-75	-2	3	-92	4	-1
52	0	10	2	-4	2	-10	8	-9	-7	-75	0	0	-91	5	0
53	-12	4	5	2	-6	-3	5	-3	-6	-74	-10	-4	-91	0	0

M is MS number. N is near future (i.e., 2011-2040), M is middle future (i.e., 2041-2070), and F is far future (i.e., 2071-2100). Green cells show an increase, while red cells show a decrease comparing to previous period.

Percent changes in the mean precipitations for the projection period are given in Table 5.9 where RCM 3 shows oscillating trends in mean precipitations for the projection periods starting with an increase in the near future for most of the MSs. RCM 5 shows a decrease in the near future for almost all MSs, then increases and decreases are shown almost evenly for the study area. RCM 13 shows a steady decrease for the whole projection period for half of the MSs, while the other half tends to have oscillating trends. Both ensembles show increase in the near future for all MSs and decreases for the rest of the projection periods for most of the MSs.

Table 5.9. Percent Changes in the Mean Precipitation for the Projection Period

	RCM 3			RCM 5			RCM 13			ENS1			ENS2		
M	**N**	**M**	**F**	**N**	**M**	**F**	**N**	**M**	**F**	**N**	**M**	**F**	**N**	**M**	**F**
1	10	0	12	33	0	0	10	3	8	3	-4	-1	10	0	0
2	13	-6	3	-38	4	5	3	3	1	1	-4	-4	2	0	0
3	6	-3	9	0	0	-3	3	1	-3	6	-6	-3	3	0	0
4	6	-2	8	-55	6	6	-3	6	-1	2	-1	-3	5	0	0
5	14	-9	4	10	-1	-5	-4	2	-2	9	-6	-6	7	0	0
6	16	-6	-1	-36	0	-1	-2	4	-7	7	-8	-6	1	0	0
7	8	-8	8	-23	2	4	4	6	-8	6	-6	-3	2	0	0
8	8	-7	10	-54	2	10	1	-3	9	11	-9	-6	7	0	0
9	0	1	8	-47	9	3	-11	8	5	3	-2	-4	4	0	0
10	6	-8	7	-14	12	-2	-3	6	-3	4	-4	-5	3	0	0
11	-1	-12	5	-44	1	-1	-7	-11	-2	10	-8	-10	12	-1	0
12	1	-10	7	9	-6	-9	-4	-6	-2	13	-10	-10	13	-1	0
13	3	-10	12	2	-3	-10	-1	-6	-6	14	-9	-10	15	-1	0
14	-3	-12	11	-3	-2	-17	-9	-9	0	13	-9	-10	12	-1	0
15	13	-7	-9	-31	-9	-26	-6	-6	-15	13	-7	-15	10	0	-1
16	11	-14	2	5	0	-21	-1	-2	-13	11	-5	-11	18	-1	-1
17	6	-14	2	-23	-5	-21	-11	0	-21	14	-10	-15	12	-1	0
18	-2	-11	-6	-36	-3	-23	-13	-4	-15	14	-11	-13	11	-1	-1
19	-4	-10	3	-31	3	-24	-9	-4	-18	15	-8	-13	9	0	0
20	-1	0	7	-18	-7	-21	-1	-6	-9	12	-6	-10	10	0	0
21	-5	-8	11	11	3	-11	-3	-6	-6	11	-8	-9	10	0	0
22	-7	-12	4	-49	-7	-16	-8	-2	-8	13	-9	-12	9	-1	0
23	10	-6	-18	27	-12	-25	-6	-11	-16	11	-12	-19	9	-1	-2
24	3	-1	9	-28	10	17	7	-5	15	0	-2	2	6	0	1
25	4	-4	7	-41	9	7	5	-5	7	4	-3	-3	7	0	0
26	-5	1	11	-65	19	19	1	-1	8	4	-3	-4	5	0	1
27	8	-5	9	1	-1	-3	6	-4	-3	8	-4	-5	7	0	0
28	4	5	13	-29	9	6	7	6	7	3	-2	-2	8	0	1
29	9	2	1	-20	4	-6	5	-1	2	6	-5	-5	2	0	0
30	4	3	10	-30	4	10	3	6	5	5	-2	-3	7	0	0
31	10	-5	9	-39	3	-3	1	2	-3	8	-6	-5	2	0	0
32	8	-8	9	7	6	6	1	1	-2	3	-5	-5	8	0	1
33	4	0	8	-52	11	11	-2	4	-2	5	-3	-4	5	0	0
34	1	-5	8	-38	3	2	-3	4	3	6	-5	-6	5	0	0
35	-1	-11	12	-37	0	1	-4	-2	-4	12	-9	-9	11	0	0
36	1	-2	17	-37	10	11	7	-4	10	8	-6	-5	7	0	1
37	11	-8	-5	-62	3	1	-6	2	-7	10	-9	-11	8	0	0
38	10	-5	2	-3	2	-3	4	7	-3	8	-6	-5	9	0	0
39	5	-5	7	-23	12	-4	1	6	4	5	-3	-4	7	0	0
40	0	5	4	-42	8	1	-9	5	0	6	-2	-6	4	0	0
41	-1	-7	9	-30	-6	-17	-9	-7	-10	9	-7	-9	8	0	0
42	14	-3	-12	-43	-16	-9	1	-4	-4	7	-10	-13	0	0	0

Table 5.9. (continued)

43	9	0	0	-46	-4	0	-4	5	2	10	-7	-9	8	0	0
44	0	-10	3	-15	2	-26	-7	-10	-15	16	-8	-12	10	0	0
45	17	-13	-7	-88	0	7	-3	-10	-6	12	-10	-15	9	-1	0
46	13	-17	-1	-5	-6	-18	-4	-3	-11	8	-5	-12	11	-1	0
47	-3	-7	1	-25	3	-24	-11	-1	-17	15	-8	-13	11	0	0
48	3	-1	9	-29	-6	-18	1	-7	-8	7	-5	-9	5	0	0
49	3	-9	8	-20	-3	-12	-7	-3	-3	6	-5	-9	5	0	0
50	10	-13	6	-6	1	-20	-3	-1	-13	10	-6	-12	13	-1	0
51	4	1	5	-21	0	-18	-1	-6	-5	8	-4	-10	8	0	0
52	1	1	7	-21	-2	-21	0	-6	-13	10	-6	-12	10	0	0
53	-5	-4	4	-17	-6	-20	-3	-8	-11	9	-7	-13	8	0	0

M is MS number. N is near future (i.e., 2011-2040), M is middle future (i.e., 2041-2070), and F is far future (i.e., 2071-2100). Green cells show an increase, while red cells show a decrease comparing to previous period.

CHAPTER 6

CONCLUSIONS

Bias correction of daily precipitation time series with five different bias correction methods for 53 locations in the southern and south-eastern regions of Turkey is conducted in this study. Daily precipitation time series of the observations and 17 RCM outputs are identified as stationary in the study area. Expected changes in the mean extreme precipitation for the near, middle, and futures are calculated using bias-corrected RCMs and their ensembles. The following conclusions are reached:

- All bias correction methods used in this study improved the performance parameters (i.e, PBIAS, RMSE, and MAE) compared to those of the uncorrected model outputs. Thus, bias-corrected model outputs should be used in climate change analysis.
- Three variations of the DBS method, namely DBS_99, DBS_99_GP, and DBS_99_LOGN are developed in this study. These variations did not improve the overal performance compared to the original method. Use of GP distribution is found to be not suitable for the mapping procedure, especially when data is limited .
- The LS method, which is the simplest bias correction method, performs very well in correcting biases. However, it results in over and underestimation of extreme values which is stated in the literature as well. So use of the LS method is not suggested if future forecasts are going to be used for the analysis of extreme events such as floods or droughts.
- The performance of LOGN distribution in the representation of extreme daily precipitation is very similar to that of the gamma distribution. AIC values of both distributions are very similar, LOGN distribution has even smaller AIC values for the MSs in the study area. Moreover, performance parameters calculated for bias corrected model outputs with DBS_99 and

DBS_99_LOGN are very similar to each other. Thus LOGN distribution is a good canditate for quantile based bias correction methods.

- Changing the partition point from 95th to 99th quantile did not improve the performance of the DBS method. All three methods developed in this study use 99th quantile while original method uses 95th quantile and all three methods are outperformed by the original method. Thus, the original DBS method is identified as the most suitable bias correction approach compared to those suggested in this study.
- An increase in the mean extreme precipitation is expected for most of the study area for the projection period (i.e., 2011-2100).
- MSs which are generally located at the shoreline showed oscillating trends (i.e., increase followed by decrease followed by increase or vise versa) in the mean extreme precipitation. Thus, a continous increase or decrease is not expected in the mean extreme precipitation for the whole projection period for these MSs. This result suggests that for extreme events such as floods, rather than regional, local mitigation strategies may be more beneficial and effective along the shoreline.
- Ensembling using mean or MLR results in accumulating all the data around mean values, thus is not suitable when the goal is to study extreme events.

For future work:

- Newly proposed bias-correction methods with fixed partition points did not imporve the bias-correction performance of the original DBS method. As future work, identifying dynamic partition points for each location may be studied.
- In the literature it is seen that separating data into two parts improved the performance comparing to no separating. Effects of separating data into more than two parts may be studied as well.

REFERENCES

Arfken, G. (1985). *Mathematical Methods for Physicists, 3rd ed.* Academic Press.

Ayugi, B., Tan, G., Ruoyun, N., Babaousmail, H., Ojara, M., Wido, H., Mumo, L., Ngoma, N. H., Nooni, I. K., & Ongoma, V. (2020). Quantile mapping bias correction on rossby centre regional climate models for precipitation analysis over Kenya, East Africa. *Water (Switzerland)*, *12*(3). https://doi.org/10.3390/w12030801

Barkış, N. B. (2022). *Investigating the effects of climate change on the surface runoff potential over Kızılırmak basin* [Middle East Technical University]. https://hdl.handle.net/11511/99563

Beck, H. E., Zimmermann, N. E., McVicar, T. R., Vergopolan, N., Berg, A., & Wood, E. F. (2018). Present and future köppen-geiger climate classification maps at 1-km resolution. *Scientific Data*, *5*, 1–12. https://doi.org/10.1038/sdata.2018.214

Benestad, R., Buonomo, E., Gutiérrez, J. M., Haensler, A., Hennemuth, B., Illy, T., Jacob, D., Keup-Thiel, E., Katragkou, E., Kotlarski, S., Nikulin, G., Otto, J., Rechid, D., Remke, T., Sieck, K., Sobolowski, S., Szabó, P., Szépszó, G., Teichmann, C., … Zsebeházi, G. (2017). *Guidance for EURO-CORDEX climate projections data use*. 1–27. https://www.euro-cordex.net/imperia/md/content/csc/cordex/euro-cordex-guidelines-version1.0-2017.08.pdf

Block, P. J., Souza Filho, F. A., Sun, L., & Kwon, H. H. (2009). A streamflow forecasting framework using multiple climate and hydrological models. *Journal of the American Water Resources Association*, *45*(4), 828–843. https://doi.org/10.1111/j.1752-1688.2009.00327.x

Boe, J., Terray, L., Habets, F., & Martin, E. (2007). Statistical and dynamical

downscaling of the Seine basin climate for hydro-meteorological studies. *International Journal of Climatology*, *2029*(August 2007), 1643–1655. https://doi.org/10.1002/joc

Bosshard, T., Kotlarski, S., Ewen, T., & Schär, C. (2011). Spectral representation of the annual cycle in the climate change signal. *Hydrology and Earth System Sciences*, *15*(9), 2777–2788. https://doi.org/10.5194/hess-15-2777-2011

Butler, A., Heffernan, J. E., Tawn, J. A., & Flather, R. A. (2007). Trend estimation in extremes of synthetic North Sea surges. *Journal of the Royal Statistical Society. Series C: Applied Statistics*, *56*(4), 395–414. https://doi.org/10.1111/j.1467-9876.2007.00583.x

Butler, A., Heffernan, J. E., Tawn, J. A., Flather, R. A., & Horsburgh, K. J. (2007). Extreme value analysis of decadal variations in storm surge elevations. *Journal of Marine Systems*, *67*(1–2), 189–200. https://doi.org/10.1016/j.jmarsys.2006.10.006

Çaktu, Y. (2022). *Identifying impacts of climate change on water resources using CMIP6 simulations: Havran basin case* [Middle East Technical University]. https://hdl.handle.net/11511/99583

Cane, D., & Milelli, M. (2010). Multimodel SuperEnsemble technique for quantitative precipitation forecasts in Piemonte region. *Natural Hazards and Earth System Sciences*, *10*(2), 265–273. https://doi.org/10.5194/nhess-10-265-2010

Casanueva, A., Kotlarski, S., Herrera, S., Fernández, J., Gutiérrez, J. M., Boberg, F., Colette, A., Christensen, O. B., Goergen, K., Jacob, D., Keuler, K., Nikulin, G., Teichmann, C., & Vautard, R. (2016). Daily precipitation statistics in a EURO-CORDEX RCM ensemble: added value of raw and bias-corrected high-resolution simulations. *Climate Dynamics*, *47*(3–4), 719–737. https://doi.org/10.1007/s00382-015-2865-x

Chen, J., Brissette, F. P., & Leconte, R. (2011). Uncertainty of downscaling

method in quantifying the impact of climate change on hydrology. *Journal of Hydrology*, *401*(3–4), 190–202. https://doi.org/10.1016/j.jhydrol.2011.02.020

Chen, J., Brissette, F. P., Poulin, A., & Leconte, R. (2011). Overall uncertainty study of the hydrological impacts of climate change for a Canadian watershed. *Water Resources Research*, *47*(12), 1–16. https://doi.org/10.1029/2011WR010602

Christensen, J. H., Boberg, F., Christensen, O. B., & Lucas-Picher, P. (2008). On the need for bias correction of regional climate change projections of temperature and precipitation. *Geophysical Research Letters*, *35*(20). https://doi.org/10.1029/2008GL035694

Coles. (2001). *An Introduction to Statistical Modelling of Extreme Values*. Springer.

Davison. (2005). *Extreme Values, Encyclopedia of Biostatistics*. Wiley.

Dickey, D. A. (2014). *Testing for unit roots in autoregressive-moving average models of unknown order*. *71*(3), 599–607.

Enayati, M., Bozorg-Haddad, O., Bazrafshan, J., Hejabi, S., & Chu, X. (2021). Bias correction capabilities of quantile mapping methods for rainfall and temperature variables. *Journal of Water and Climate Change*, *12*(2), 401–419. https://doi.org/10.2166/wcc.2020.261

Engin, B. E. (2015). *Uncertainty assessment in projection of the extreme river flows, the case of Ömerli catchment, İstanbul* [Middle East Technical University]. http://etd.lib.metu.edu.tr/upload/12618526/index.pdf

Ersoy, N. E. (2022). *IMPACT OF CLIMATE CHANGE OVER THE VARIABILITY OF DROUGHT CHARACTERISTICS OVER 25 BASINS OF TURKEY* [Middle East Technical University]. https://hdl.handle.net/11511/96769

Feigenwinter, I., Kotlarski, S., Casanueva, A., Fischer, A., Schwierz, C., & Liniger, M. A. (2018). Exploring quantile mapping as a tool to produce user tailored

climate scenarios for Switzerland. *Technical Report MeteoSwiss*, *270*. https://www.meteoschweiz.admin.ch/home/service-und-publikationen/publikationen.subpage.html/de/data/publications/2018/11/exploring-quantile-mapping-as-a-tool-to-produce-user-tailored-climate-scenarios-for-switzerland.html?topic=/content/meteoswiss/tags/to

Forbes, C., Hastings, N., Evans, M., & Peacock, B. (2010). Statistical Distributions. In *Introduction to Power Analysis: Two-Group Studies*. https://doi.org/10.4135/9781506343105.n6

Fujihara, Y., Tanaka, K., Watanabe, T., Nagano, T., & Kojiri, T. (2008). Assessing the impacts of climate change on the water resources of the Seyhan River Basin in Turkey: Use of dynamically downscaled data for hydrologic simulations. *Journal of Hydrology*, *353*(1–2), 33–48. https://doi.org/10.1016/j.jhydrol.2008.01.024

Ghimire, U., Srinivasan, G., & Agarwal, A. (2019). Assessment of rainfall bias correction techniques for improved hydrological simulation. *International Journal of Climatology*, *39*(4), 2386–2399. https://doi.org/10.1002/joc.5959

Gilleland, E. (2022). *Package "extRemes."*

Graham, L. P., Andreáasson, J., & Carlsson, B. (2007). Assessing climate change impacts on hydrology from an ensemble of regional climate models, model scales and linking methods - A case study on the Lule River basin. *Climatic Change*, *81*(SUPPL. 1), 293–307. https://doi.org/10.1007/s10584-006-9215-2

Graham, L. P., Hagemann, S., Jaun, S., & Beniston, M. (2007). On interpreting hydrological change from regional climate models. *Climatic Change*, *81*(SUPPL. 1), 97–122. https://doi.org/10.1007/s10584-006-9217-0

Grillakis, M. G., Koutroulis, A. G., & Tsanis, I. K. (2013). Multisegment statistical bias correction of daily GCM precipitation output. *Journal of Geophysical Research Atmospheres*, *118*(8), 3150–3162. https://doi.org/10.1002/jgrd.50323

Gudmundsson, L., Bremnes, J. B., Haugen, J. E., & Engen-Skaugen, T. (2012). Technical Note: Downscaling RCM precipitation to the station scale using statistical transformations – A comparison of methods. *Hydrology and Earth System Sciences*, *16*(9), 3383–3390. https://doi.org/10.5194/hess-16-3383-2012

Haerter, J. O., Hagemann, S., Moseley, C., & Piani, C. (2011). Climate model bias correction and the role of timescales. *Hydrology and Earth System Sciences*, *15*(3), 1065–1079. https://doi.org/10.5194/hess-15-1065-2011

Haylock, M. R., Cawley, G. C., Harpham, C., Wilby, R. L., & Goodess, C. M. (2006). Downscaling heavy precipitation over the United Kingdom: A comparison of dynamical and statistical methods and their future scenarios. *International Journal of Climatology*, *26*(10), 1397–1415. https://doi.org/10.1002/joc.1318

Heo, J. H., Ahn, H., Shin, J. Y., Kjeldsen, T. R., & Jeong, C. (2019). Probability distributions for a quantile mapping technique for a bias correction of precipitation data: A case study to precipitation data under climate change. *Water (Switzerland)*, *11*(7). https://doi.org/10.3390/w11071475

Hodson, T. O. (2022). Root-mean-square error (RMSE) or mean absolute error (MAE): when to use them or not. *Geoscientific Model Development*, *15*(14), 5481–5487. https://doi.org/10.5194/gmd-15-5481-2022

Ines, A. V. M., & Hansen, J. W. (2006). Bias correction of daily GCM rainfall for crop simulation studies. *Agricultural and Forest Meteorology*, *138*(1–4), 44–53. https://doi.org/10.1016/j.agrformet.2006.03.009

Jenkinson, A. F. (1955). The frequency distribution of the annual maximum (or minimum) values of meteorological elements. *Quarterly Journal of the Royal Meteorological Society*, *81*(348), 158–171. https://doi.org/10.1002/qj.49708134804

Johnson, F., & Sharma, A. (2011). Accounting for interannual variability: A

comparison of options for water resources climate change impact assessments. *Water Resources Research*, *47*(4), 1–20. https://doi.org/10.1029/2010WR009272

Kara, F., & Yucel, I. (2015). Climate change effects on extreme flows of water supply area in Istanbul: utility of regional climate models and downscaling method. *Environmental Monitoring and Assessment*, *187*(9). https://doi.org/10.1007/s10661-015-4808-8

Kim, S., Joo, K., Kim, H., Shin, J. Y., & Heo, J. H. (2021). Regional quantile delta mapping method using regional frequency analysis for regional climate model precipitation. *Journal of Hydrology*, *596*(October), 125685. https://doi.org/10.1016/j.jhydrol.2020.125685

Kwiatkowski, D., Phillips, P. C. B., Schmidt, P., & Shin, Y. (1992). Testing the null hypothesis of stationarity against the alternative of a unit root. How sure are we that economic time series have a unit root? *Journal of Econometrics*, *54*(1–3), 159–178. https://doi.org/10.1016/0304-4076(92)90104-Y

Lakku, N. K. G., & Behera, M. R. (2022). Skill and Inter-Model Comparison of Regional and Global Climate Models in Simulating Wind Speed over South Asian Domain. *Climate*, *10*(6). https://doi.org/10.3390/cli10060085

Leander, R., & Buishand, T. A. (2007). Resampling of regional climate model output for the simulation of extreme river flows. *Journal of Hydrology*, *332*(3–4), 487–496. https://doi.org/10.1016/j.jhydrol.2006.08.006

Leander, R., Buishand, T. A., van den Hurk, B. J. J. M., & de Wit, M. J. M. (2008). Estimated changes in flood quantiles of the river Meuse from resampling of regional climate model output. *Journal of Hydrology*, *351*(3–4), 331–343. https://doi.org/10.1016/j.jhydrol.2007.12.020

Lenderink, G., Buishand, A., & Van Deursen, W. (2007). Estimates of future discharges of the river Rhine using two scenario methodologies: Direct versus delta approach. *Hydrology and Earth System Sciences*, *11*(3), 1145–1159.

https://doi.org/10.5194/hess-11-1145-2007

Lun, Y., Liu, L., Cheng, L., Li, X., Li, H., & Xu, Z. (2021). Assessment of GCMs simulation performance for precipitation and temperature from CMIP5 to CMIP6 over the Tibetan Plateau. *International Journal of Climatology*, *41*(7), 3994–4018. https://doi.org/10.1002/joc.7055

Luo, M., Liu, T., Meng, F., Duan, Y., Frankl, A., Bao, A., & De Maeyer, P. (2018). Comparing bias correction methods used in downscaling precipitation and temperature from regional climate models: A case study from the Kaidu River Basin in Western China. *Water (Switzerland)*, *10*(8). https://doi.org/10.3390/w10081046

Mann, H. (1945). Nonparametric Tests Against Trend Author (s): Henry B . Mann Published by : The Econometric Society Stable URL : https://www.jstor.org/stable/1907187 REFERENCES Linked references are available on JSTOR for this article : You may need to log in to JSTOR. *Econometrica*, *13*(3), 245–259.

Maraun, D., Wetterhall, F., Ireson, A. M., Chandler, R. E., Kendon, E. J., Widmann, M., Brienen, S., Rust, H. W., Sauter, T., Themel, M., Venema, V. K. C., Chun, K. P., Goodess, C. M., Jones, R. G., Onof, C., Vrac, M., & Thiele-Eich, I. (2010). Precipitation downscaling under climate change: Recent developments to bridge the gap between dynamical models and the end user. *Reviews of Geophysics*, *48*(3), 1–34. https://doi.org/10.1029/2009RG000314

Maraun, Douglas. (2013). Bias correction, quantile mapping, and downscaling: Revisiting the inflation issue. *Journal of Climate*, *26*(6), 2137–2143. https://doi.org/10.1175/JCLI-D-12-00821.1

Mendez, M., Maathuis, B., Hein-Griggs, D., & Alvarado-Gamboa, L.-F. (2020). Performance Evaluation of Bias Correction Methods for Climate Change Monthly Precipitation Projections over Costa Rica. *Water*, *12*(2).

Mesta Yoleri, B. (2022). *Impact of Climate change in The Southern Mediterranean of Turkey: A Method to Assess Oymapınar Reservoir's Inflow Projections* (Issue June).

Moore, K., Pierson, D., Pettersson, K., Schneiderman, E., & Samuelsson, P. (2008). Effects of warmer world scenarios on hydrologic inputs to Lake Mälaren, Sweden and implications for nutrient loads. *Hydrobiologia*, *599*(1), 191–199. https://doi.org/10.1007/s10750-007-9197-8

Moravej, M. (2016). Investigating climate change using AK stationarity test in the Lake Urmia basin. *International Journal of Hydrology Science and Technology*, *6*(4), 382–407. https://doi.org/10.1504/IJHST.2016.079349

Olsson, J., Berggren, K., Olofsson, M., & Viklander, M. (2009). Applying climate model precipitation scenarios for urban hydrological assessment: A case study in Kalmar City, Sweden. *Atmospheric Research*, *92*(3), 364–375. https://doi.org/10.1016/j.atmosres.2009.01.015

Özkaya, A. (2017). *ASSESSMENT OF DIFFERENT RAINFALL PRODUCTS IN FLOOD SIMULATIONS* [Middle East Technical University]. http://etd.lib.metu.edu.tr/upload/12620990/index.pdf

Park, C., Lee, G., Kim, G., & Cha, D. (2020). Intl Journal of Climatology - 2020 - Park - Future changes in precipitation for identified sub-regions in East Asia using.pdf. *International Journal of Climatology*, *41*.

Pastén-Zapata, E., Jones, J. M., Moggridge, H., & Widmann, M. (2020). Evaluation of the performance of Euro-CORDEX Regional Climate Models for assessing hydrological climate change impacts in Great Britain: A comparison of different spatial resolutions and quantile mapping bias correction methods. *Journal of Hydrology*, *584*(February), 124653. https://doi.org/10.1016/j.jhydrol.2020.124653

Piani, C., Weedon, G. P., Best, M., Gomes, S. M., Viterbo, P., Hagemann, S., & Haerter, J. O. (2010). Statistical bias correction of global simulated daily

precipitation and temperature for the application of hydrological models. *Journal of Hydrology*, *395*(3–4), 199–215. https://doi.org/10.1016/j.jhydrol.2010.10.024

Rana, A., Foster, K., Bosshard, T., Olsson, J., & Bengtsson, L. (2014). Impact of climate change on rainfall over Mumbai using Distribution-based Scaling of Global Climate Model projections. *Journal of Hydrology: Regional Studies*, *1*, 107–128. https://doi.org/10.1016/j.ejrh.2014.06.005

Salathé, E. P. (2003). Comparison of various precipitation downscaling methods for the simulation of streamflow in a rainshadow river basin. *International Journal of Climatology*, *23*(8), 887–901. https://doi.org/10.1002/joc.922

Sato, Y., Kojiri, T., Michihiro, Y., Suzuki, Y., & Nakakita, E. (2013). Assessment of climate change impacts on river discharge in Japan using the super-high-resolution MRI-AGCM. *Hydrological Processes*, *27*(23), 3264–3279. https://doi.org/10.1002/hyp.9828

Schmidli, J., Frei, C., & Vidale, P. L. (2006). Downscaling from GCM precipitation: A benchmark for dynamical and statistical downscaling methods. *International Journal of Climatology*, *26*(5), 679–689. https://doi.org/10.1002/joc.1287

Seaby, L. P., Refsgaard, J. C., Sonnenborg, T. O., Stisen, S., Christensen, J. H., & Jensen, K. H. (2013). Assessment of robustness and significance of climate change signals for an ensemble of distribution-based scaled climate projections. *Journal of Hydrology*, *486*, 479–493. https://doi.org/10.1016/j.jhydrol.2013.02.015

Sen, P. K. (1968). Estimates of the Regression Coefficient Based on Kendall ' s Tau Author (s): Pranab Kumar Sen Source : Journal of the American Statistical Association , Vol . 63 , No . 324 (Dec ., 1968), pp . Published by : Taylor & Francis , Ltd . on behalf of the A. *Journal of the American Statistical Association*, *63*(324), 1379–1389.

https://www.jstor.org/stable/2285891

Stefanidis, S., Dafis, S., & Stathis, D. (2020). Evaluation of regional climate models (Rcms) performance in simulating seasonal precipitation over mountainous central pindus (greece). *Water (Switzerland)*, *12*(10). https://doi.org/10.3390/w12102750

Sun. (2011). *Water Resources Research - 2011 - Sun - Hydroclimatic projections for the Murray-Darling Basin based on an ensemble derived.pdf*.

Sunyer, M. A., Hundecha, Y., Lawrence, D., Madsen, H., Willems, P., Martinkova, M., Vormoor, K., Bürger, G., Hanel, M., Kriaučiuniene, J., Loukas, A., Osuch, M., & Yücel, I. (2015). Inter-comparison of statistical downscaling methods for projection of extreme precipitation in Europe. *Hydrology and Earth System Sciences*, *19*(4), 1827–1847. https://doi.org/10.5194/hess-19-1827-2015

Teutschbein, C., & Seibert, J. (2010). Regional climate models for hydrological impact studies at the catchment scale: A review of recent modeling strategies. *Geography Compass*, *4*(7), 834–860. https://doi.org/10.1111/j.1749-8198.2010.00357.x

Teutschbein, C., & Seibert, J. (2012). Bias correction of regional climate model simulations for hydrological climate-change impact studies: Review and evaluation of different methods. *Journal of Hydrology*, *456–457*, 12–29. https://doi.org/10.1016/j.jhydrol.2012.05.052

van Roosmalen, L., Sonnenborg, T. O., Jensen, K. H., & Christensen, J. H. (2011). Comparison of Hydrological Simulations of Climate Change Using Perturbation of Observations and Distribution-Based Scaling. *Vadose Zone Journal*, *10*(1), 136–150. https://doi.org/10.2136/vzj2010.0112

Walker, A., & Braglia, L. (2018). *Package "openxlsx."*

Wilcke, R. A. I., Mendlik, T., & Gobiet, A. (2013). Multi-variable error correction

of regional climate models. *Climatic Change*, *120*(4), 871–887. https://doi.org/10.1007/s10584-013-0845-x

Wilks, D. S. (1995). *Statistical Methods in the Atmospheric Sciences: An Introduction*. Academic Press.

Yang, W., Andréasson, J., Graham, L. P., Olsson, J., Rosberg, J., & Wetterhall, F. (2010). Distribution-based scaling to improve usability of regional climate model projections for hydrological climate change impacts studies. *Hydrology Research*, *41*(3–4), 211–229. https://doi.org/10.2166/nh.2010.004

Yılmaz, E., & Darende, V. (2021). Türkiye'de yağış ölçümü yapılan manuel-otomatik meteoroloji gözlem istasyonu verilerinin karşılaştırılması. *Türk Coğrafya Dergisi*, *77*, 53–66. https://doi.org/10.17211/tcd.834500

Yousefi, K. (2020). *ESTIMATION OF BIAS-CORRECTED HIGH-RESOLUTION RADAR PRECIPITATION MAPS USING THE RADAR AND RAIN GAUGE NETWORK OVER TURKEY* [Middle East Technical University]. http://etd.lib.metu.edu.tr/upload/12625578/index.pdf

APPENDICES

A. Stationarity Tests Results

A.1 Combined Results of ADF and KPSS tests for whole datasets

		RCMs																
M	**O**	**1**	**2**	**3**	**4**	**5**	**6**	**7**	**8**	**9**	**10**	**11**	**12**	**13**	**14**	**15**	**16**	**17**
1	S	S	S	S	IN	S	IN	S	IN	S	S	S	S	S	IN	S	S	S
2	S	S	S	S	S	IN	IN	S	S	S	S	S	S	S	IN	S	IN	S
3	S	S	S	S	S	S	S	S	S	IN	S	S	S	S	IN	S	S	S
4	S	S	S	S	IN	IN	IN	S	S	S	S	S	S	S	IN	S	IN	S
5	S	IN	S	S	S	S	IN	S	S	S	S	S	S	S	IN	S	S	S
6	S	IN	S	S	S	IN	IN	S	S	S	S	S	S	S	IN	S	S	IN
7	S	S	S	S	S	IN	IN	S	S	S	S	S	S	S	IN	S	S	IN
8	S	S	S	S	IN	IN	IN	S	S	S	S	S	S	S	IN	S	S	S
9	S	S	S	S	S	IN	IN	S	S	S	S	S	S	S	IN	S	S	S
10	S	S	S	S	S	S	IN	S	S	S	S	S	S	S	IN	S	S	S
11	S	S	S	IN	IN	IN	S	S	S	S	S	S	S	S	IN	S	S	S
12	S	S	S	S	S	S	S	S	S	S	S	S	S	S	IN	S	S	S
13	S	S	S	S	S	S	S	S	S	S	S	S	S	S	IN	S	S	S
14	S	S	S	S	S	S	IN	S	S	S	S	S	S	S	IN	S	S	S
15	S	S	S	S	S	IN	S	S	S	S	S	S	S	S	S	S	S	S
16	S	S	S	S	S	S	S	S	S	S	S	S	S	S	S	S	S	S
17	S	S	S	S	S	S	IN	S	S	S	S	S	S	S	S	S	S	S
18	S	S	S	IN	S	IN	S	S	S	S	S	S	S	S	IN	S	S	S
19	S	S	S	IN	S	IN	S	S	S	S	S	S	S	S	IN	S	S	S
20	S	S	S	S	S	S	S	S	S	S	S	S	S	S	IN	S	S	S
21	S	S	S	S	S	S	S	S	S	S	S	S	S	S	IN	S	S	S
22	S	S	S	S	IN	IN	S	S	S	S	S	S	S	S	IN	S	S	S
23	S	S	S	S	IN	S	IN	S	S	S	S	S	S	S	IN	S	S	S
24	S	S	S	S	S	IN	IN	S	S	IN	S	S	S	S	IN	S	S	IN
25	S	S	S	S	IN	IN	IN	S	S	S	S	S	S	S	IN	S	S	S
26	S	S	S	S	IN	IN	IN	S	S	S	S	S	S	S	IN	S	S	IN
27	S	S	S	S	S	S	S	S	S	S	S	S	S	S	IN	S	S	IN
28	S	S	S	S	S	IN	IN	S	S	IN	S	S	S	S	IN	S	S	IN
29	S	IN	S	S	S	IN	IN	S	S	S	S	S	S	S	IN	S	S	IN
30	S	S	S	S	S	IN	IN	S	S	S	S	S	S	S	IN	S	S	S
31	S	IN	S	S	IN	IN	IN	S	S	S	S	S	S	S	IN	S	S	S
32	S	S	S	S	S	S	S	IN	S	IN	S	S	S	S	IN	S	S	S
33	S	S	S	S	IN	IN	IN	IN	S	IN	S	S	S	S	IN	S	S	S
34	S	S	S	S	S	IN	IN	S	S	S	S	S	S	S	IN	S	S	S

A.1 (continued)

35	S	S	S	S	S	IN	IN	S	S	S	S	S	S	S	IN	S	S	S
36	S	S	S	S	S	IN	IN	S	S	S	S	S	S	S	IN	S	S	IN
37	S	IN	S	S	IN	IN	IN	S	S	S	S	S	S	S	IN	S	S	IN
38	S	IN	S	S	S	S	IN	S	S	S	S	S	S	S	IN	S	S	S
39	S	IN	S	S	S	IN	IN	S	S	S	S	S	S	S	IN	S	S	IN
40	S	S	S	S	S	IN	IN	S	S	IN	S	S	S	S	IN	S	IN	S
41	S	S	S	IN	S	IN	S	S	S	S	S	S	S	S	IN	S	S	S
42	S	IN	S	S	S	IN	S	S	S	S	S	S	S	S	IN	S	S	S
43	S	IN	S	S	S	IN	IN	S	S	S	S	S	S	S	S	S	S	S
44	S	S	S	IN	S	S	S	S	S	S	S	S	S	S	IN	S	S	S
45	S	IN	S	S	IN	IN	S	S	S	S	S	S	S	S	S	S	S	S
46	S	S	S	S	S	S	S	S	S	S	S	S	S	S	S	S	S	S
47	S	S	S	IN	S	S	S	S	S	S	S	S	S	S	IN	S	S	S
48	S	S	S	S	IN	IN	S	S	S	S	S	S	S	S	IN	S	S	S
49	S	S	S	S	IN	S	S	S	S	S	S	S	S	S	S	S	S	S
50	S	S	S	S	S	S	IN	S	S	S	S	S	S	S	S	S	S	S
51	S	S	S	S	S	S	S	S	S	S	S	S	S	S	IN	S	S	S
52	S	S	S	S	S	S	S	S	S	S	S	S	S	S	IN	S	S	S
53	S	S	S	S	S	S	S	S	S	S	S	S	S	S	IN	S	S	S

A.2 Combined Results of ADF and KPSS tests for extreme parts

		RCMs																
M	**O**	**1**	**2**	**3**	**4**	**5**	**6**	**7**	**8**	**9**	**10**	**11**	**12**	**13**	**14**	**15**	**16**	**17**
1	S	S	S	S	S	S	S	S	S	S	S	S	S	S	S	S	S	S
2	S	S	S	S	S	S	S	IN	S	S	IN	S	S	S	S	S	S	S
3	S	IN	S	S	S	S	S	S	S	S	S	S	S	S	S	S	S	S
4	S	S	S	S	S	S	S	S	S	IN	S	S	S	S	S	S	S	S
5	S	S	S	S	IN	IN	S	S	S	S	S	S	S	S	S	S	S	S
6	S	S	S	S	S	S	IN	S	S	S	IN	S	S	S	S	S	S	S
7	S	S	IN	S	S	IN	S	S	S	S	S	IN	S	S	S	S	S	S
8	S	S	S	S	IN	IN	S	S	S	S	S	S	S	S	S	IN	S	S
9	S	S	S	S	S	S	S	S	IN	S	S	S	S	S	S	S	S	S
10	S	S	S	S	S	S	S	S	S	S	S	S	S	S	S	S	S	S
11	IN	S	S	S	S	S	S	S	IN	S	S	S	S	S	S	S	S	S
12	S	S	S	S	S	S	S	S	S	S	S	S	S	S	S	S	S	S
13	S	S	S	S	S	S	S	S	S	S	S	S	S	S	S	S	S	S
14	S	S	S	S	S	S	IN	S	S	S	S	S	S	S	S	S	S	S
15	S	S	S	S	S	S	IN	S	S	S	S	S	S	S	S	S	IN	S
16	S	S	S	S	S	S	IN	S	IN	IN	S	S	S	S	S	S	S	S
17	S	S	S	IN	S	S	IN	S	IN	S	S	S	S	S	IN	S	S	S

A.2 (continued)

18	S	S	S	S	S	S	S	S	S	IN	S	S	S	S	S	S	IN	S
19	IN	S	S	S	S	S	S	S	S	S	S	S	S	S	S	S	S	S
20	S	S	S	IN	S	S	S	S	S	S	S	S	S	S	S	S	S	S
21	S	S	S	S	S	S	S	S	S	S	S	S	S	S	S	S	S	S
22	S	S	S	IN	IN	IN	S	S	S	S	S	S	S	S	S	IN	S	S
23	S	S	S	S	IN	S	S	S	IN	S	S	S	S	S	S	S	S	S
24	S	S	S	S	S	S	S	S	S	S	S	S	S	S	S	S	S	S
25	S	S	S	S	S	S	S	S	S	S	S	S	S	S	S	S	S	S
26	S	S	S	S	S	IN	S	S	S	S	S	S	S	S	S	S	S	S
27	S	S	S	S	S	S	S	S	S	S	S	S	IN	S	S	S	S	S
28	S	S	S	S	S	S	S	S	S	S	S	S	S	S	S	S	S	S
29	S	S	S	S	S	IN	S	S	S	S	S	S	S	S	S	S	S	S
30	S	S	S	S	S	S	S	S	S	S	S	S	S	S	S	IN	S	S
31	S	S	S	S	S	S	IN	S	S	S	S	S	S	S	IN	S	S	S
32	S	S	S	S	S	S	IN	IN	S	S	S	S	S	S	S	S	S	S
33	S	S	S	IN	S	S	S	S	S	S	S	S	S	S	S	S	S	S
34	S	S	S	S	S	S	S	S	S	S	S	S	S	S	S	S	S	S
35	S	S	S	IN	S	S	S	S	S	S	S	S	S	S	S	S	S	S
36	S	S	S	S	S	S	S	S	S	S	S	S	S	S	S	S	S	S
37	S	S	S	S	S	S	S	S	S	S	S	S	S	IN	S	S	S	S
38	S	S	S	S	S	S	S	S	S	IN	S	S	S	S	S	S	S	S
39	S	S	S	S	S	S	S	S	S	S	S	IN	S	S	S	S	S	S
40	IN	S	IN	S	S	S	S	S	S	S	IN	S	S	S	S	S	S	S
41	S	S	S	S	IN	S	S	S	IN	S	S	S	S	S	S	S	S	S
42	S	S	S	S	S	S	S	S	S	S	S	S	S	S	S	S	S	S
43	IN	S	S	S	S	S	IN	S	S	S	S	S	S	S	S	S	S	S
44	S	S	S	S	S	S	S	S	S	S	S	S	S	S	S	IN	S	S
45	S	S	S	S	S	S	S	S	S	S	S	S	S	S	S	S	S	S
46	S	S	S	S	S	S	S	S	IN	S	S	IN	S	IN	S	S	S	S
47	IN	S	S	S	S	S	S	S	S	S	S	S	S	S	S	S	IN	S
48	S	S	S	S	S	S	S	IN	S	S	S	S	S	S	S	S	S	IN
49	S	IN	IN	S	S	S	S	S	S	S	S	S	S	S	S	S	S	S
50	S	S	S	S	S	S	IN	S	S	IN	S	S	S	S	S	S	S	S
51	S	S	S	S	S	S	IN	S	S	S	S	S	S	S	S	S	S	S
52	S	S	S	S	S	S	S	S	S	S	S	S	IN	S	S	S	S	S
53	S	S	S	S	S	S	S	S	S	S	S	S	S	S	S	S	S	S

B. CDFs of Remaining MSs

B.1 CDFs of Remaining MSs Corrected by DBS Method

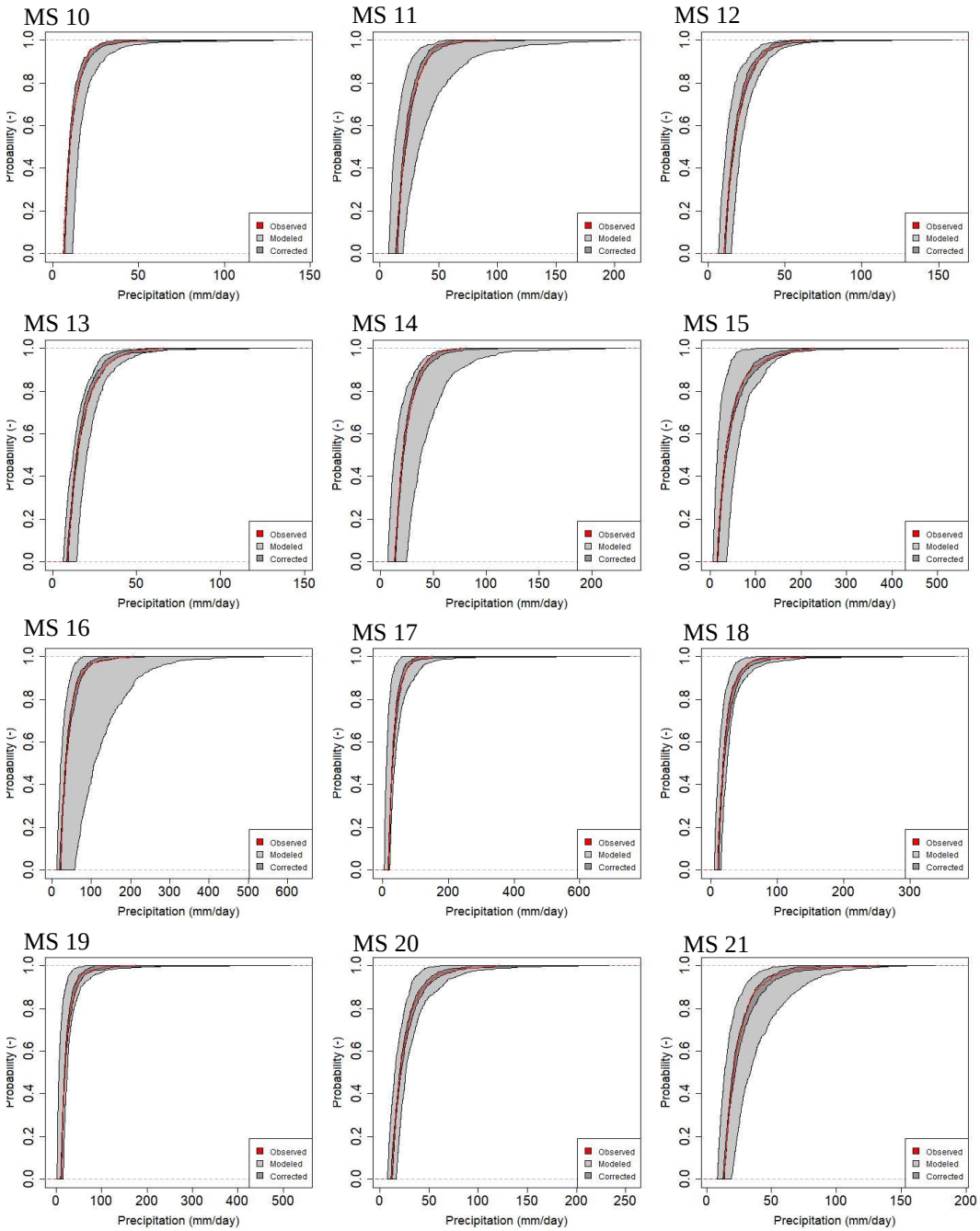

MS 22

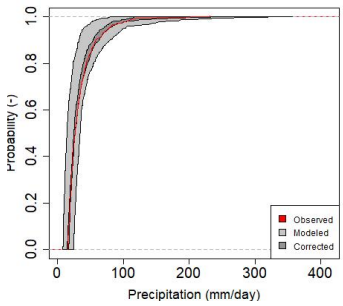

MS 23

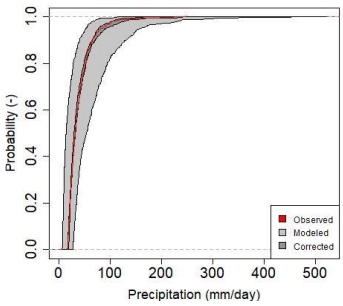

MS 24

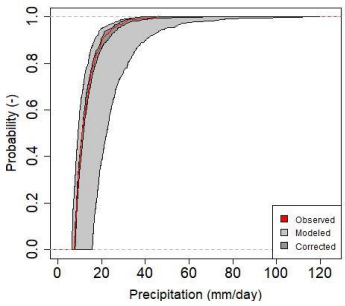

MS 25

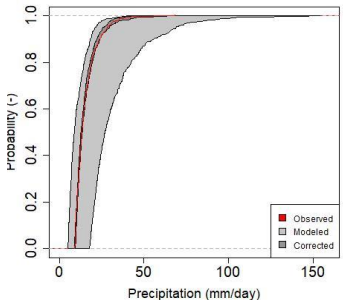

MS 26

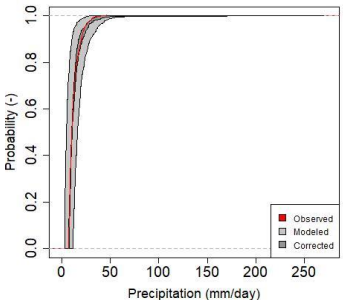

MS 27

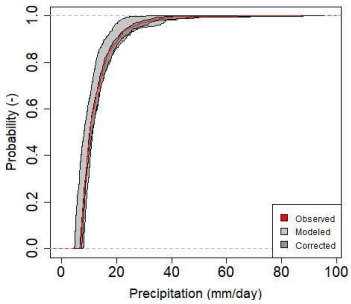

MS 28

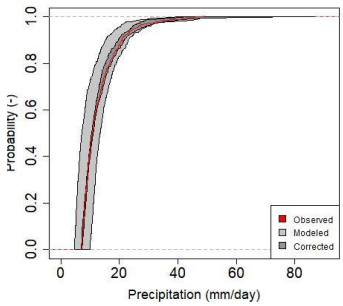

MS 29

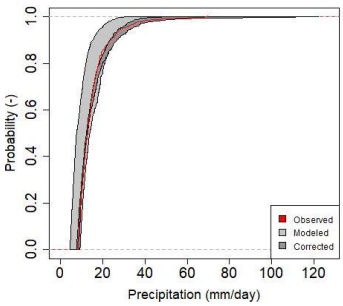

MS 30

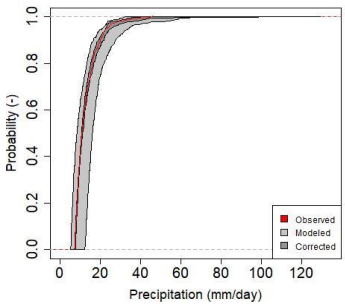

MS 31

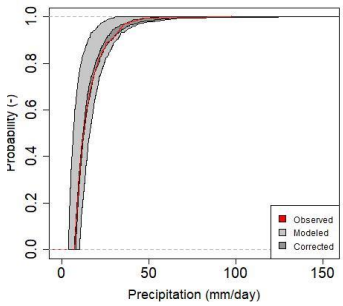

MS 32

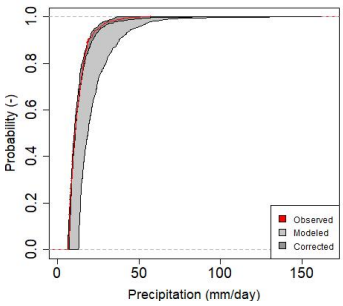

MS 33

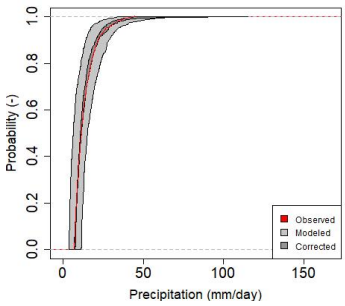

MS 34

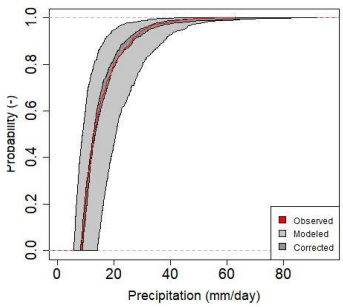

MS 35

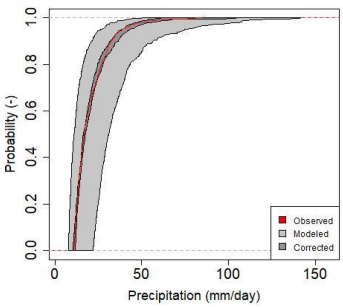

MS 36

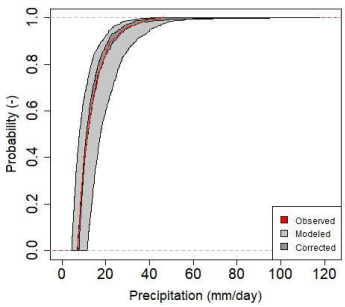

MS 37

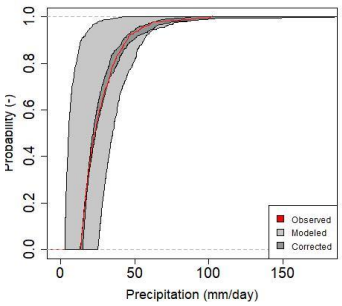

MS 38

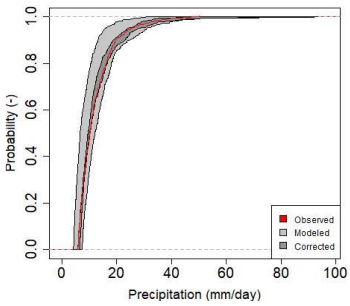

MS 39

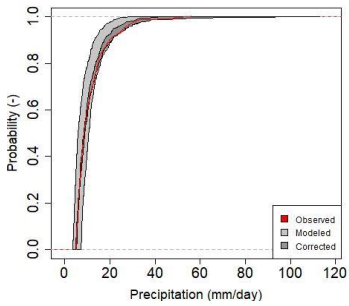

MS 40

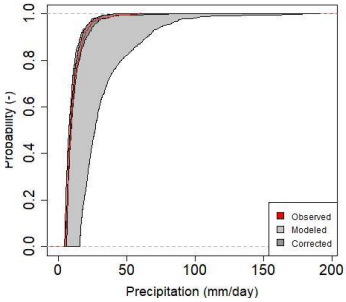

MS 41

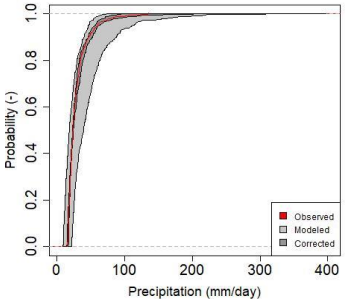

MS 42

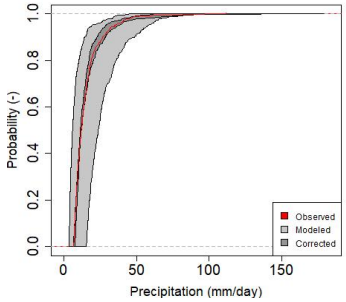

MS 43

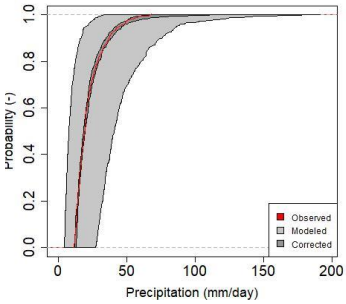

MS 44

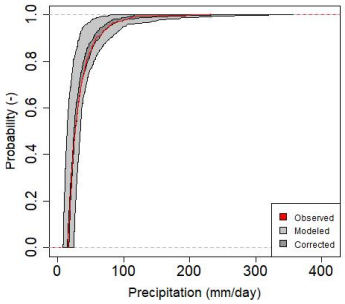

MS 45

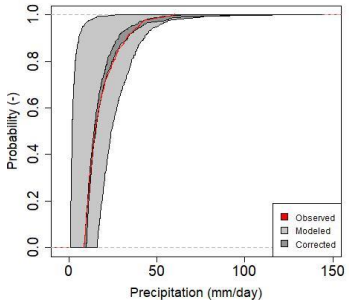

MS 46

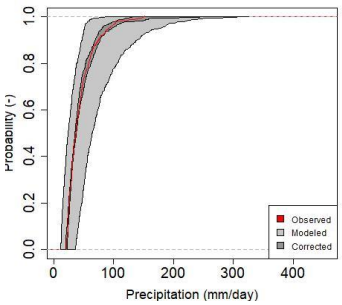

MS 47

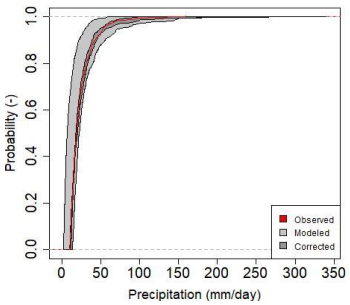

MS 48

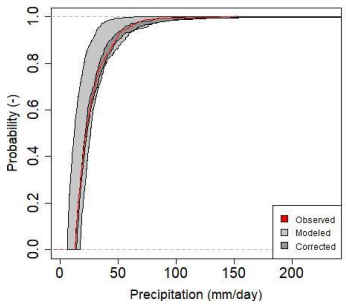

MS 49

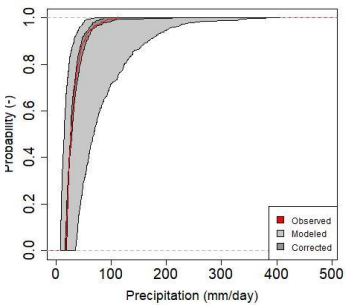

MS 50

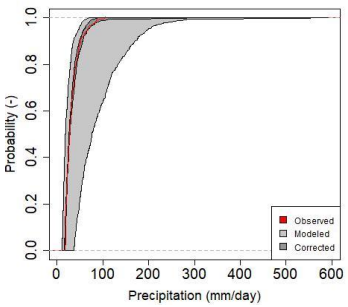

MS 51

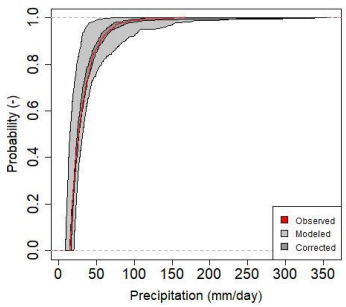

MS 52

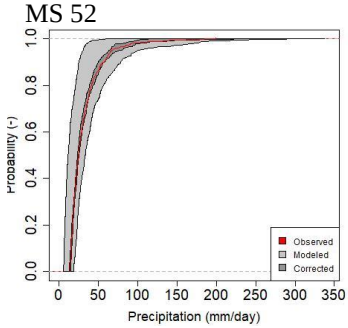
Probability (-)
0.0
0.2
0.4
0.6
0.8
1.0
0
50
100
150
200
250
300
350
Precipitation (mm/day)
Observed
Modeled
Corrected

MS 53

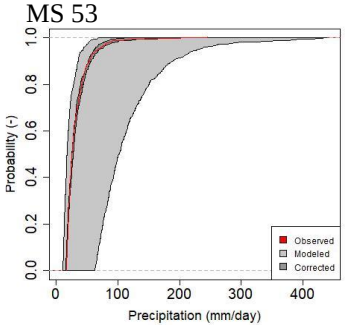
Probability (-)
0.0
0.2
0.4
0.6
0.8
1.0
0
100
200
300
400
Precipitation (mm/day)
Observed
Modeled
Corrected

B.2 CDFs of Remaining MSs Corrected by DBS_99 Method

MS 10

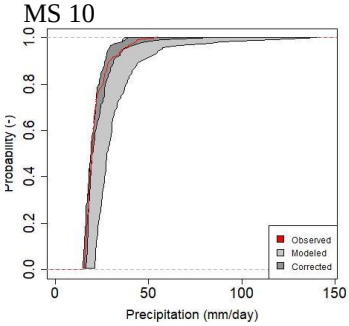

MS 11

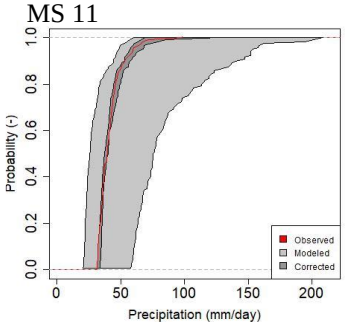

MS 12

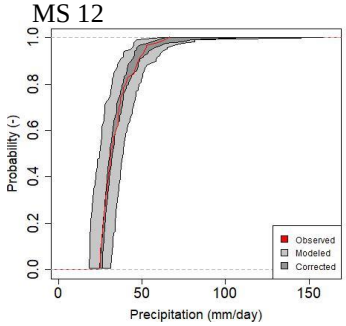

MS 13

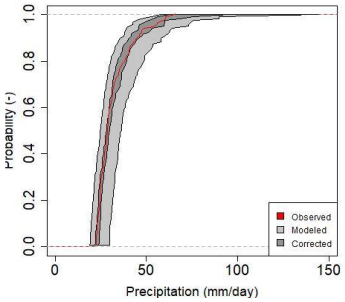

MS 14

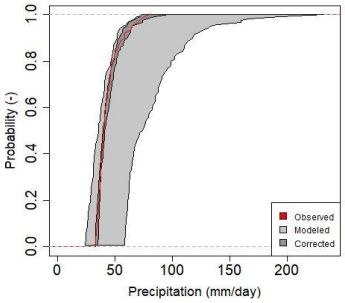

MS 15

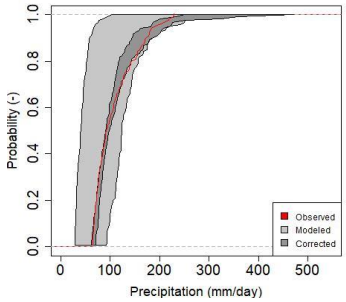

MS 16

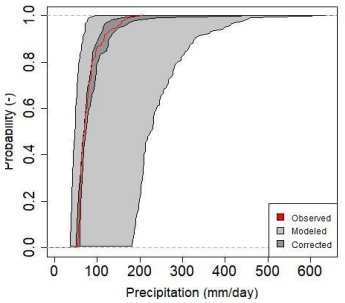

MS 17

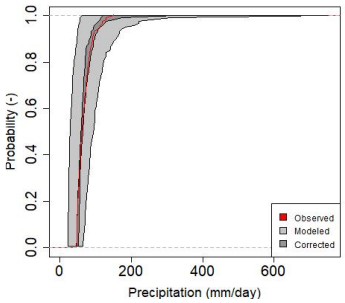

MS 18

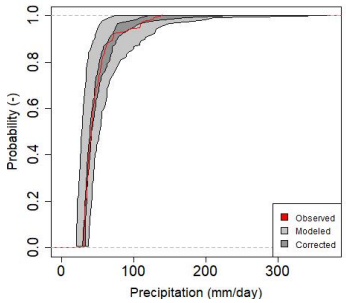

MS 19

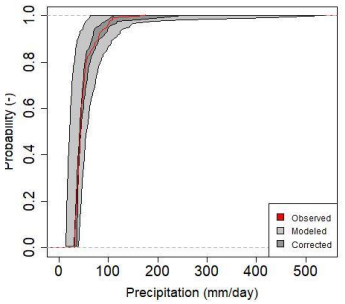

MS 20

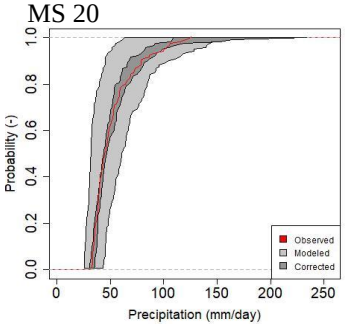

MS 21

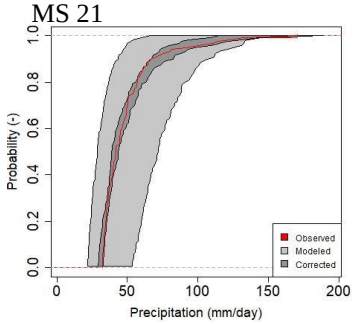

MS 22

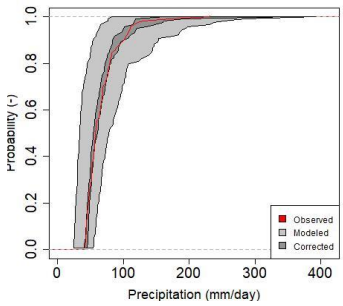

MS 23

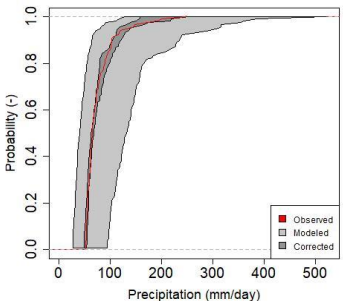

MS 24

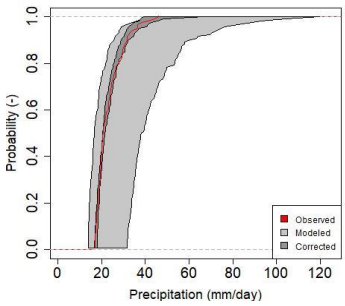

MS 25

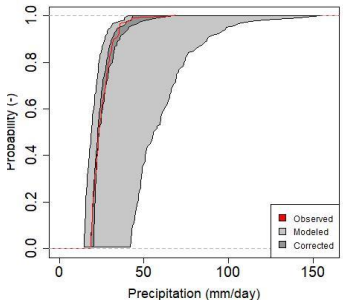

MS 26

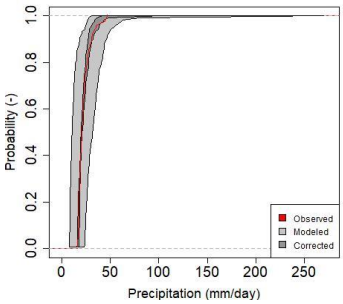

MS 27

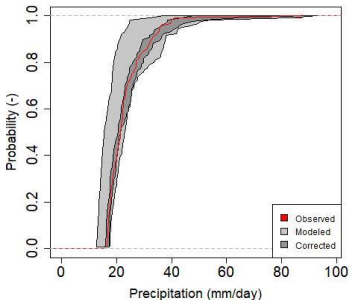

MS 28

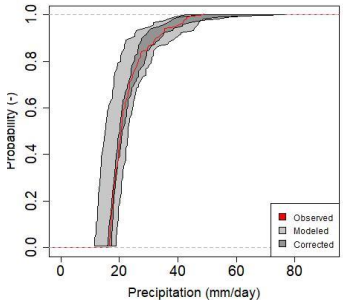

MS 29

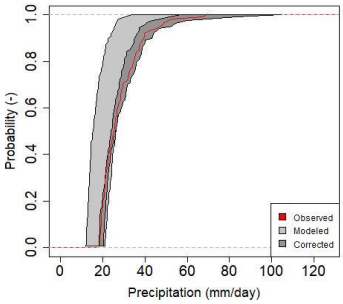

MS 30

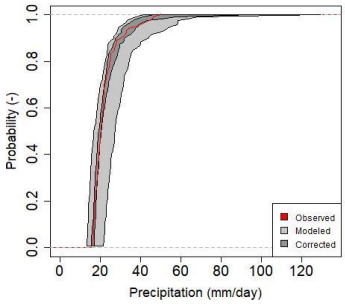

MS 31

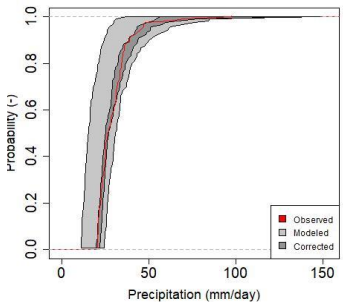

MS 32

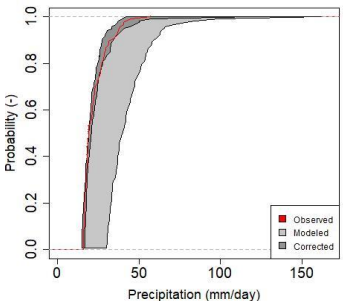

MS 33

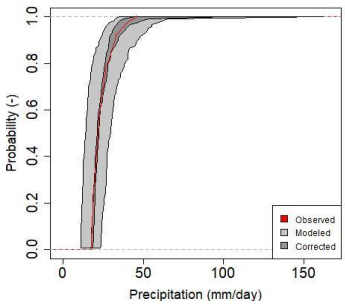

MS 34

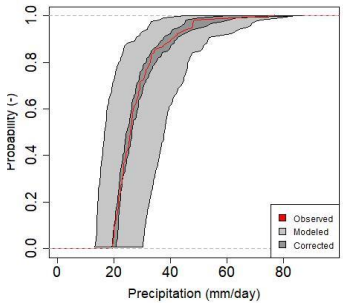

MS 35

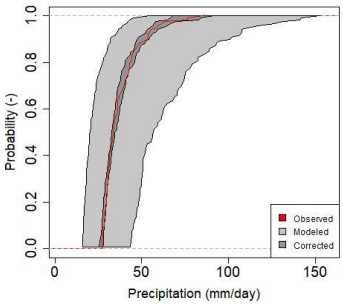

MS 36

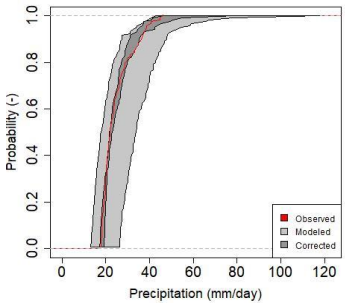

MS 37

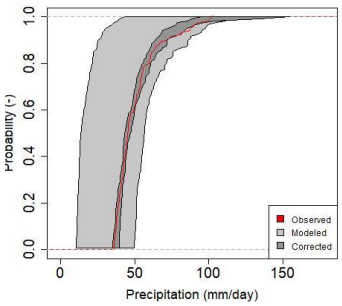

MS 38

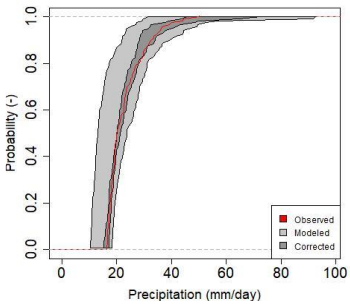

MS 39

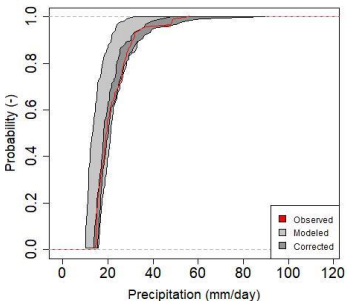

MS 40

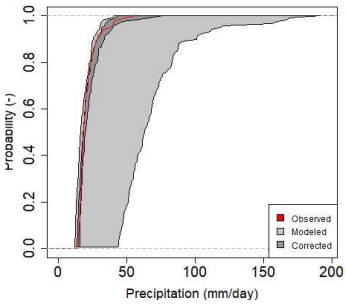

MS 41

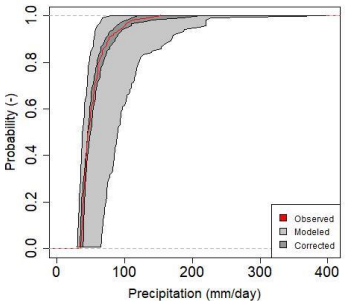

MS 42

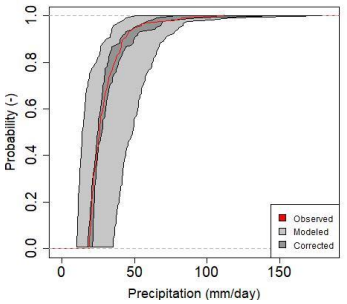

MS 43

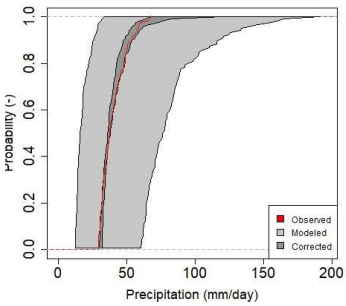

MS 44

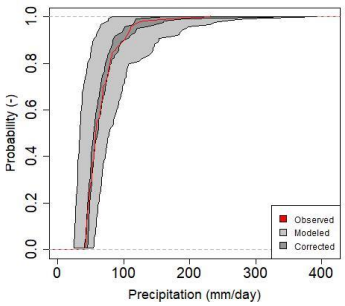

MS 45

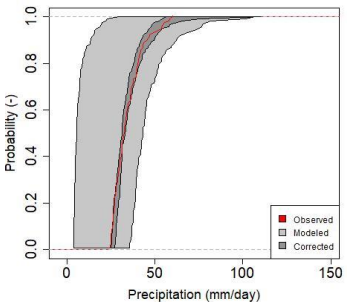

MS 46

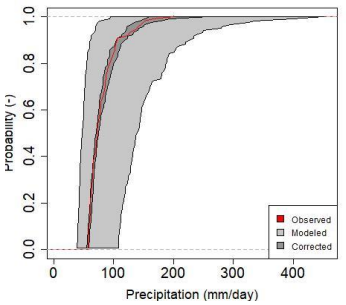

MS 47

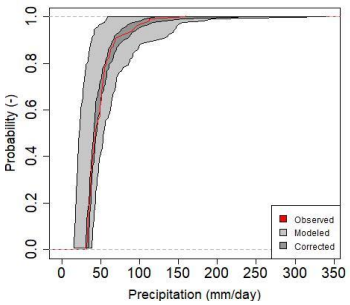

MS 48

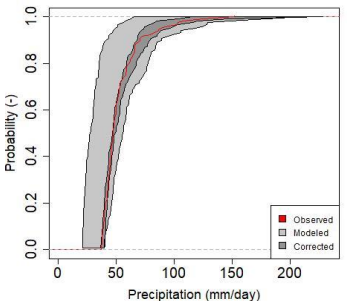

MS 49

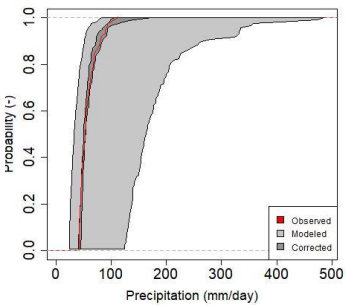

MS 50

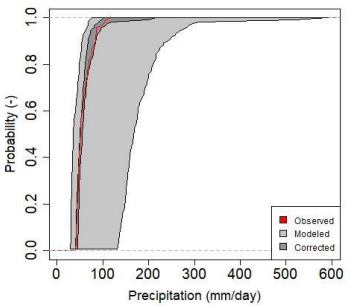

MS 51

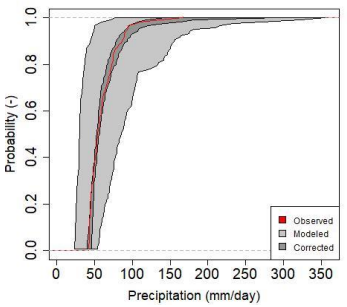

MS 52

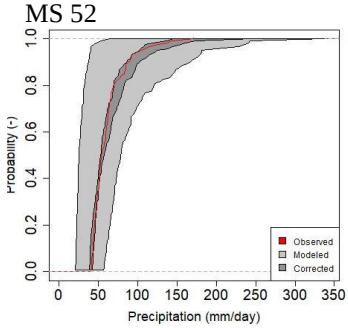
Probability (-)
0.0
0.2
0.4
0.6
0.8
1.0
0
50
100
150
200
250
300
350
Precipitation (mm/day)
Observed
Modeled
Corrected

MS 53

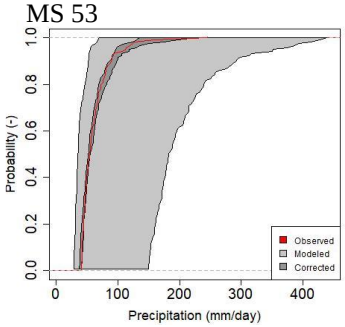
Probability (-)
0.0
0.2
0.4
0.6
0.8
1.0
0
100
200
300
400
Precipitation (mm/day)
Observed
Modeled
Corrected

B.3 CDFs of Remaining MSs Corrected by DBS_99_GP Method

MS 10

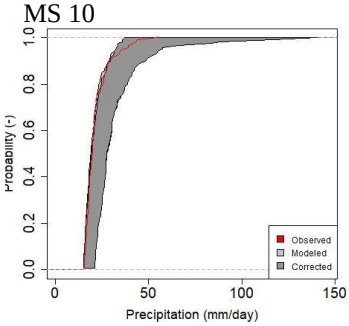

MS 11

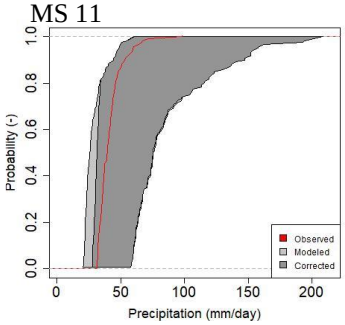

MS 12

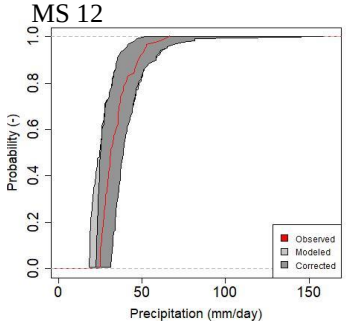

MS 13

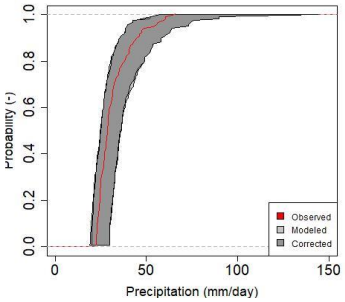

MS 14

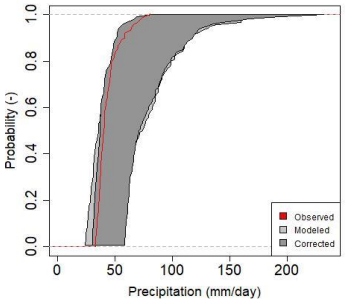

MS 15

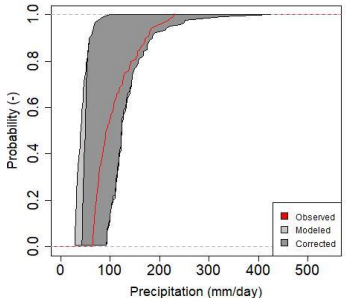

MS 16

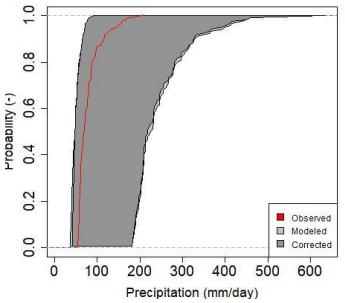

MS 17

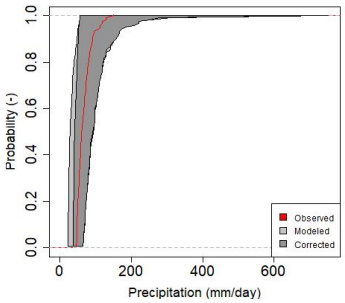

MS 18

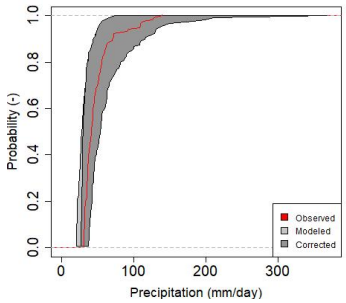

MS 19

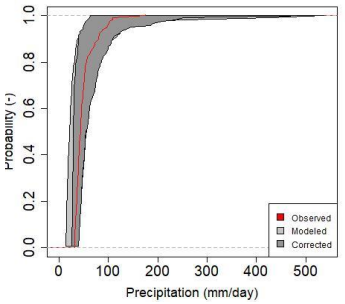

MS 20

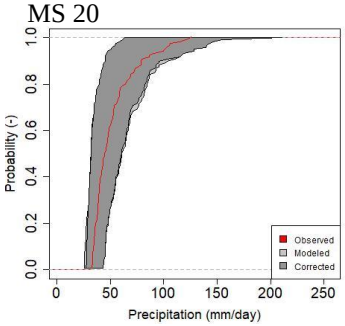

MS 21

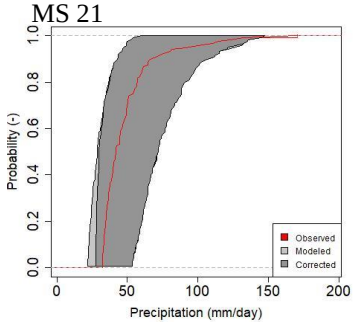

MS 22

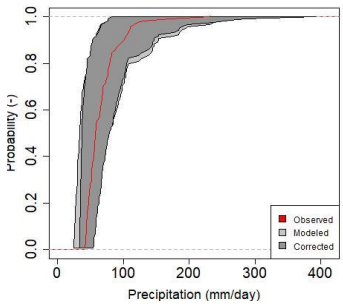

MS 23

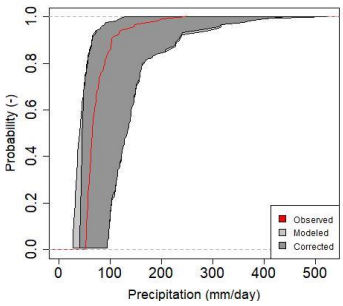

MS 24

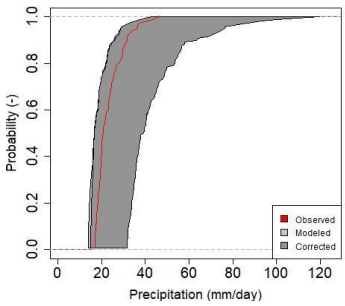

MS 25

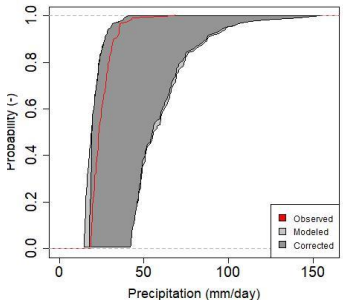

MS 26

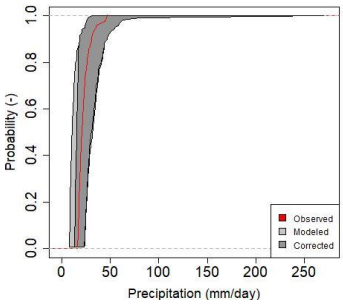

MS 27

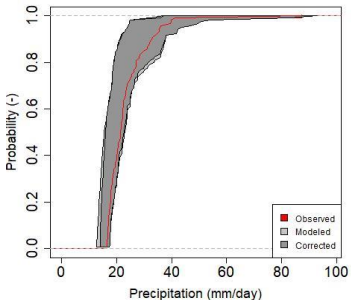

MS 28

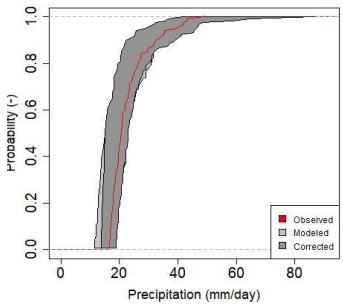

MS 29

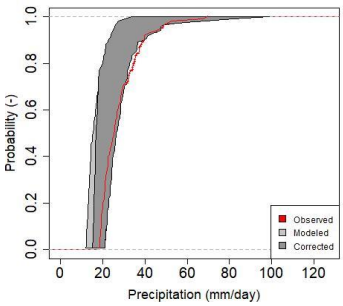

MS 30

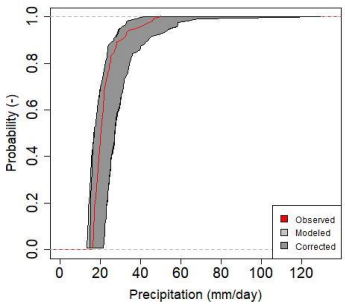

MS 31

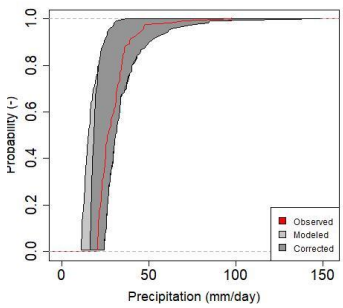

MS 32

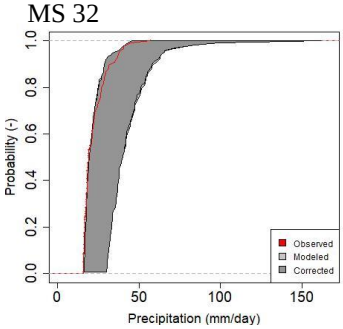

MS 33

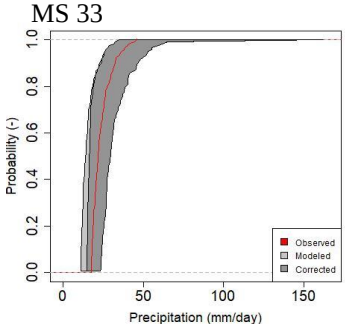

MS 34

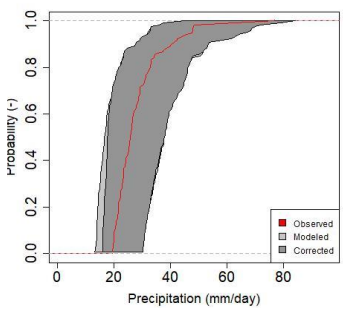

MS 35

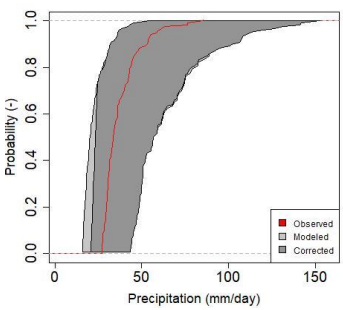

MS 36

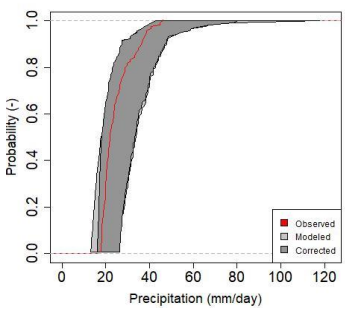

MS 37

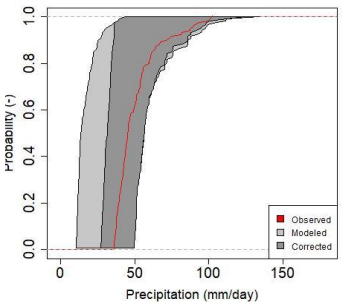

MS 38

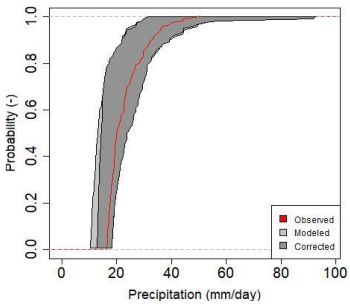

MS 39

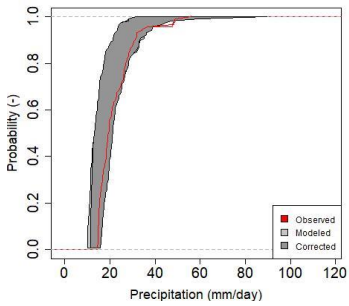

MS 40

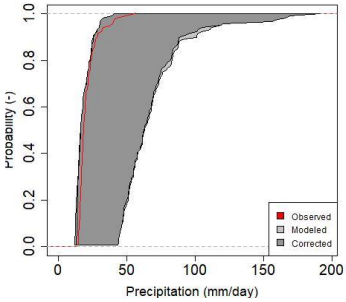

MS 41

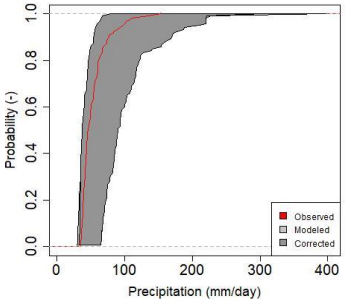

MS 42

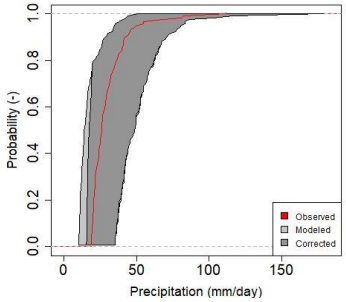

MS 43

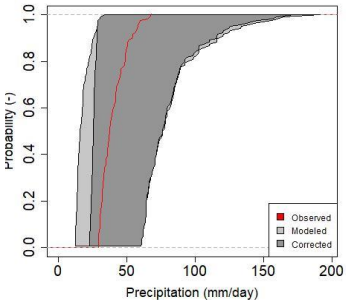

MS 44

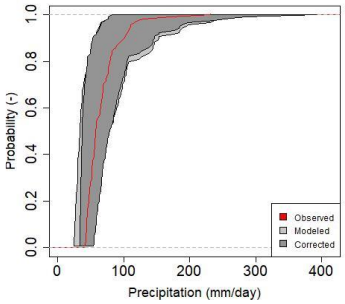

MS 45

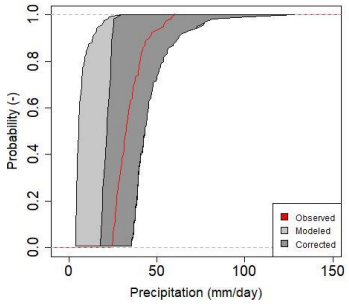

MS 46

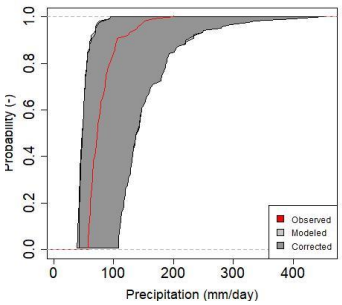

MS 47

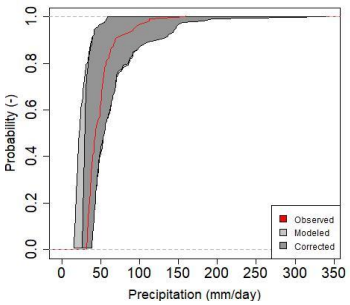

MS 48

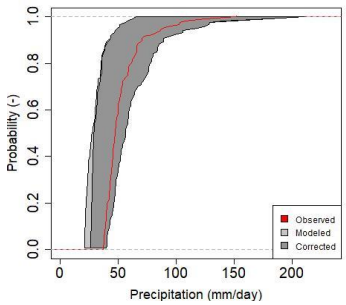

MS 49

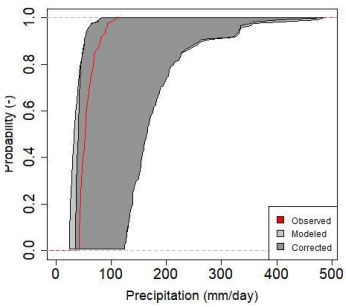

MS 50

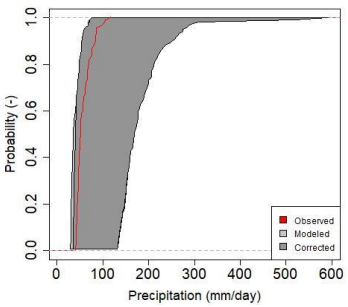

MS 51

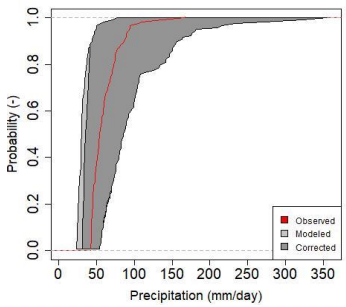

MS 52

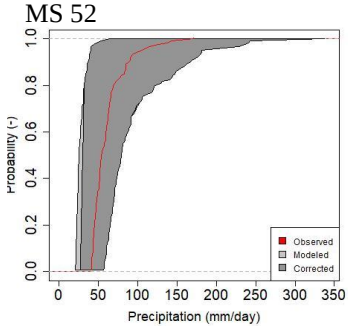
Probability (-)
0.0
0.2
0.4
0.6
0.8
1.0
0
50
100
150
200
250
300
350
Precipitation (mm/day)
Observed
Modeled
Corrected

MS 53

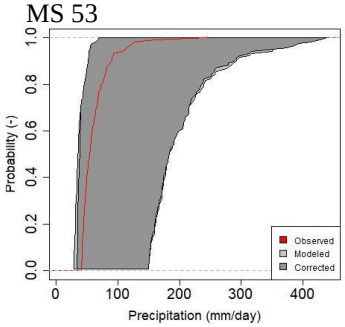
Probability (-)
0.0
0.2
0.4
0.6
0.8
1.0
0
100
200
300
400
Precipitation (mm/day)
Observed
Modeled
Corrected

B.4 CDFs of Remaining MSs Corrected by DBS_99_LOGN Method

MS 10

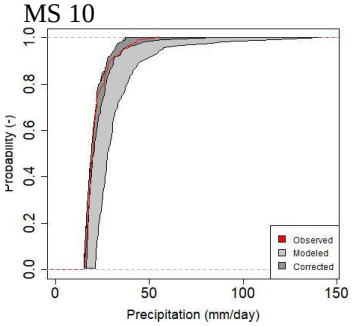

MS 11

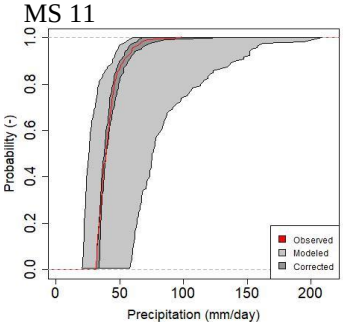

MS 12

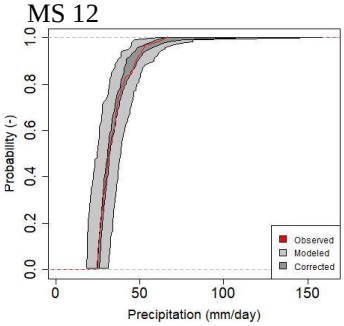

MS 13

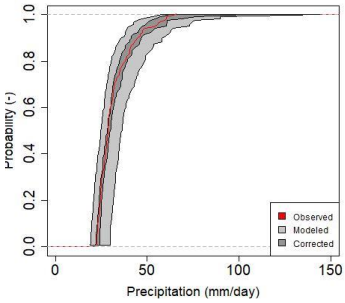

MS 14

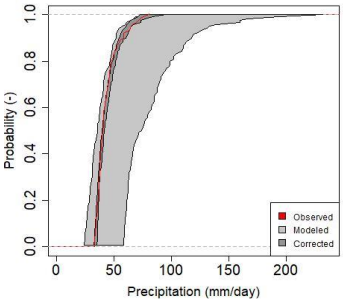

MS 15

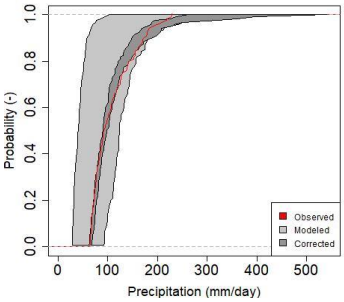

MS 16

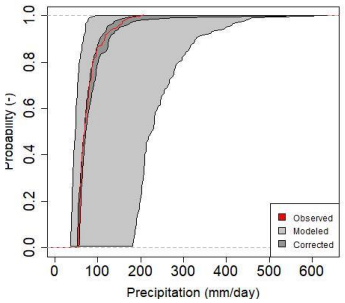

MS 17

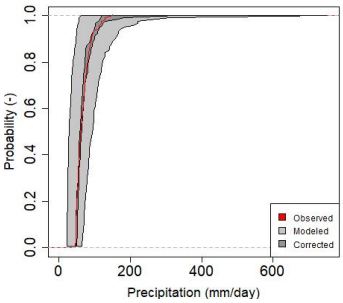

MS 18

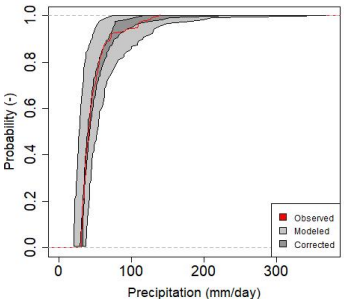

MS 19

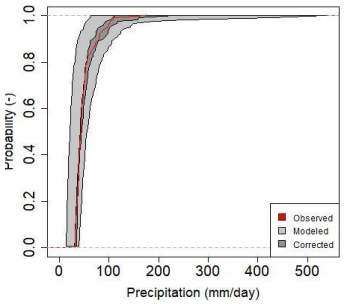

MS 20

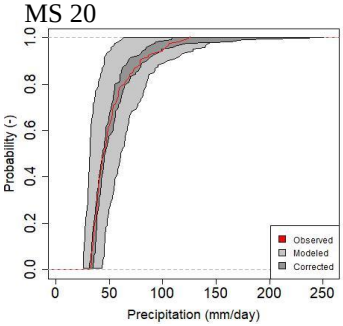

MS 21

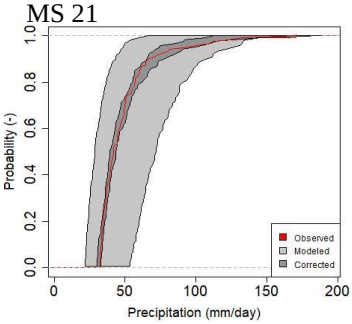

MS 22

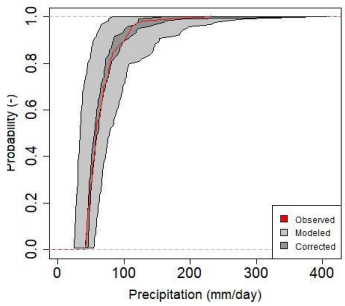

MS 23

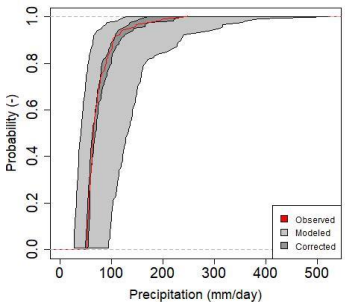

MS 24

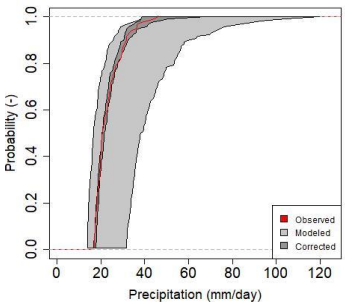

MS 25

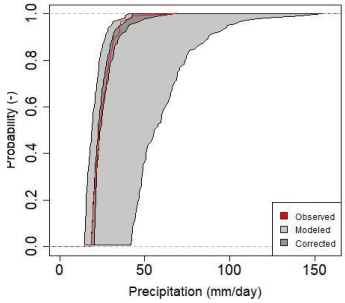

MS 26

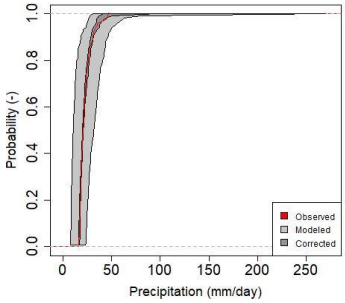

MS 27

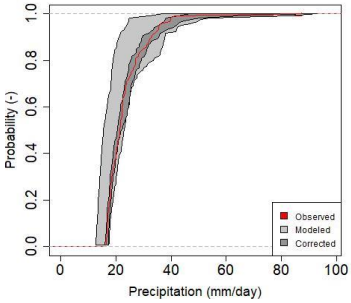

MS 28

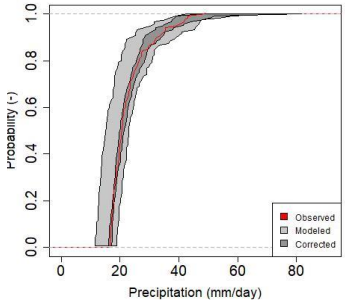

MS 29

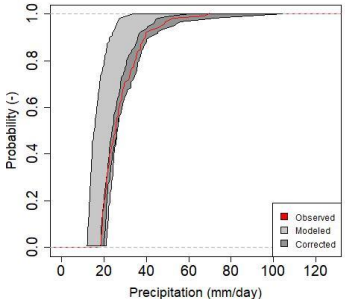

MS 30

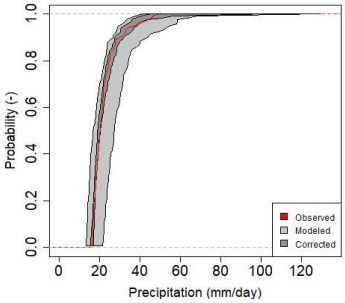

MS 31

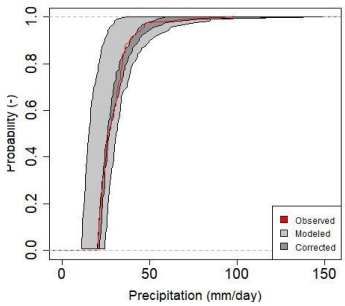

MS 32

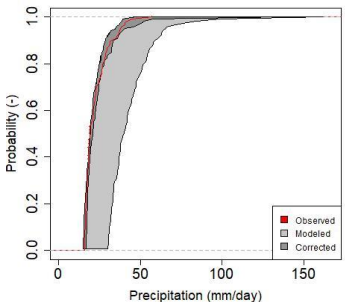

MS 33

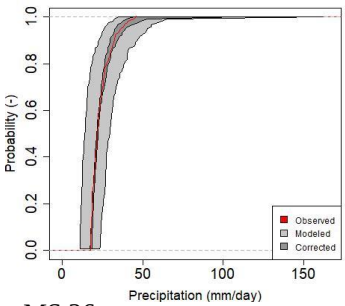

MS 34

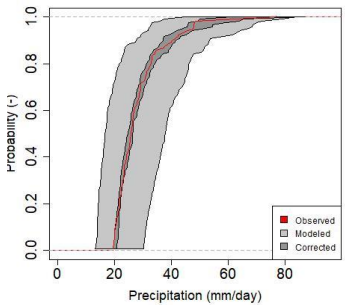

MS 35

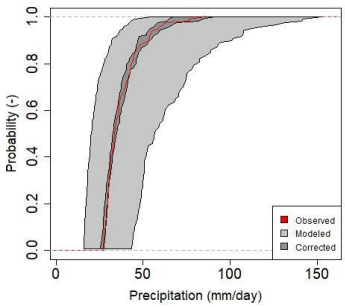

MS 36

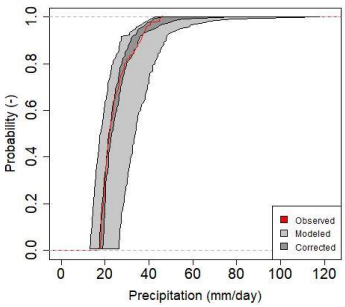

MS 37

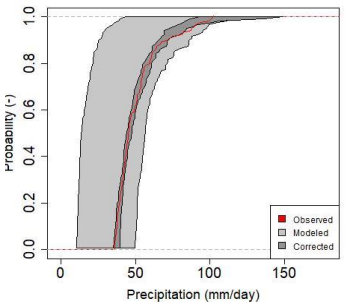

MS 38

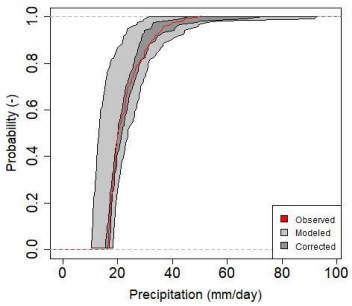

MS 39

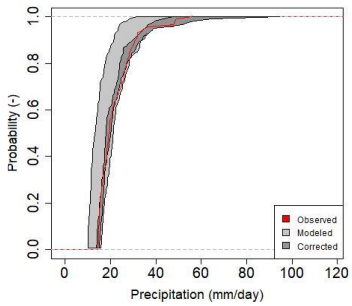

MS 40

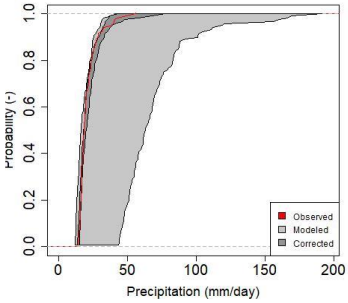

MS 41

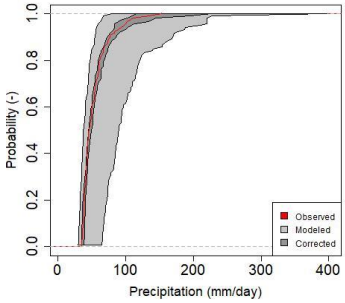

MS 42

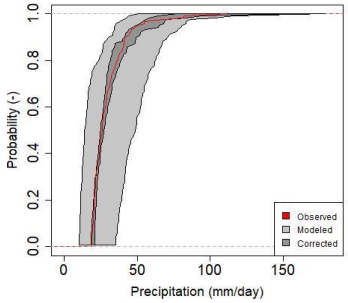

MS 43

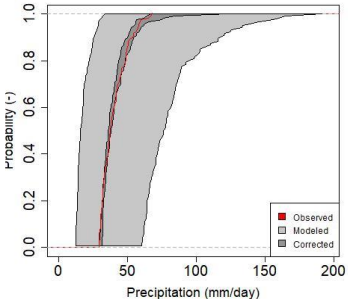

MS 44

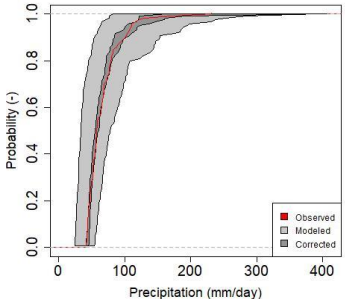

MS 45

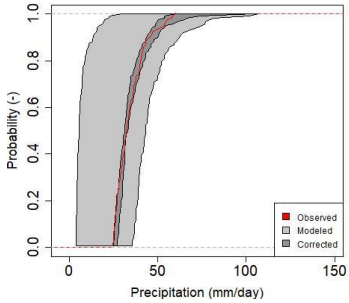

MS 46

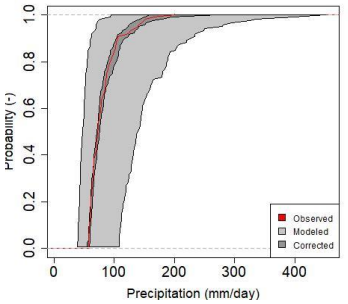

MS 47

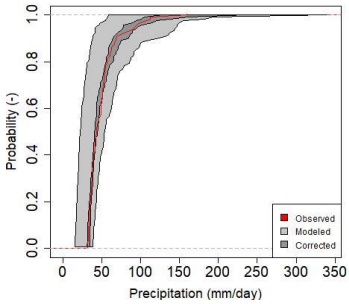

MS 48

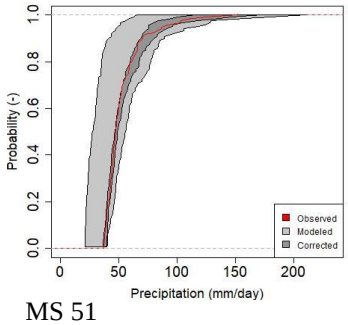

MS 49

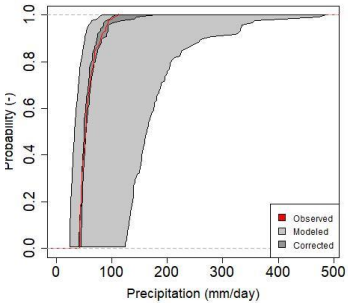

MS 50

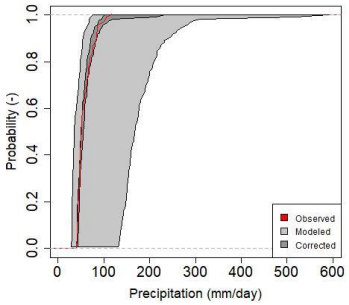

MS 51

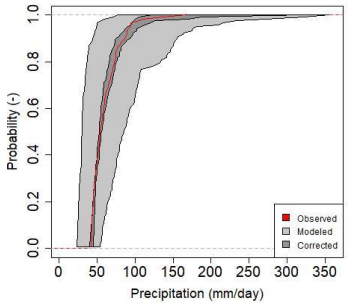

MS 52

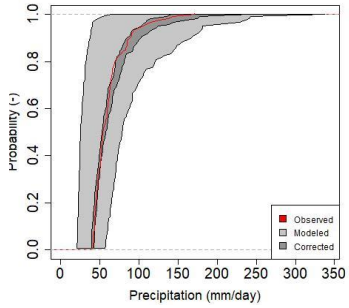
Probability (-)
0.0
0.2
0.4
0.6
0.8
1.0
0
50
100
150
200
250
300
350
Precipitation (mm/day)
Observed
Modeled
Corrected

MS 53

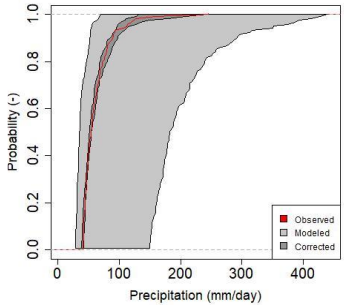
Probability (-)
0.0
0.2
0.4
0.6
0.8
1.0
0
100
200
300
400
Precipitation (mm/day)
Observed
Modeled
Corrected

C. RMSE and MAE Values of Remaining MSs for the Best Three RCMs

C.1 MAE Values of Remaining MSs

	RCM3						RCM5						RCM13					
M	U	LS	D1	D2	D3	D4	U	LS	D1	D2	D3	D4	U	LS	D1	D2	D3	D4
1	5.4	4.4	4.8	4.7	5.1	4.7	4.8	4.6	4.7	4.7	4.8	4.7	5.6	4.9	4.8	4.8	5.2	4.8
2	4.1	4.7	4.7	4.7	4.4	4.7	4.4	4.6	4.7	4.6	4.5	4.6	4.3	6.0	4.8	4.8	4.6	4.8
3	4.4	3.8	4.2	4.2	4.3	4.2	3.9	4.1	4.2	4.1	4.0	4.1	4.6	4.2	4.3	4.2	4.5	4.2
4	3.9	5.2	4.7	4.6	4.3	4.6	4.6	4.3	4.6	4.6	4.5	4.6	4.0	6.2	4.7	4.7	4.4	4.7
5	6.1	6.4	6.9	6.8	6.4	6.8	6.1	6.4	6.8	6.8	6.3	6.8	6.3	7.1	6.9	6.9	6.6	6.9
6	6.0	6.4	6.8	6.7	6.3	6.7	6.0	6.4	6.7	6.7	6.2	6.7	6.3	6.9	6.8	6.8	6.5	6.8
7	4.2	4.2	4.5	4.5	4.3	4.5	4.2	4.3	4.5	4.5	4.3	4.5	4.2	4.6	4.6	4.5	4.3	4.5
8	3.9	4.5	4.5	4.5	4.2	4.5	4.2	4.4	4.5	4.4	4.3	4.4	3.9	5.1	4.6	4.5	4.2	4.5
9	3.6	4.3	4.1	4.0	3.9	4.1	4.5	3.7	4.0	4.0	4.2	4.0	3.4	5.0	4.1	4.1	3.7	4.1
10	4.6	4.0	4.2	4.2	4.5	4.2	4.5	3.9	4.2	4.2	4.3	4.2	4.7	4.8	4.2	4.2	4.5	4.2
11	7.7	8.9	8.4	8.4	8.2	8.4	7.8	8.7	8.4	8.4	8.2	8.4	9.0	11.9	8.7	8.7	9.2	8.7
12	6.7	6.3	6.7	6.7	6.7	6.7	6.5	7.1	6.8	6.8	6.7	6.8	7.8	6.9	6.9	6.9	7.3	6.9
13	6.5	5.9	6.1	6.1	6.3	6.1	6.0	6.2	6.1	6.2	6.0	6.2	7.2	6.6	6.3	6.3	6.7	6.3
14	8.9	9.0	8.5	8.5	9.0	8.5	9.9	9.0	8.6	8.5	9.4	8.5	11.3	10.5	8.8	8.8	10.6	8.8
15	15.4	16.6	18.5	18.4	15.9	18.4	16.9	17.7	18.8	18.8	16.9	18.8	17.2	19.4	19.3	19.2	17.4	19.2
16	13.2	14.4	14.8	15.0	13.8	15.0	14.5	16.1	15.3	15.3	14.9	15.5	14.6	16.7	15.4	15.5	14.6	15.5
17	10.3	13.5	12.6	12.7	11.4	12.7	13.9	15.6	13.0	13.0	14.4	13.0	11.3	18.0	13.2	13.2	12.2	13.2
18	7.8	9.0	8.7	8.8	8.2	8.8	8.5	9.1	9.0	9.0	8.6	8.9	8.4	11.5	9.0	9.1	8.8	9.1
19	8.0	10.2	9.2	9.2	8.6	9.2	9.1	10.0	9.3	9.3	9.2	9.3	8.7	12.3	9.3	9.4	9.2	9.4
20	9.3	8.6	9.5	9.6	9.1	9.6	8.9	10.3	9.8	9.8	9.1	9.9	10.6	9.5	9.8	9.8	10.0	9.8
21	8.6	9.3	9.4	9.5	8.9	9.5	8.0	9.8	9.4	9.5	8.7	9.5	9.2	10.0	9.6	9.6	9.3	9.6
22	11.2	16.8	14.4	14.6	12.6	14.5	11.5	15.8	14.4	14.7	12.7	14.6	11.4	21.1	14.9	15.1	12.9	15.0
23	12.9	14.2	14.0	14.0	13.5	13.9	15.1	15.8	14.3	14.1	15.2	14.1	14.1	15.7	14.3	14.3	14.3	14.3
24	4.7	5.2	4.6	4.6	4.7	4.6	4.9	4.4	4.7	4.6	4.7	4.6	5.0	5.9	4.7	4.7	5.0	4.7
25	4.9	6.0	5.3	5.4	5.3	5.4	5.2	5.1	5.3	5.3	5.2	5.3	5.2	7.7	5.5	5.5	5.6	5.5
26	3.9	4.9	4.4	4.4	4.2	4.4	4.7	4.3	4.4	4.4	4.5	4.4	4.2	6.2	4.5	4.5	4.5	4.5
27	4.6	4.3	4.7	4.6	4.6	4.6	4.3	4.7	4.6	4.6	4.5	4.6	4.9	4.7	4.7	4.7	4.9	4.7
28	4.4	4.4	4.6	4.5	4.5	4.5	4.4	4.4	4.6	4.5	4.4	4.5	4.6	5.1	4.6	4.6	4.7	4.6
29	5.2	4.9	5.6	5.5	5.3	5.5	4.8	5.3	5.4	5.5	5.0	5.5	5.2	5.2	5.6	5.5	5.3	5.5
30	4.4	4.3	4.5	4.5	4.5	4.5	4.8	4.2	4.5	4.5	4.6	4.5	4.5	5.0	4.6	4.6	4.6	4.6
31	4.8	5.3	5.7	5.7	5.2	5.7	5.3	5.4	5.7	5.7	5.4	5.6	4.9	6.0	5.8	5.7	5.3	5.7
32	5.7	4.3	4.5	4.4	5.3	4.5	4.9	4.1	4.5	4.4	4.6	4.4	6.1	5.1	4.6	4.6	5.6	4.6
33	4.3	4.7	4.7	4.6	4.5	4.6	4.5	4.5	4.7	4.6	4.5	4.6	4.5	5.4	4.8	4.8	4.7	4.8
34	5.1	5.7	5.6	5.6	5.4	5.6	5.5	5.4	5.7	5.7	5.5	5.7	5.2	6.6	5.8	5.8	5.5	5.8
35	7.6	6.7	7.2	7.2	7.2	7.2	7.4	7.1	7.2	7.2	7.2	7.2	8.4	7.7	7.4	7.4	7.7	7.4
36	5.1	4.7	4.9	4.8	5.1	4.8	5.0	4.8	4.8	4.8	4.9	4.8	5.3	5.2	4.9	4.9	5.1	4.9
37	7.6	9.7	9.7	9.6	8.6	9.6	7.9	9.5	9.7	9.6	8.7	9.7	7.8	10.9	9.9	9.9	8.8	9.9
38	4.6	4.1	4.4	4.3	4.5	4.3	3.9	4.3	4.3	4.3	4.1	4.3	4.5	4.2	4.4	4.4	4.4	4.4
39	3.8	3.7	4.0	4.0	3.9	4.0	3.9	4.0	4.1	4.1	3.9	4.1	3.9	4.0	4.1	4.1	3.9	4.1
40	4.2	4.2	4.2	4.2	4.2	4.2	5.6	3.8	4.1	4.1	4.8	4.1	4.1	5.2	4.2	4.2	4.2	4.2
41	10.0	10.1	10.4	10.5	10.2	10.5	10.4	10.9	10.7	10.7	10.5	10.8	11.3	11.7	10.7	10.8	11.2	10.8
42	5.2	5.3	5.7	5.6	5.4	5.6	5.8	5.3	5.7	5.7	5.6	5.7	5.5	5.7	5.8	5.7	5.7	5.7
43	6.4	7.9	7.8	7.7	7.1	7.7	7.2	7.4	7.8	7.7	7.4	7.7	6.4	8.1	7.9	7.8	7.1	7.8
44	11.3	12.0	12.4	12.2	11.8	12.2	12.3	12.6	12.3	12.2	12.2	12.2	12.4	12.6	12.5	12.4	12.6	12.4
45	4.9	7.2	6.4	6.4	5.6	6.4	6.4	6.4	6.5	6.5	6.4	6.5	5.1	8.7	6.6	6.5	5.8	6.5
46	14.0	14.7	15.1	15.1	14.4	15.1	14.3	16.2	15.6	15.4	14.9	15.4	15.7	18.1	15.8	15.9	15.3	15.9
47	7.9	9.5	9.0	9.0	8.4	9.0	9.0	9.5	9.3	9.1	9.3	9.2	8.9	12.7	9.2	9.3	9.2	9.3
48	8.8	9.3	10.0	9.9	9.1	9.9	8.8	10.2	10.1	10.0	9.3	10.0	9.6	10.3	10.2	10.2	9.7	10.2
49	9.7	12.5	11.4	11.4	10.7	11.4	10.3	13.1	11.4	11.3	11.0	11.4	10.4	13.2	11.6	11.6	11.2	11.6
50	10.6	11.0	11.0	11.0	10.8	11.0	11.5	12.1	11.0	11.1	11.6	11.1	12.0	12.9	11.3	11.4	11.6	11.4
51	9.8	10.5	11.5	11.4	10.3	11.4	11.4	12.1	11.9	11.6	11.7	11.6	11.2	11.7	11.7	11.6	11.1	11.6
52	9.9	10.7	11.5	11.5	10.3	11.5	9.8	12.4	11.7	11.7	10.5	11.7	11.7	11.6	11.7	11.8	11.4	11.8
53	10.4	11.3	11.7	11.7	10.9	11.7	11.0	12.0	11.7	11.7	11.2	11.7	11.0	12.6	11.9	12.0	11.2	12.0

C.2 MAE Values of Remaining MSs

	RCM3						RCM5						RCM13					
M	U	LS	D1	D2	D3	D4	U	LS	D1	D2	D3	D4	U	LS	D1	D2	D3	D4
1	2.5	2.0	2.1	2.1	2.1	2.1	2.2	2.0	2.0	2.0	2.1	2.0	2.5	2.1	2.1	2.1	2.2	2.1
2	1.6	1.9	1.9	1.9	1.8	1.9	1.9	1.9	1.9	1.9	1.9	1.9	1.7	2.0	1.9	1.9	1.9	1.9
3	1.9	1.6	1.6	1.6	1.6	1.6	1.5	1.6	1.5	1.6	1.5	1.6	1.8	1.6	1.6	1.6	1.6	1.6
4	1.5	1.9	1.9	1.8	1.8	1.8	2.0	1.8	1.8	1.8	1.8	1.8	1.5	1.9	1.9	1.9	1.8	1.9
5	2.5	2.6	2.7	2.7	2.6	2.7	2.5	2.6	2.6	2.7	2.6	2.7	2.5	2.6	2.7	2.7	2.6	2.7
6	2.2	2.4	2.4	2.5	2.4	2.5	2.3	2.4	2.4	2.4	2.3	2.4	2.4	2.4	2.4	2.4	2.4	2.4
7	1.5	1.5	1.5	1.5	1.5	1.5	1.5	1.5	1.5	1.5	1.5	1.5	1.5	1.6	1.6	1.6	1.5	1.6
8	1.3	1.6	1.6	1.6	1.5	1.6	1.6	1.6	1.6	1.6	1.5	1.6	1.4	1.6	1.6	1.6	1.5	1.6
9	1.2	1.5	1.4	1.4	1.4	1.4	1.8	1.4	1.4	1.4	1.5	1.4	1.2	1.5	1.4	1.4	1.4	1.4
10	1.9	1.6	1.6	1.6	1.6	1.6	1.9	1.6	1.6	1.6	1.6	1.6	1.9	1.6	1.6	1.6	1.7	1.6
11	3.0	3.4	3.4	3.3	3.3	3.3	3.1	3.4	3.4	3.4	3.3	3.4	3.5	3.6	3.5	3.5	3.6	3.5
12	2.8	2.6	2.6	2.6	2.6	2.6	2.5	2.7	2.6	2.6	2.6	2.6	3.3	2.6	2.8	2.8	2.8	2.8
13	2.5	2.2	2.3	2.3	2.3	2.3	2.2	2.3	2.3	2.3	2.2	2.3	2.9	2.3	2.3	2.4	2.4	2.4
14	3.3	3.3	3.3	3.3	3.3	3.3	3.8	3.3	3.3	3.3	3.4	3.3	4.2	3.4	3.4	3.4	3.7	3.4
15	4.8	5.2	5.3	5.4	4.9	5.4	5.5	5.4	5.5	5.5	5.3	5.5	5.5	5.4	5.6	5.7	5.4	5.7
16	4.7	5.2	5.2	5.2	5.0	5.2	5.0	5.3	5.3	5.3	5.2	5.3	5.5	5.4	5.6	5.6	5.4	5.6
17	3.3	4.4	4.4	4.3	4.1	4.3	4.1	4.5	4.4	4.4	4.4	4.4	3.9	4.6	4.7	4.6	4.4	4.6
18	2.4	2.7	2.7	2.7	2.6	2.7	2.8	2.8	2.8	2.8	2.8	2.8	2.6	2.8	2.8	2.8	2.8	2.8
19	2.3	2.9	2.9	2.8	2.7	2.8	2.8	2.9	2.9	2.9	2.9	2.9	2.6	2.9	2.9	2.9	2.9	2.9
20	3.6	3.1	3.2	3.2	3.2	3.2	3.0	3.2	3.2	3.2	3.1	3.2	4.0	3.2	3.3	3.4	3.4	3.4
21	3.3	3.6	3.5	3.5	3.4	3.5	2.9	3.6	3.5	3.5	3.4	3.5	3.6	3.6	3.6	3.6	3.6	3.6
22	3.4	5.3	5.2	5.1	4.6	5.1	3.7	5.4	5.2	5.1	4.7	5.1	3.6	5.5	5.5	5.5	4.9	5.4
23	4.2	4.5	4.6	4.6	4.5	4.6	4.8	4.6	4.7	4.7	4.8	4.7	4.8	4.5	4.8	4.8	4.8	4.8
24	2.0	1.9	1.9	1.9	1.9	1.9	2.2	1.9	1.9	1.9	1.9	1.9	2.1	2.0	2.0	2.0	2.0	2.0
25	2.2	2.4	2.4	2.4	2.4	2.4	2.5	2.4	2.4	2.4	2.4	2.4	2.2	2.6	2.5	2.5	2.5	2.5
26	1.6	1.8	1.8	1.8	1.7	1.8	2.0	1.8	1.8	1.8	1.8	1.8	1.7	1.9	1.8	1.8	1.8	1.8
27	2.0	1.8	1.8	1.8	1.8	1.8	1.7	1.8	1.8	1.8	1.8	1.8	2.0	1.8	1.8	1.8	1.9	1.8
28	1.9	1.8	1.9	1.8	1.8	1.8	1.9	1.8	1.8	1.8	1.8	1.8	1.9	1.9	1.9	1.9	1.9	1.9
29	2.3	2.1	2.2	2.2	2.2	2.2	2.0	2.2	2.2	2.2	2.1	2.2	2.2	2.2	2.2	2.2	2.2	2.2
30	1.9	1.9	1.9	1.9	1.9	1.9	2.2	1.8	1.9	1.9	1.9	1.9	1.9	1.9	1.9	1.9	1.9	1.9
31	1.8	2.1	2.1	2.1	2.0	2.1	2.1	2.1	2.1	2.1	2.1	2.1	1.9	2.1	2.1	2.1	2.0	2.1
32	2.3	1.7	1.7	1.7	1.9	1.7	2.1	1.7	1.8	1.8	1.8	1.8	2.3	1.8	1.8	1.8	1.9	1.8
33	1.7	1.9	1.8	1.8	1.8	1.8	1.9	1.8	1.8	1.8	1.8	1.8	1.8	1.9	1.9	1.9	1.9	1.9
34	2.2	2.4	2.4	2.4	2.3	2.4	2.5	2.4	2.4	2.4	2.4	2.4	2.3	2.5	2.5	2.5	2.4	2.5
35	3.2	2.8	2.8	2.9	2.9	2.9	3.0	2.8	2.8	2.8	2.9	2.8	3.6	2.9	3.0	3.0	3.1	3.0
36	2.0	1.9	1.9	1.9	1.9	1.9	2.0	1.8	1.8	1.8	1.8	1.8	2.1	1.9	1.9	1.9	1.9	1.9
37	2.7	3.6	3.7	3.7	3.4	3.7	3.0	3.6	3.6	3.7	3.4	3.7	2.8	3.6	3.7	3.7	3.5	3.7
38	1.8	1.5	1.6	1.6	1.6	1.6	1.5	1.6	1.5	1.5	1.5	1.5	1.8	1.6	1.6	1.6	1.6	1.6
39	1.4	1.4	1.4	1.4	1.3	1.4	1.4	1.4	1.4	1.4	1.3	1.4	1.4	1.4	1.4	1.4	1.4	1.4
40	1.6	1.5	1.5	1.5	1.5	1.5	2.3	1.5	1.5	1.5	1.6	1.5	1.5	1.6	1.5	1.5	1.5	1.5
41	3.9	4.1	4.1	4.0	4.0	4.0	4.1	4.1	4.1	4.1	4.1	4.1	4.3	4.2	4.2	4.1	4.2	4.1
42	1.8	1.9	1.9	1.9	1.9	1.9	2.2	1.9	1.9	1.9	1.9	1.9	1.9	1.9	1.9	1.9	1.9	1.9
43	2.4	3.0	3.1	3.1	2.9	3.1	2.9	3.0	3.0	3.0	3.0	3.0	2.5	3.0	3.1	3.1	3.0	3.1
44	4.0	4.2	4.3	4.3	4.2	4.3	4.5	4.3	4.3	4.3	4.3	4.3	4.4	4.3	4.4	4.4	4.4	4.4
45	1.6	2.3	2.3	2.2	2.0	2.2	2.4	2.3	2.3	2.3	2.3	2.3	1.7	2.4	2.3	2.3	2.1	2.3
46	5.0	5.2	5.3	5.3	5.2	5.3	5.1	5.4	5.5	5.5	5.4	5.5	5.9	5.5	5.7	5.7	5.6	5.7
47	2.3	2.8	2.8	2.8	2.7	2.8	2.7	2.8	2.8	2.8	2.8	2.8	2.7	2.9	2.9	2.9	2.9	2.9
48	3.3	3.5	3.5	3.6	3.4	3.6	3.2	3.5	3.5	3.6	3.4	3.6	3.7	3.6	3.7	3.7	3.6	3.7
49	3.7	4.6	4.5	4.5	4.4	4.5	4.0	4.6	4.5	4.5	4.4	4.5	4.0	4.6	4.6	4.6	4.5	4.6
50	3.9	4.0	4.0	4.0	4.0	4.0	4.0	4.0	4.0	4.0	4.0	4.0	4.6	4.2	4.2	4.2	4.3	4.2
51	3.7	4.0	4.1	4.1	3.9	4.1	3.8	4.1	4.1	4.1	4.0	4.1	4.4	4.0	4.2	4.2	4.1	4.2
52	3.5	3.7	3.8	3.8	3.6	3.8	3.1	3.8	3.8	3.8	3.6	3.8	4.3	3.8	3.9	4.0	3.9	4.0
53	3.9	4.2	4.2	4.2	4.1	4.2	4.1	4.3	4.3	4.3	4.2	4.3	4.2	4.3	4.4	4.4	4.3	4.4

D. Observed versus Bias Corrected and Uncorrected Model Outputs

D.1 Observed versus bias corrected and uncorrected model outputs of RCM 3

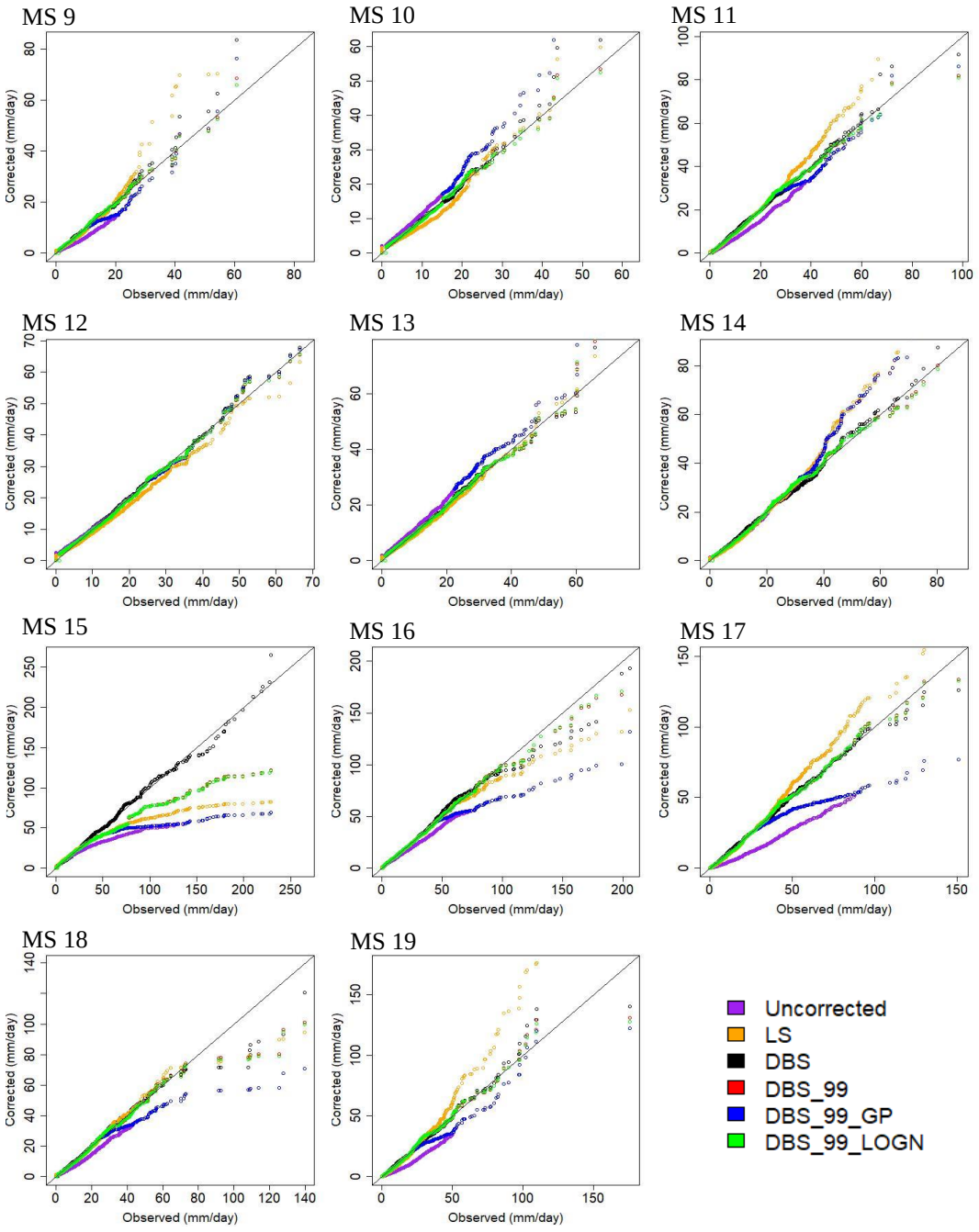

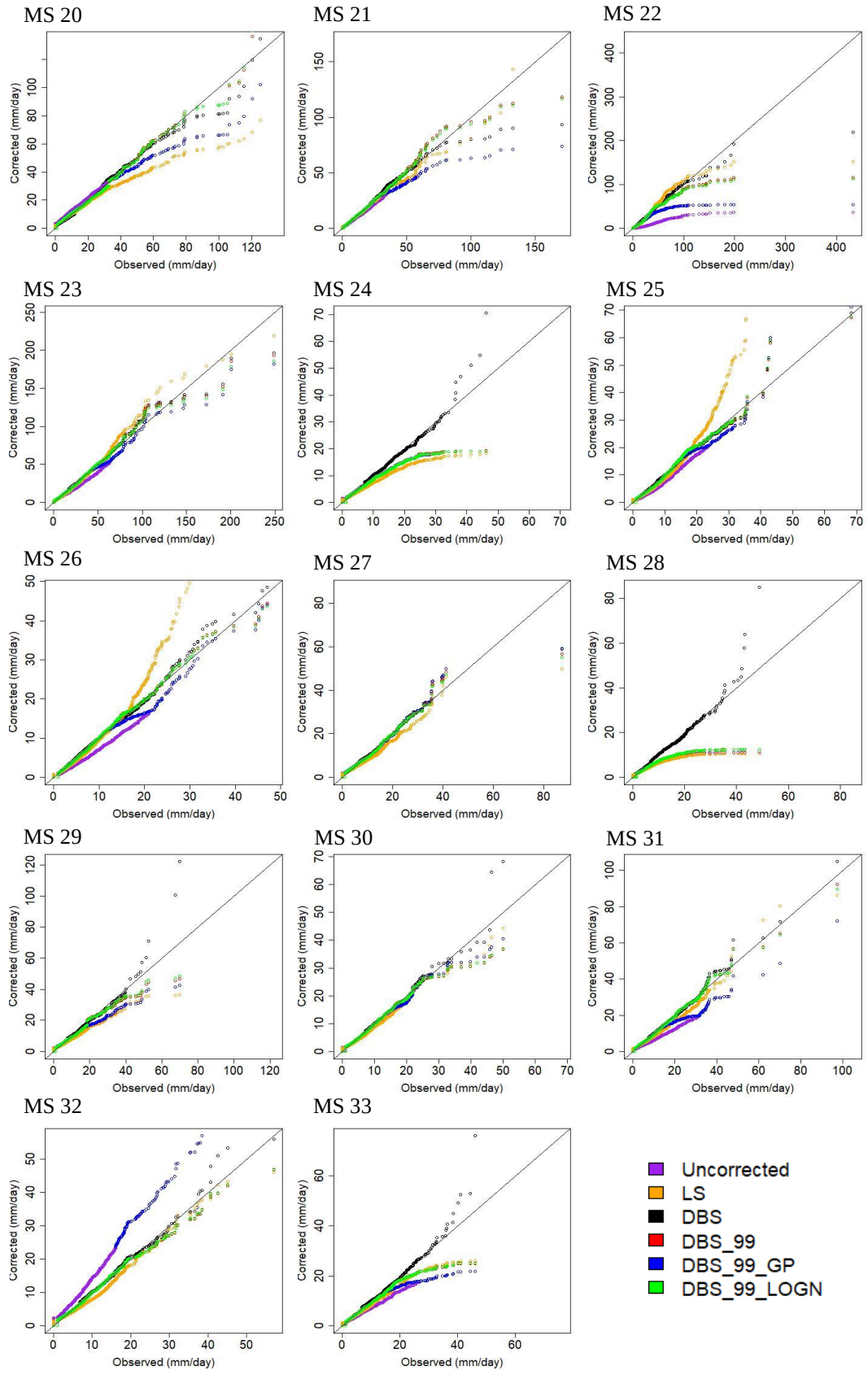
MS 20
MS 21
MS 22
MS 23
MS 24
MS 25
MS 26
MS 27
MS 28
MS 29
MS 30
MS 31
MS 32
MS 33
Corrected (mm/day)
Observed (mm/day)
Uncorrected
LS
DBS
DBS_99
DBS_99_GP
DBS_99_LOGN

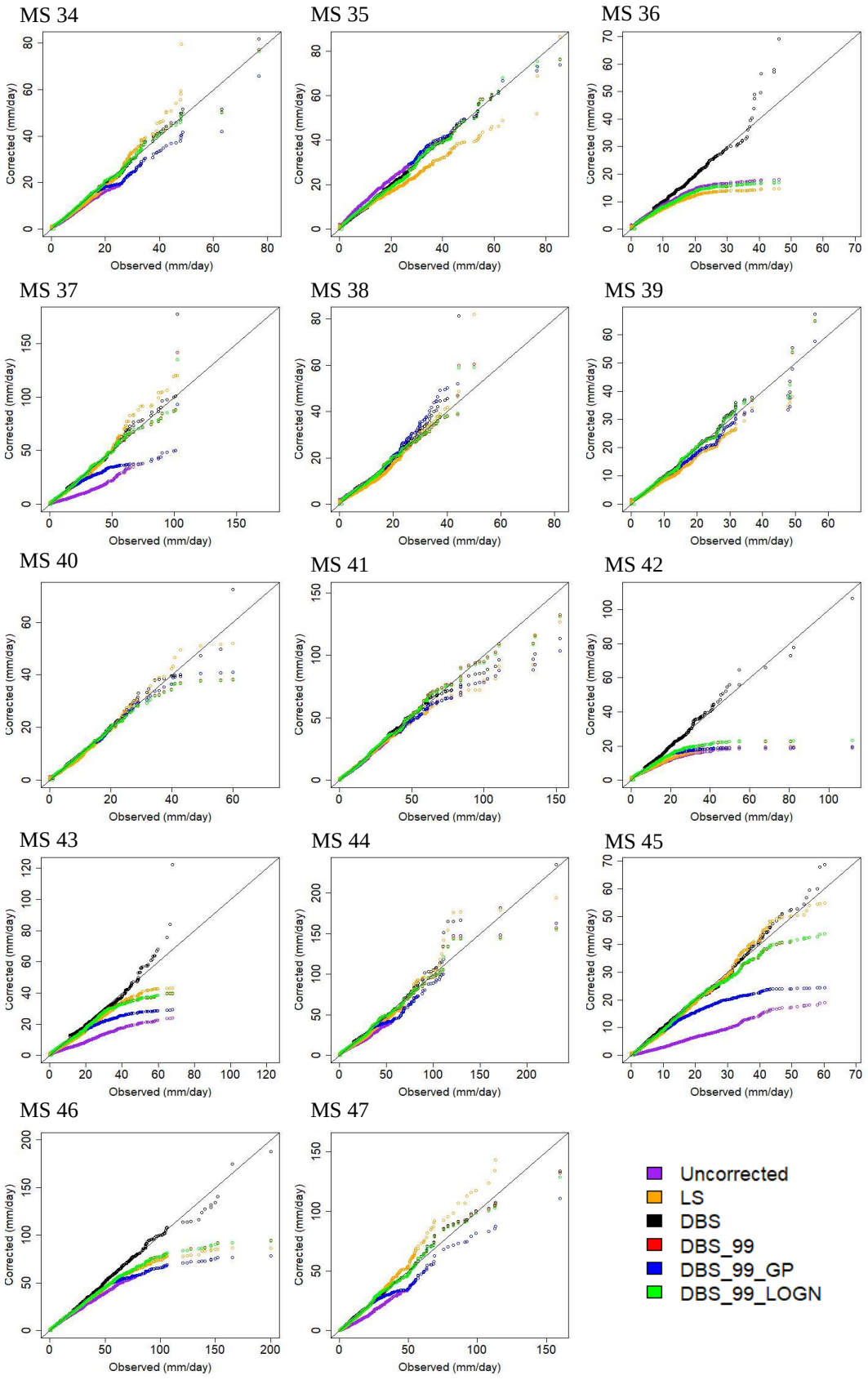
MS 34
MS 35
MS 36
MS 37
MS 38
MS 39
MS 40
MS 41
MS 42
MS 43
MS 44
MS 45
MS 46
MS 47
Corrected (mm/day)
Observed (mm/day)
Uncorrected
LS
DBS
DBS_99
DBS_99_GP
DBS_99_LOGN

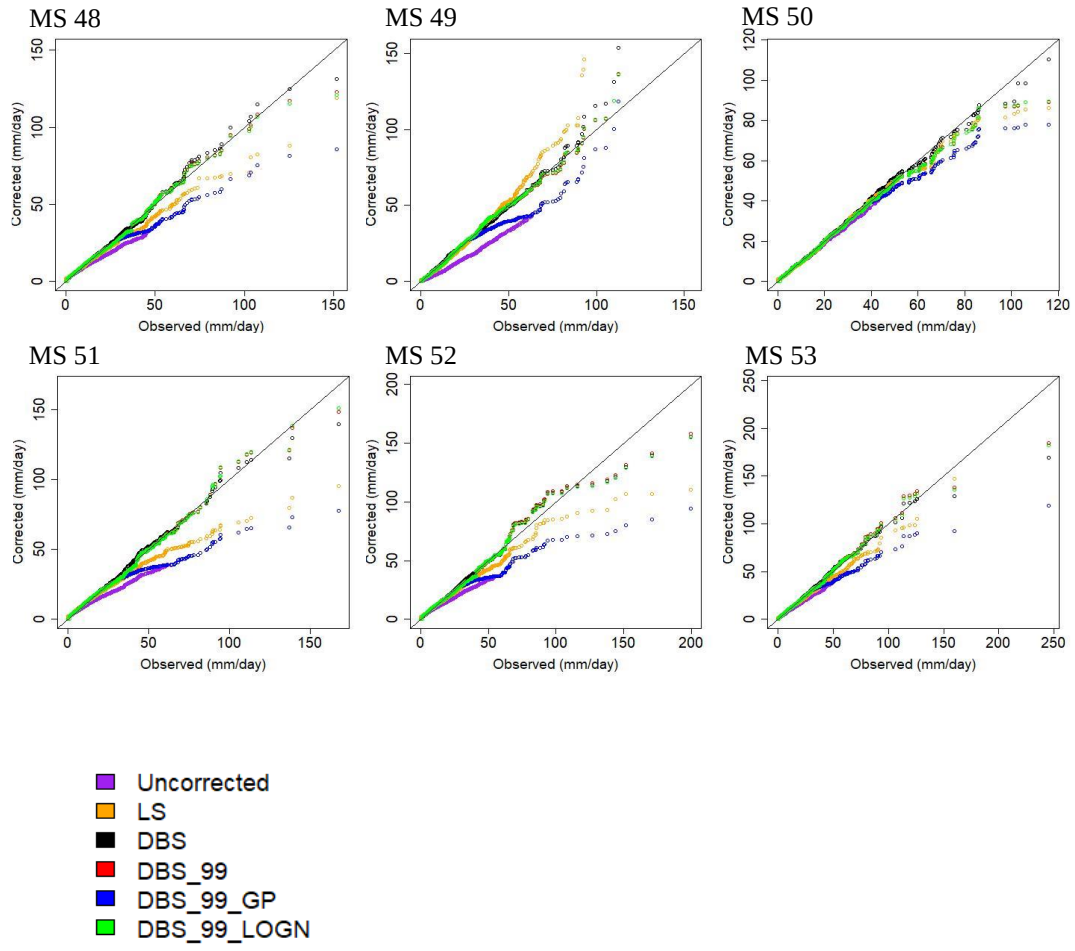
MS 48
MS 49
MS 50
MS 51
MS 52
MS 53
Corrected (mm/day)
Observed (mm/day)
Uncorrected
LS
DBS
DBS_99
DBS_99_GP
DBS_99_LOGN

D.2 Observed versus bias corrected and uncorrected model outputs

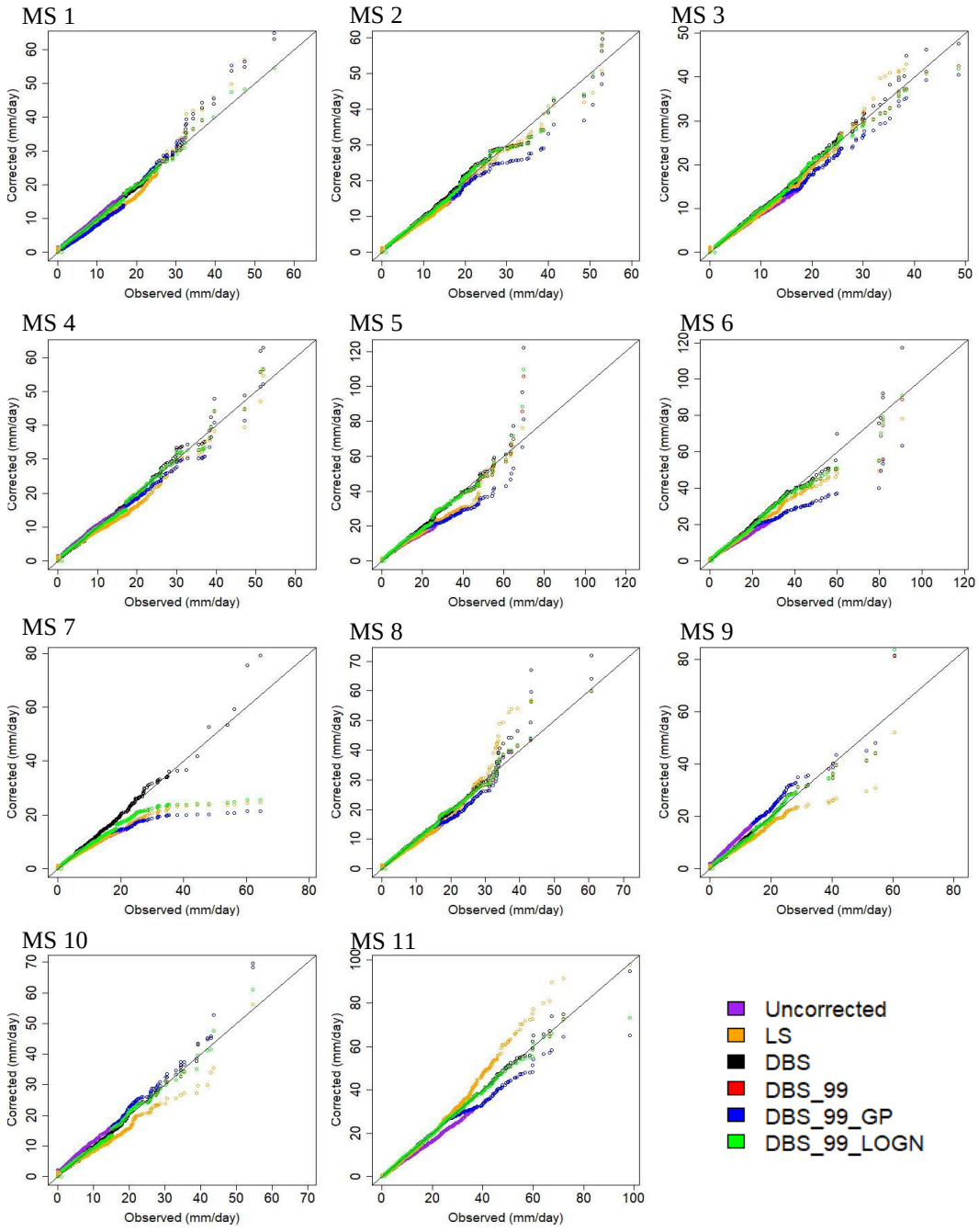

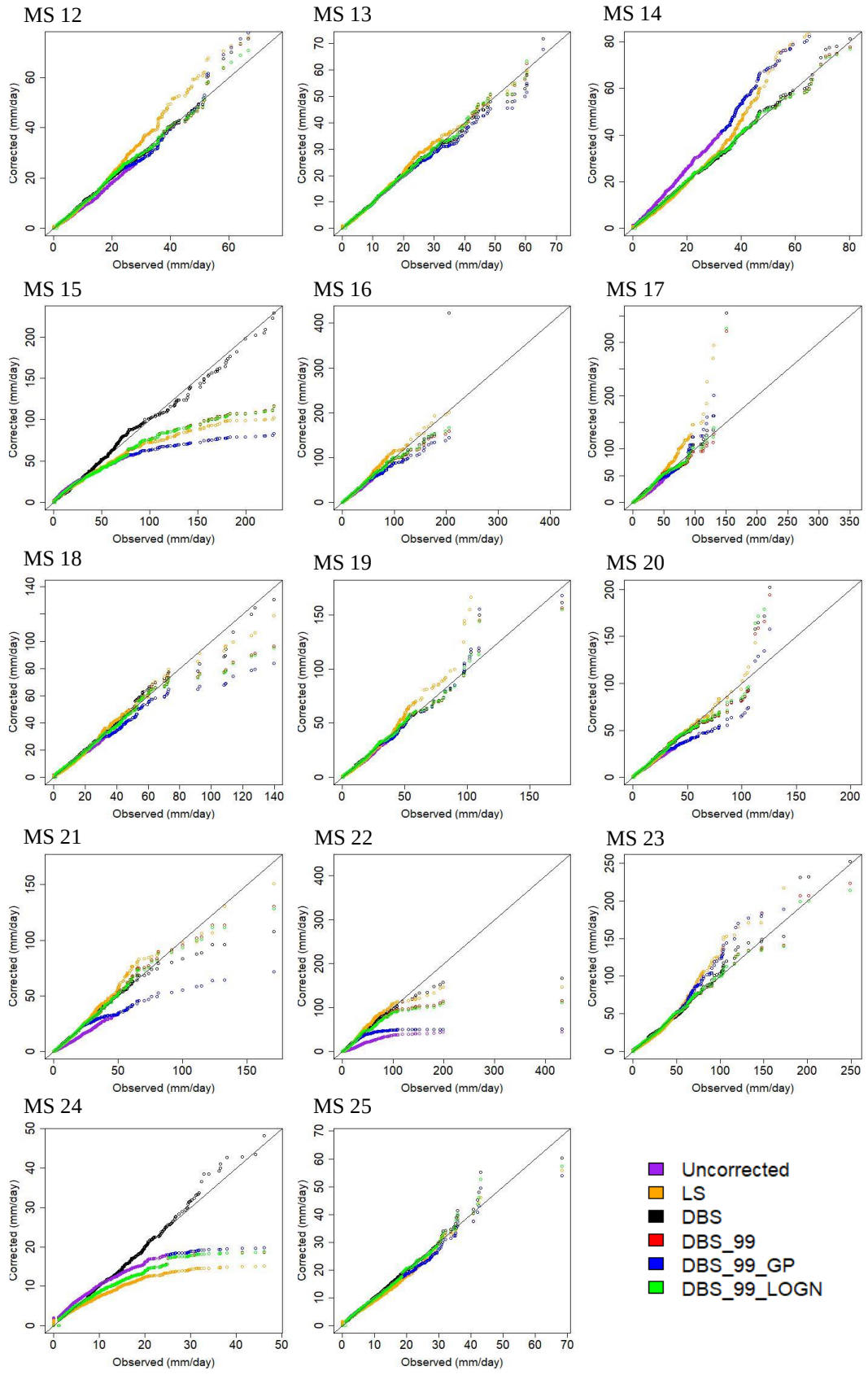
MS 12
MS 13
MS 14
MS 15
MS 16
MS 17
MS 18
MS 19
MS 20
MS 21
MS 22
MS 23
MS 24
MS 25
Corrected (mm/day)
Observed (mm/day)
Uncorrected
LS
DBS
DBS_99
DBS_99_GP
DBS_99_LOGN

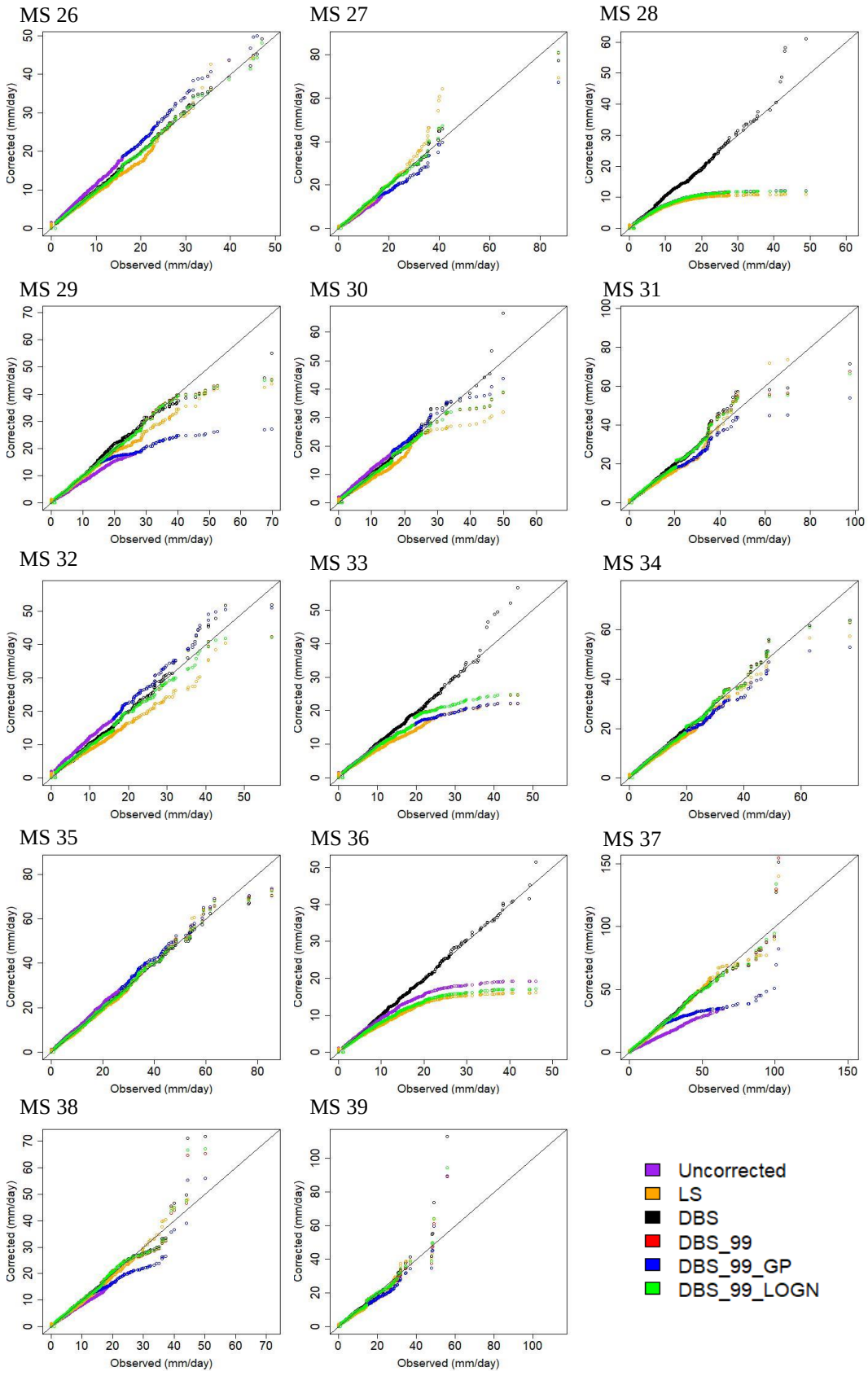
MS 26
MS 27
MS 28
MS 29
MS 30
MS 31
MS 32
MS 33
MS 34
MS 35
MS 36
MS 37
MS 38
MS 39
Corrected (mm/day)
Observed (mm/day)
Uncorrected
LS
DBS
DBS_99
DBS_99_GP
DBS_99_LOGN

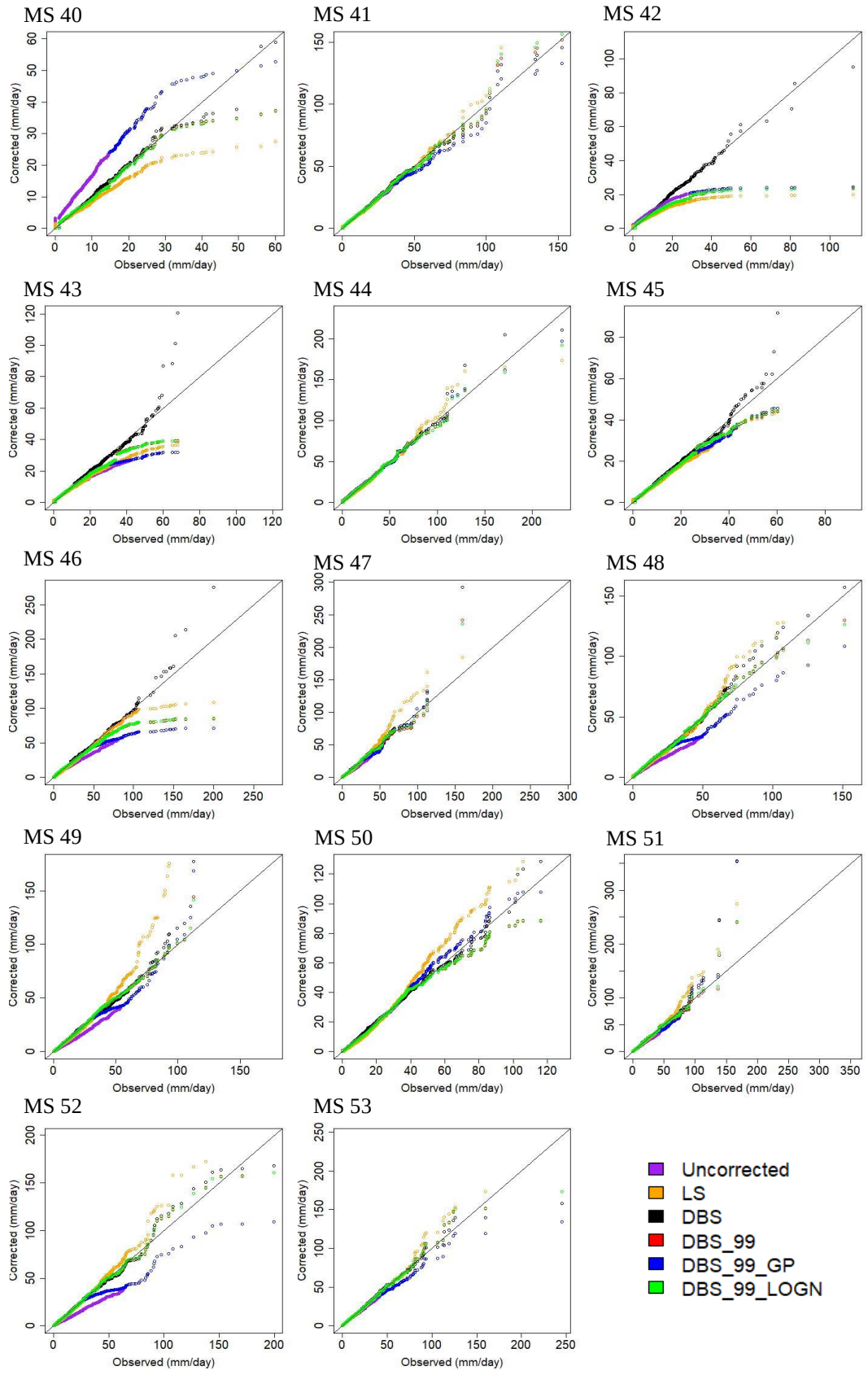
MS 40
MS 41
MS 42
MS 43
MS 44
MS 45
MS 46
MS 47
MS 48
MS 49
MS 50
MS 51
MS 52
MS 53
Corrected (mm/day)
Observed (mm/day)
Uncorrected
LS
DBS
DBS_99
DBS_99_GP
DBS_99_LOGN

D.3 Observed versus bias corrected and uncorrected model outputs of RCM 13

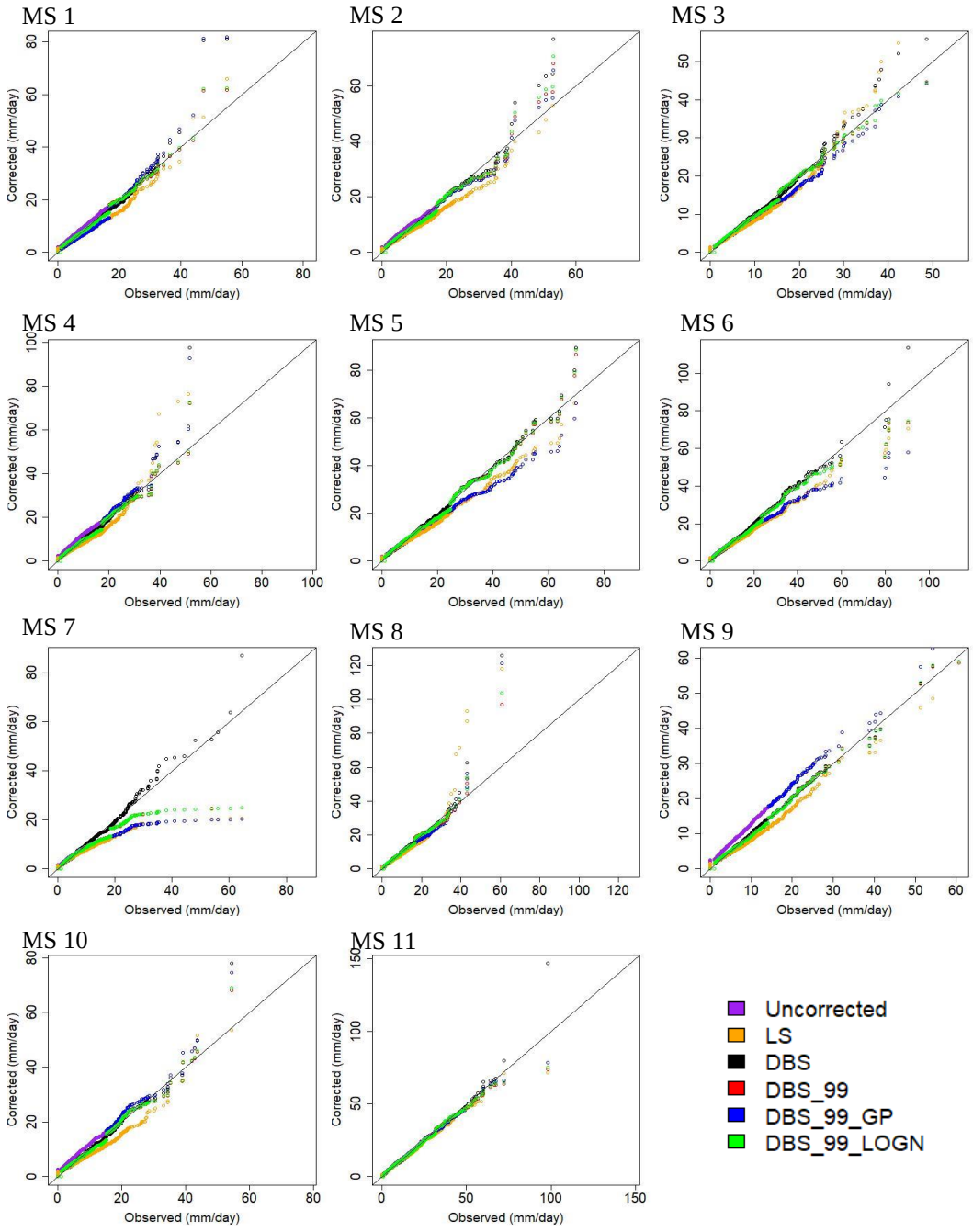

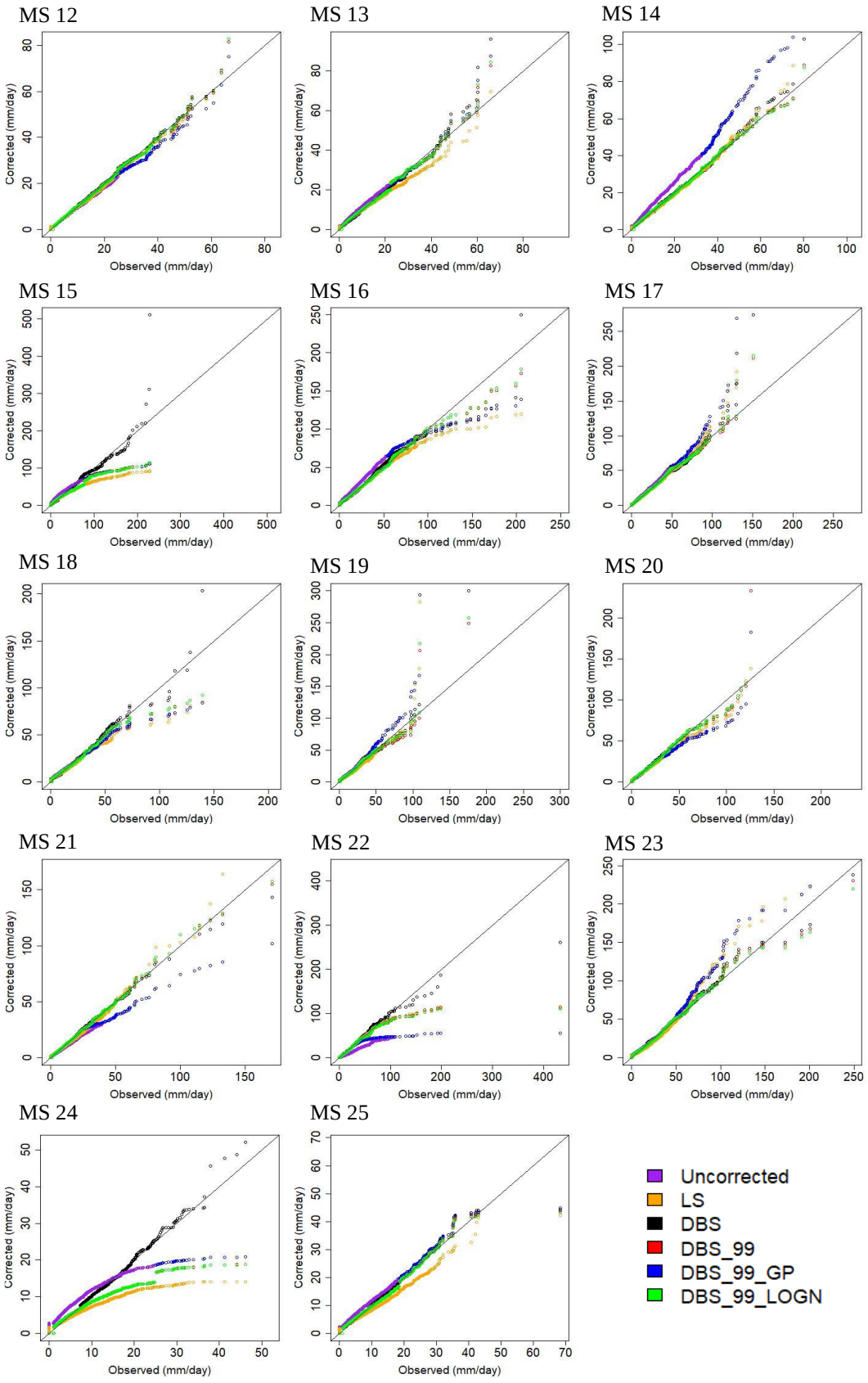
MS 12
MS 13
MS 14
MS 15
MS 16
MS 17
MS 18
MS 19
MS 20
MS 21
MS 22
MS 23
MS 24
MS 25
Corrected (mm/day)
Observed (mm/day)
Uncorrected
LS
DBS
DBS_99
DBS_99_GP
DBS_99_LOGN

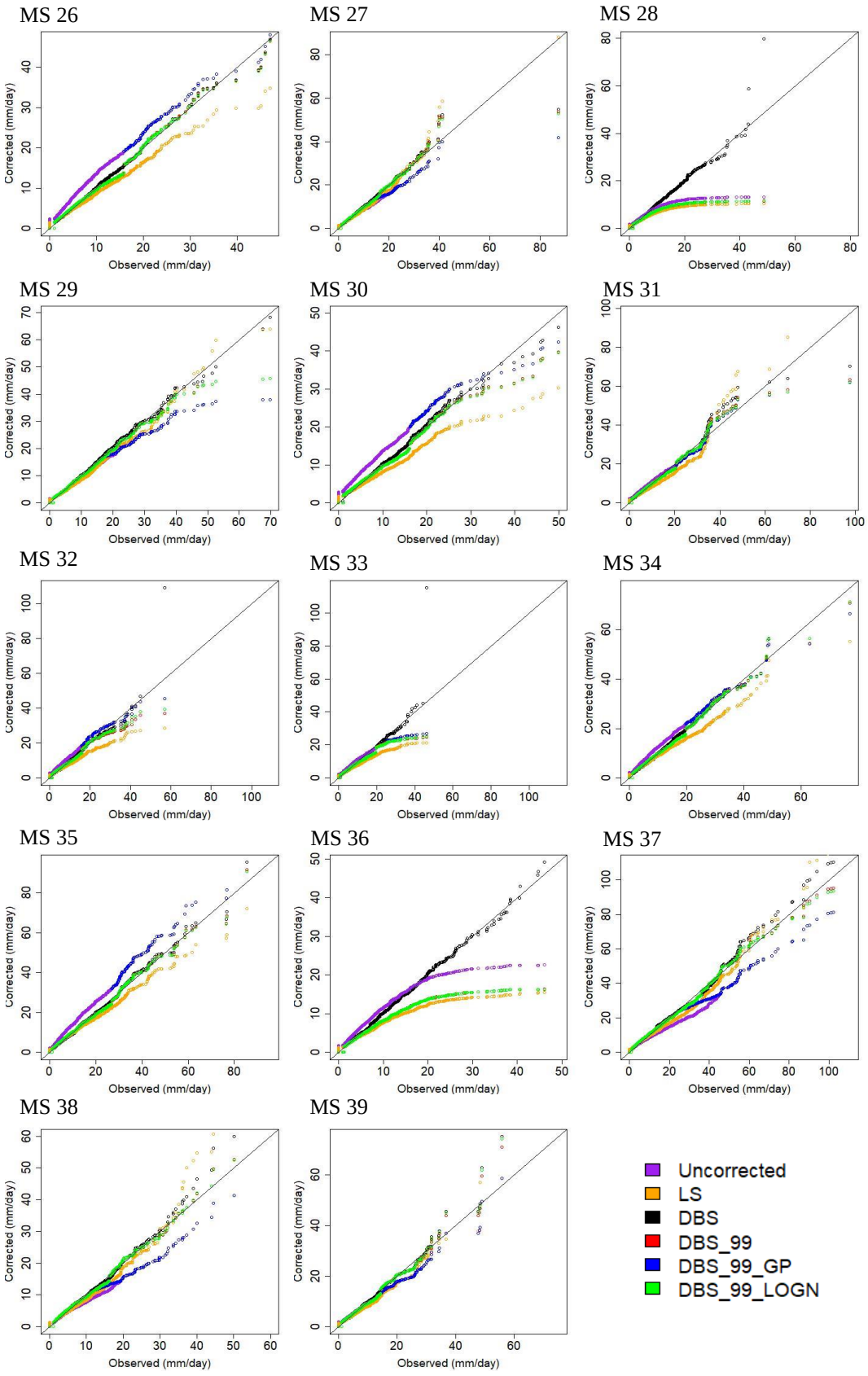
MS 26
MS 27
MS 28
MS 29
MS 30
MS 31
MS 32
MS 33
MS 34
MS 35
MS 36
MS 37
MS 38
MS 39
Corrected (mm/day)
Observed (mm/day)
Uncorrected
LS
DBS
DBS_99
DBS_99_GP
DBS_99_LOGN

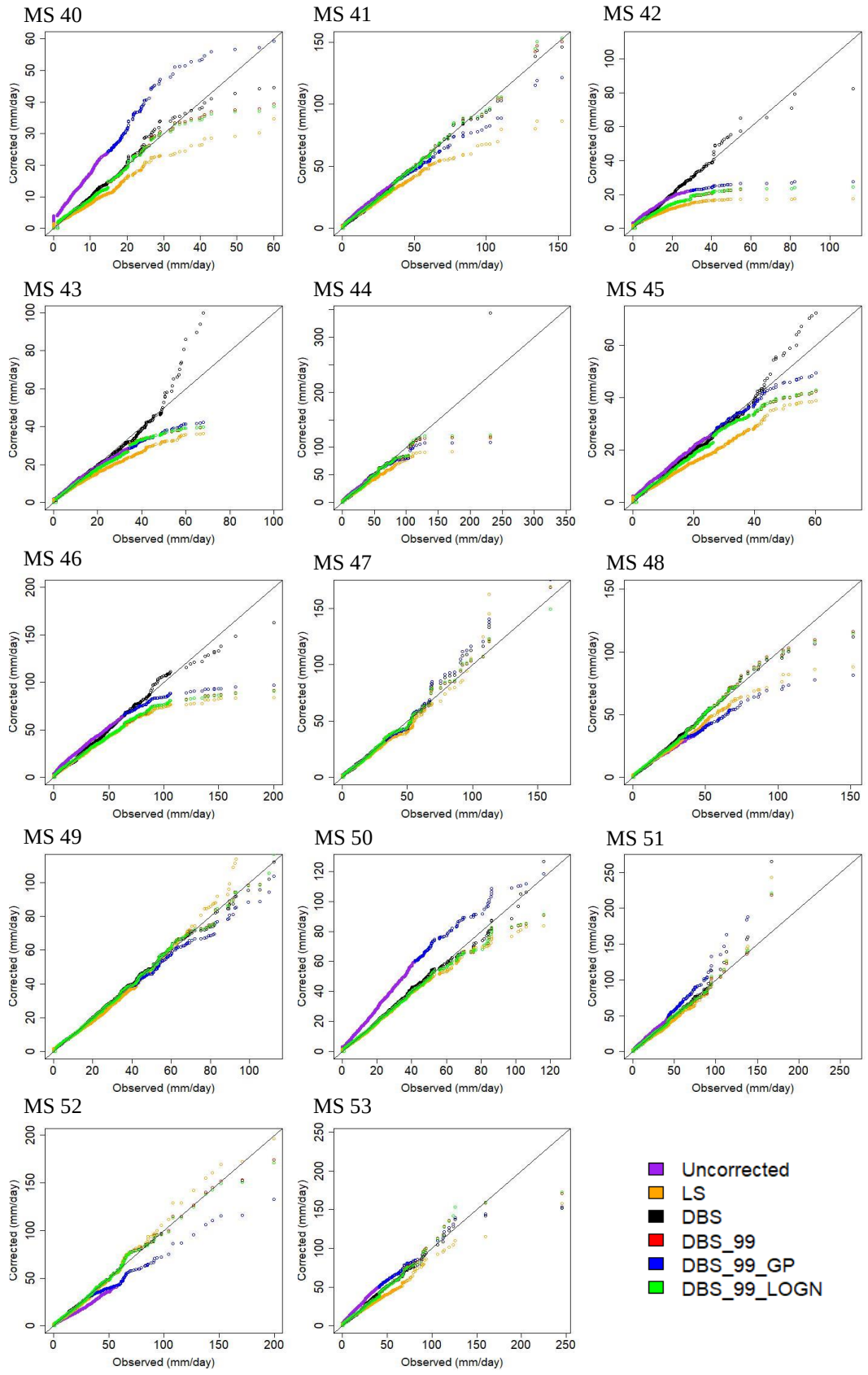
MS 40
MS 41
MS 42
MS 43
MS 44
MS 45
MS 46
MS 47
MS 48
MS 49
MS 50
MS 51
MS 52
MS 53
Corrected (mm/day)
Observed (mm/day)
Uncorrected
LS
DBS
DBS_99
DBS_99_GP
DBS_99_LOGN

E. Box Plots of Extreme Parts of Remaining MSs

E.1 Box Plots of Extreme Parts (2011-2040)

MS 10

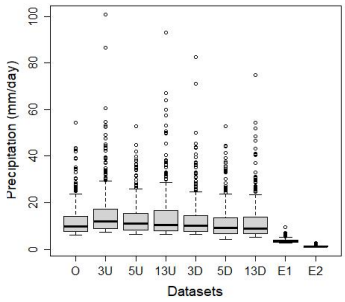

MS 11

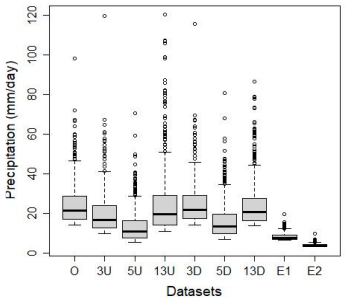

MS 12

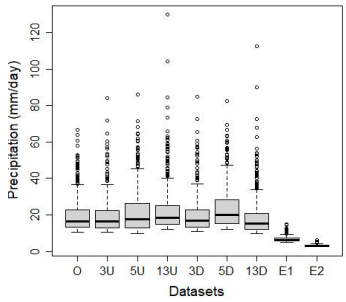

MS 13

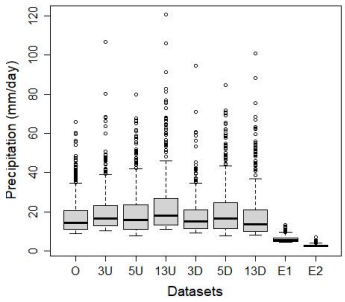

MS 14

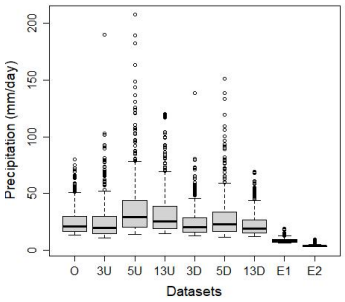

MS 15

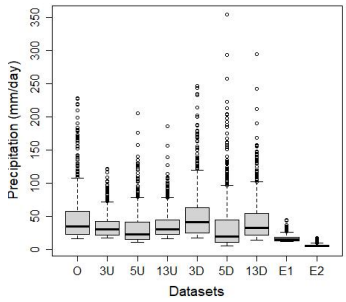

MS 16

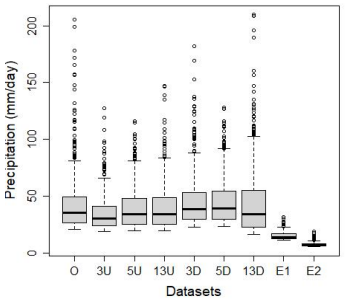

MS 17

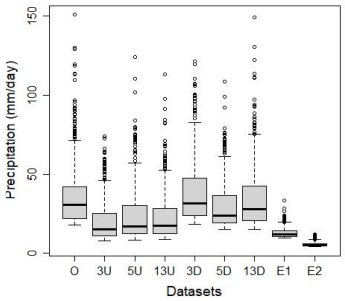

MS 18

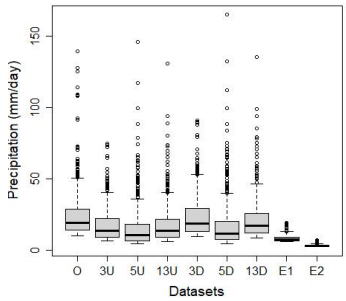

MS 19

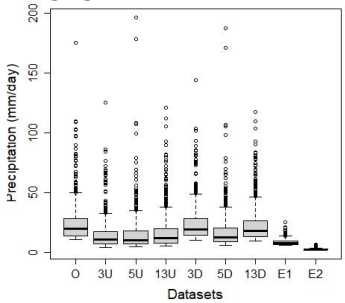

MS 20

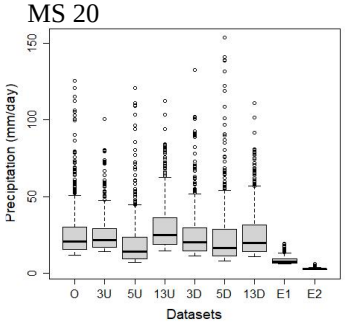

MS 21

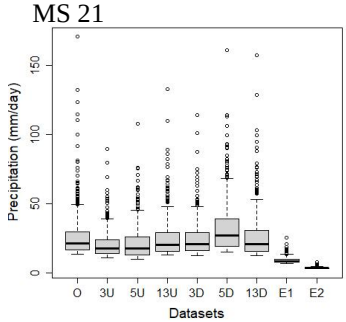

MS 22

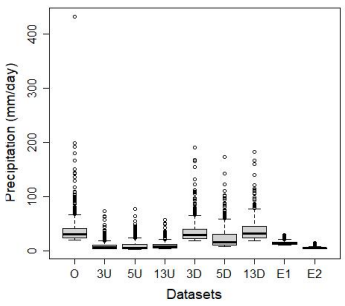

MS 23

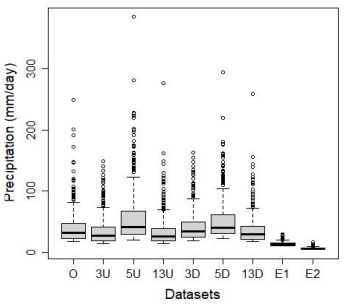

MS 24

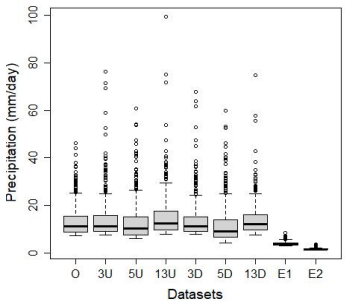

MS 25

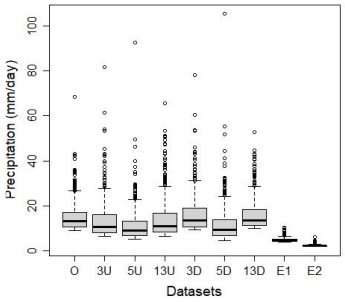

MS 26

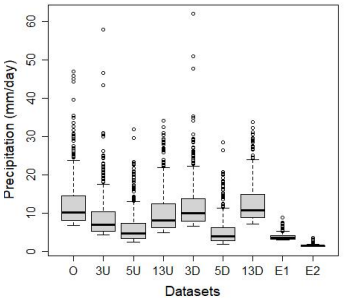

MS 27

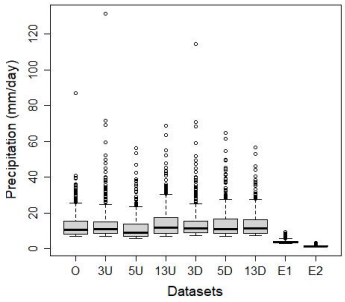

MS 28

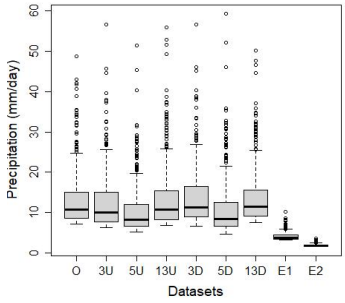

MS 29

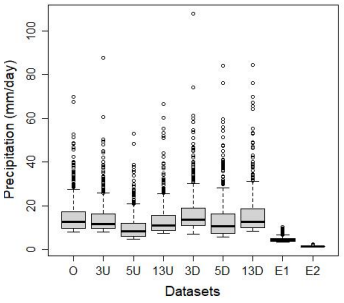

MS 30

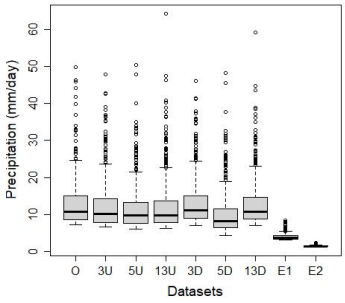

MS 31

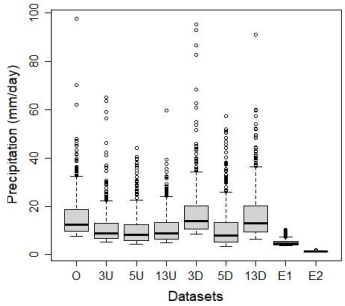

MS 32

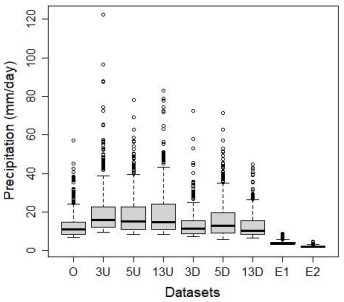

MS 33

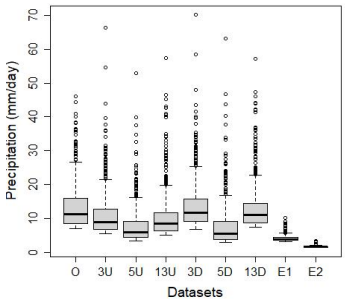

MS 34

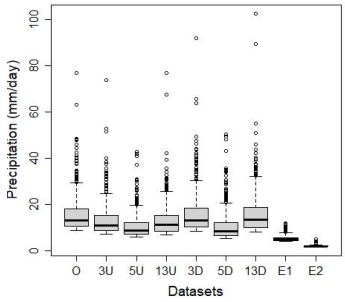

MS 35

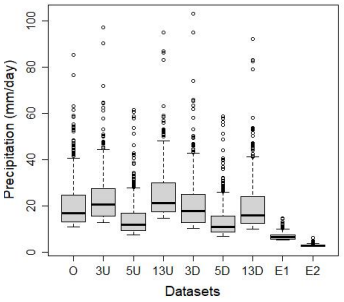

MS 36

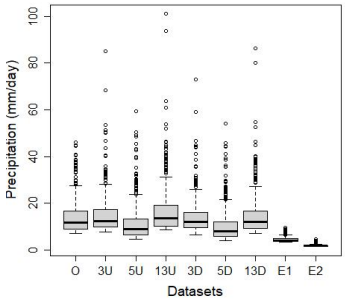

MS 37

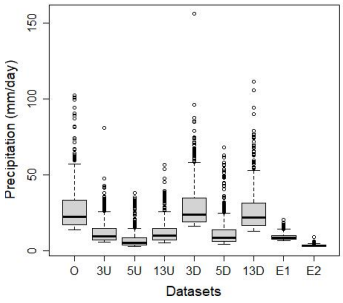

MS 38

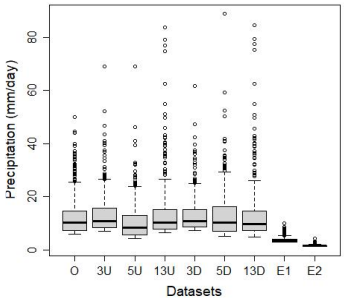

MS 39

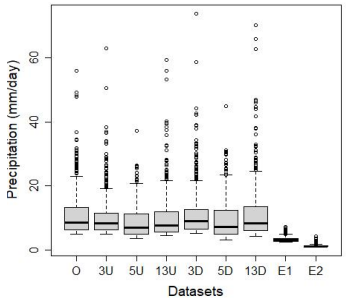

MS 40

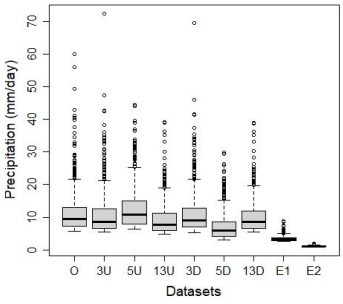

MS 41

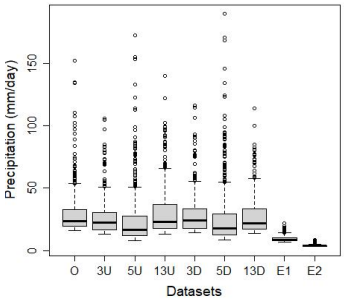

MS 42

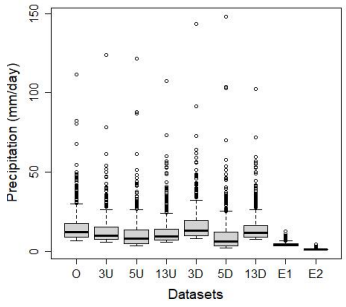

MS 43

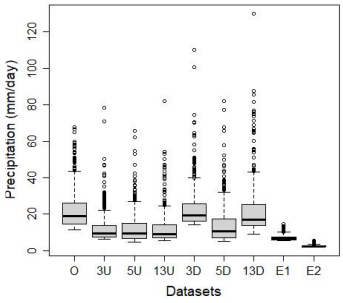

MS 44

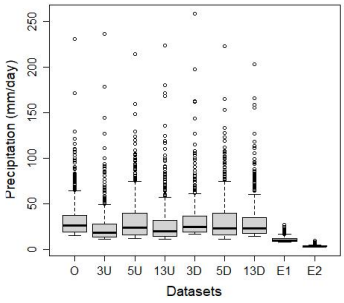

MS 45

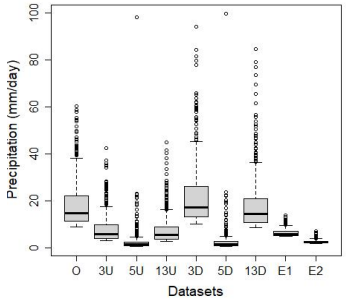

MS 46

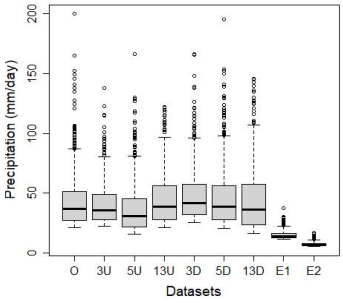

MS 47

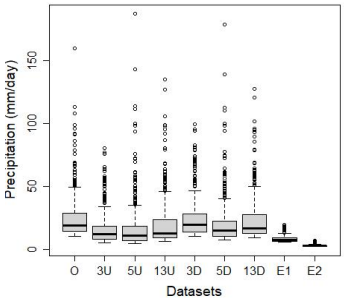

MS 48

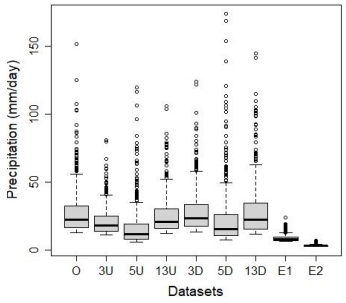

MS 49

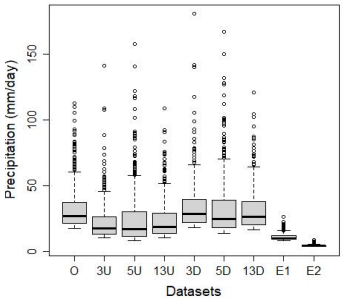

MS 50

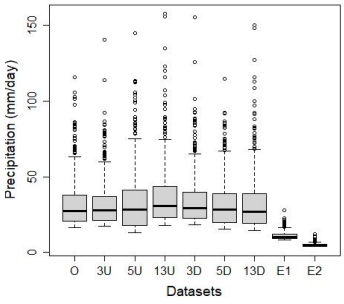

MS 51

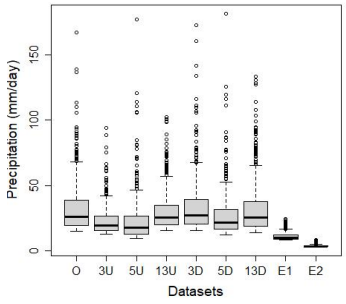

MS 52

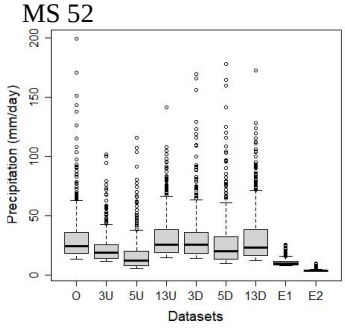
Precipitation (mm/day)
0
50
100
150
200
O
3U
5U
13U
3D
5D
13D
E1
E2
Datasets

MS 53

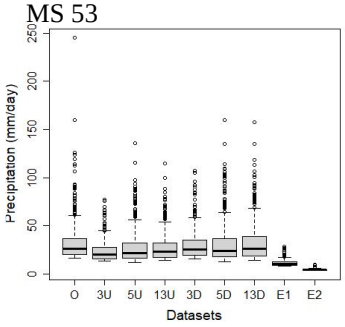
Precipitation (mm/day)
0
50
100
150
200
250
O
3U
5U
13U
3D
5D
13D
E1
E2
Datasets

E.2 Box Plots of Extreme Parts (2041-2070)

MS 10

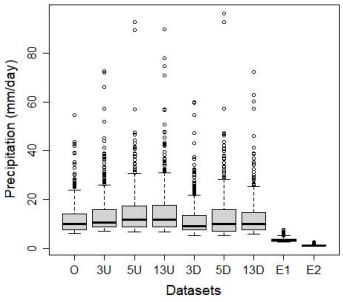

MS 11

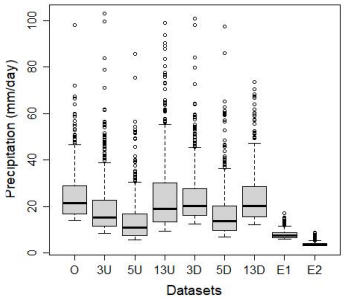

MS 12

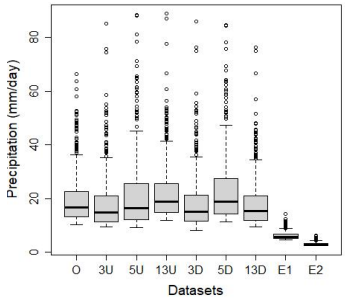

MS 13

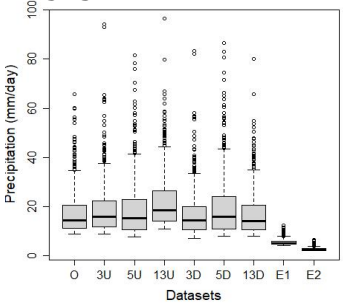

MS 14

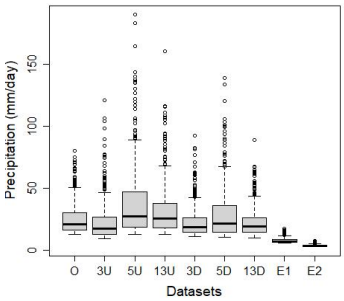

MS 15

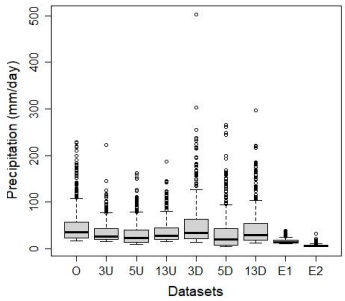

MS 16

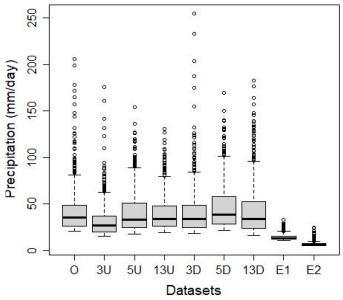

MS 17

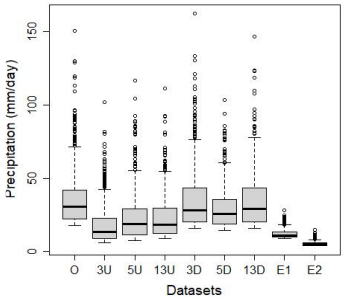

MS 18

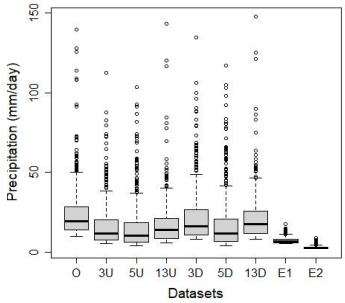

MS 19

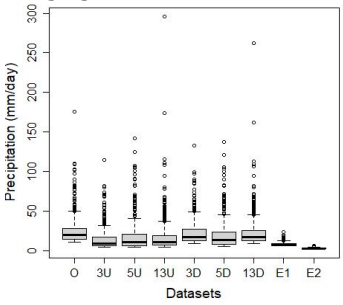

MS 20

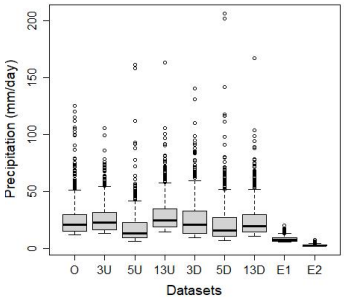

MS 21

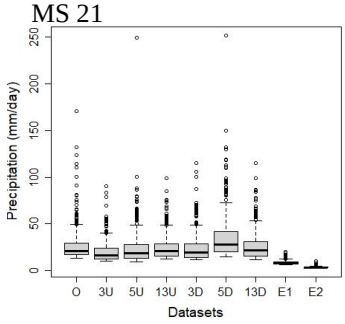

MS 22

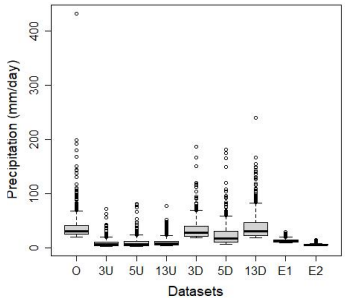

MS 23

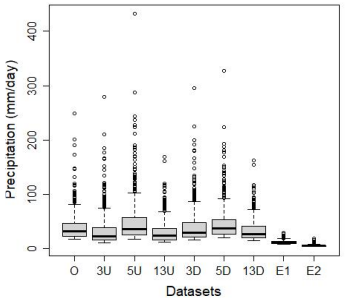

MS 24

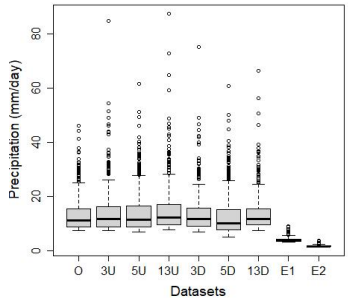

MS 25

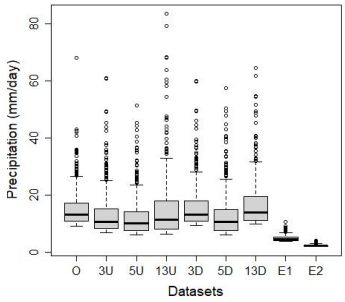

MS 26

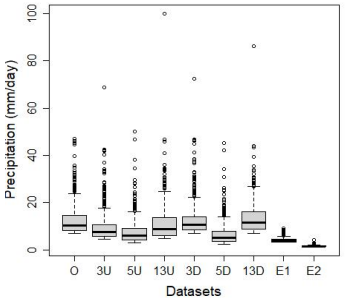

MS 27

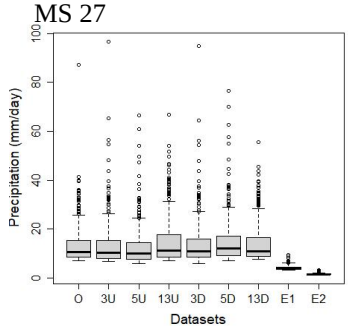

MS 28

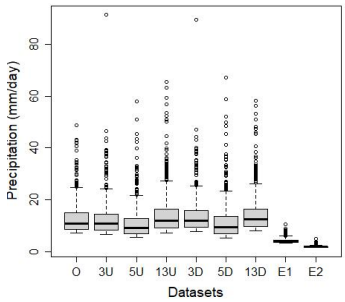

MS 29

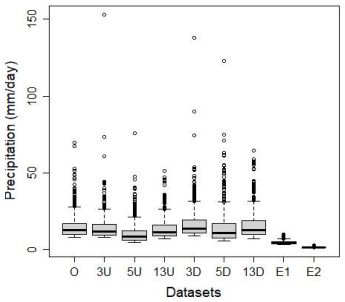

MS 30

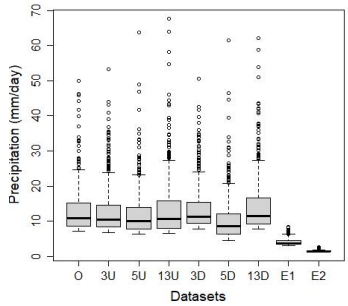

MS 31

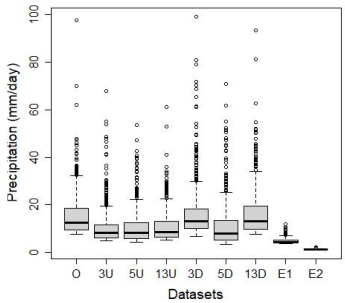

MS 32

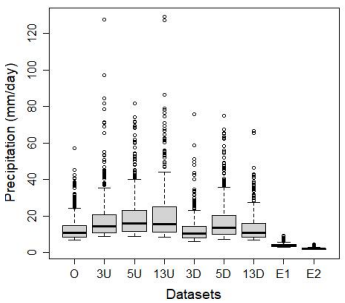

MS 33

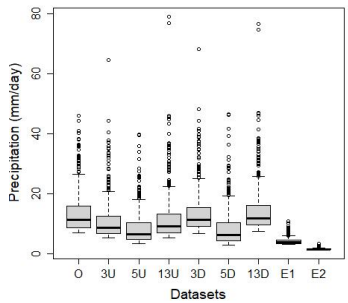

MS 34

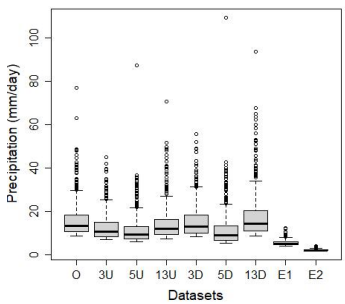

MS 35

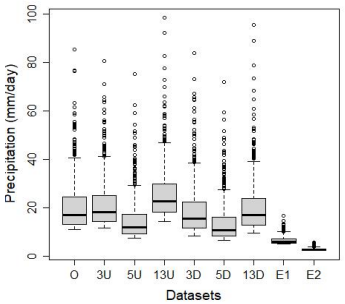

MS 36

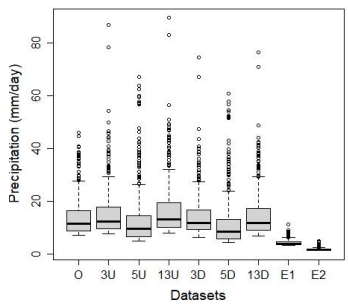

MS 37

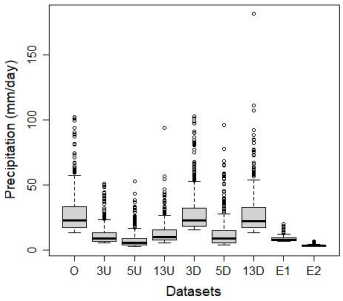

MS 38

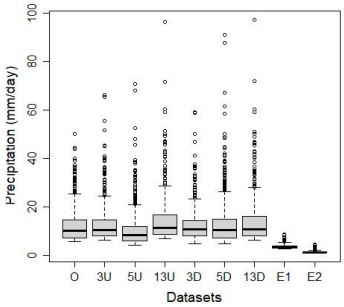

MS 39

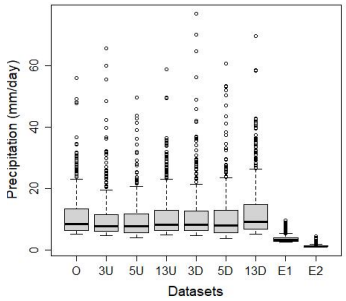

MS 40

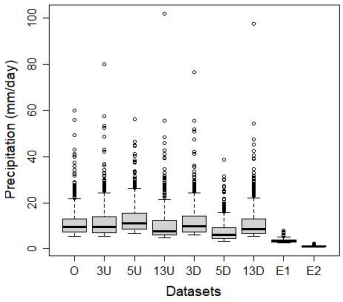

MS 41

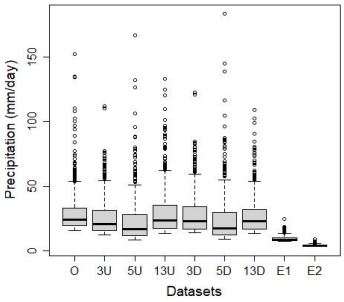

MS 42

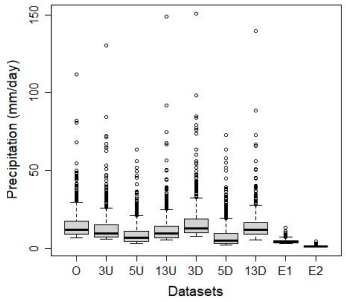

MS 43

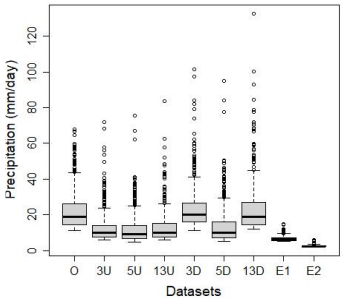

MS 44

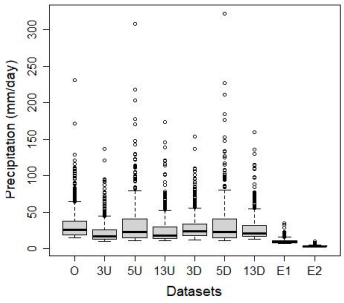

MS 45

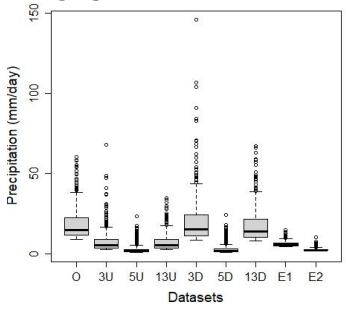

MS 46

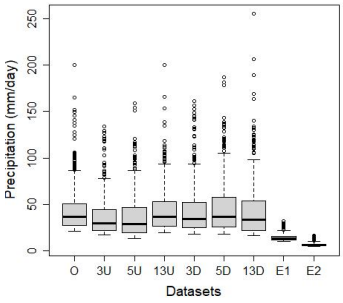

MS 47

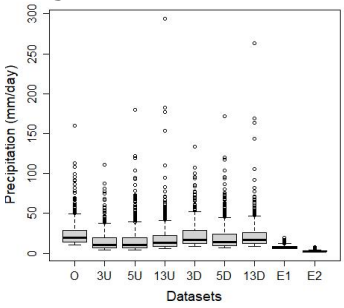

MS 48

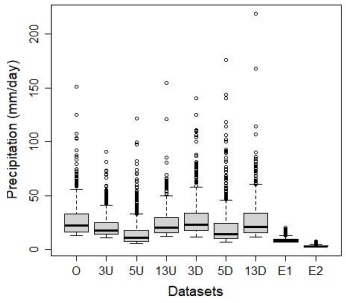

MS 49

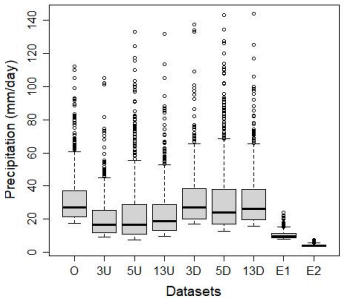

MS 50

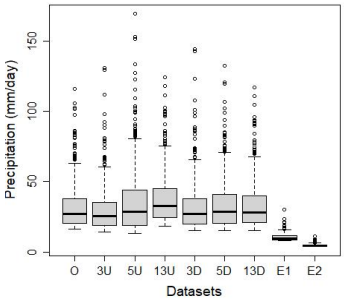

MS 51

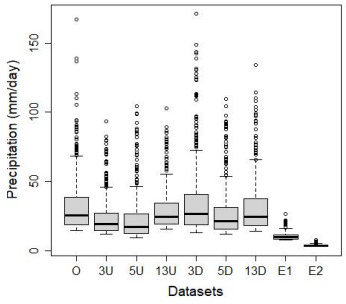

MS 52

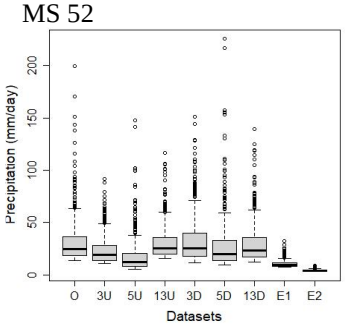
Precipitation (mm/day)
0
50
100
150
200
O
3U
5U
13U
3D
5D
13D
E1
E2
Datasets

MS 53

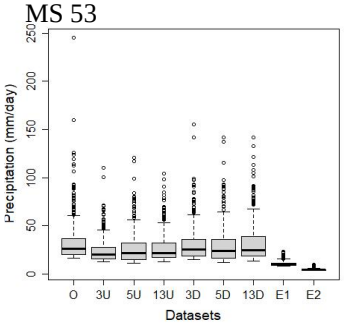
Precipitation (mm/day)
0
50
100
150
200
250
O
3U
5U
13U
3D
5D
13D
E1
E2
Datasets

E.3 Box Plots of Extreme Parts (2071-2100)

MS 10

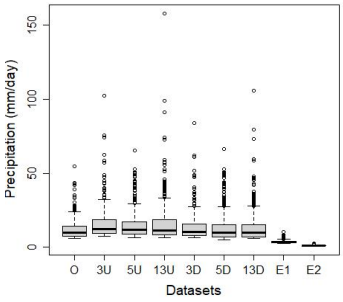

MS 11

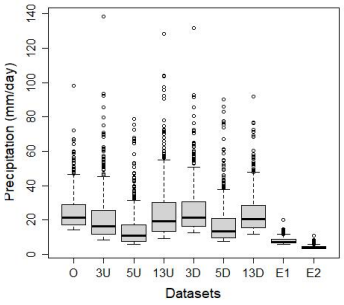

MS 12

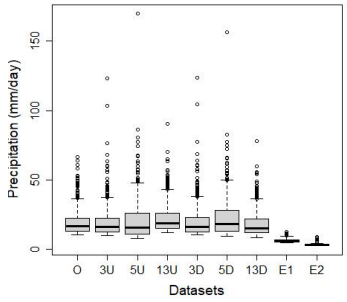

MS 13

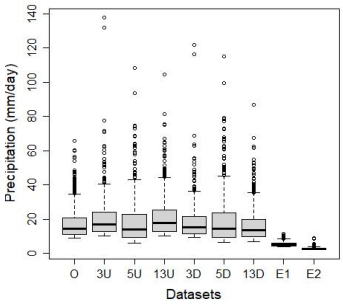

MS 14

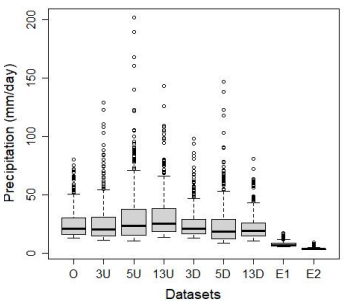

MS 15

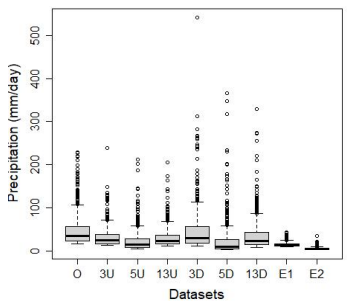

MS 16

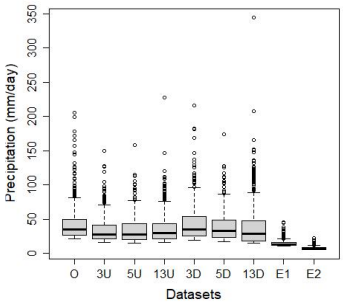

MS 17

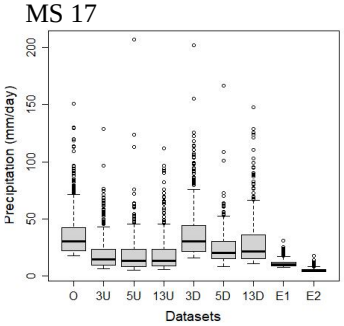

MS 18

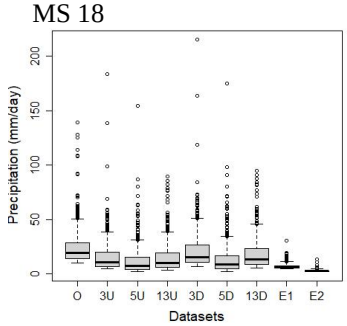

MS 19

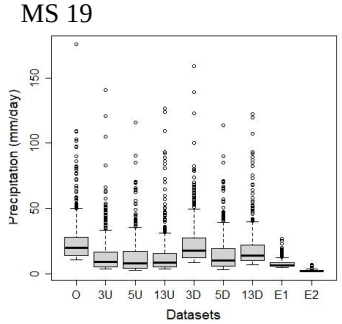

MS 20

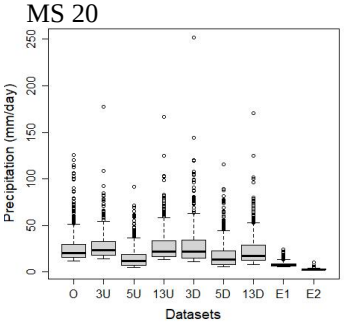

MS 21

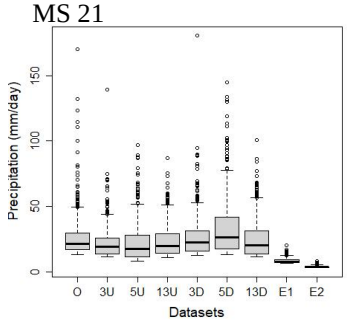

MS 22

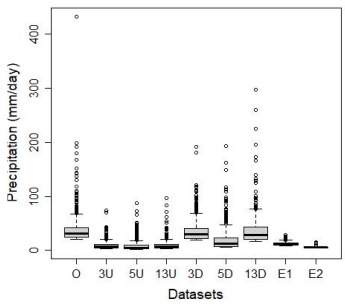

MS 23

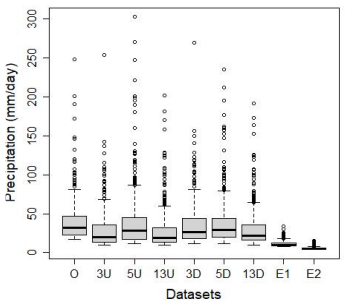

MS 24

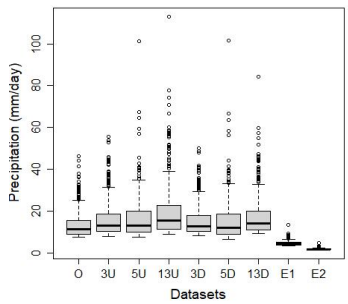

MS 25

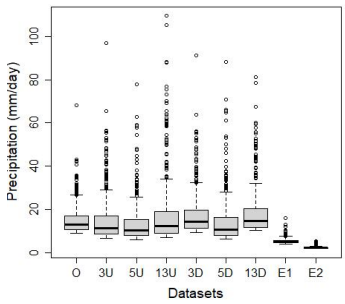

MS 26

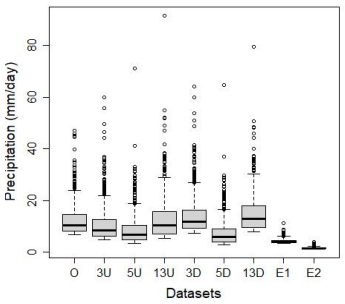

MS 27

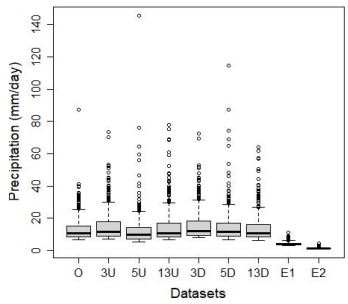

MS 28

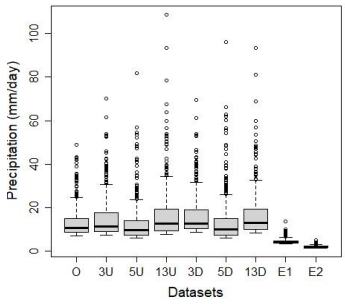

MS 29

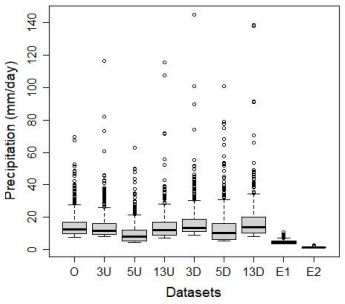

MS 30

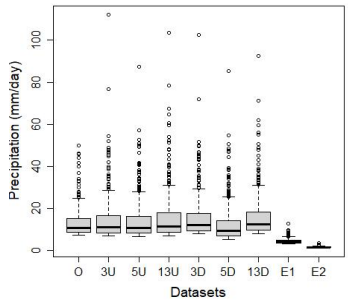

MS 31

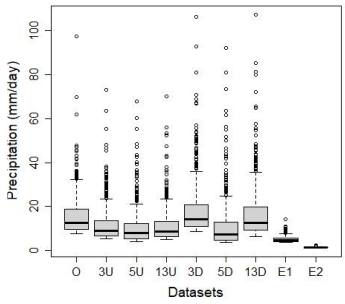

MS 32

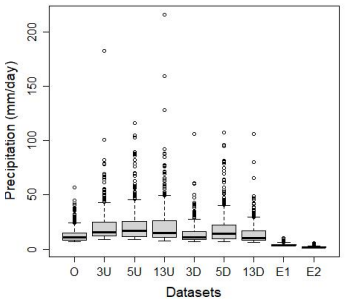

MS 33

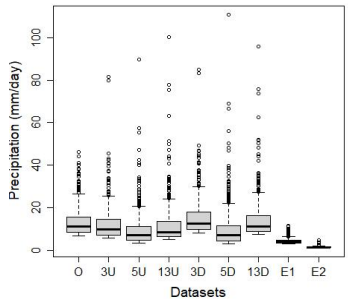

MS 34

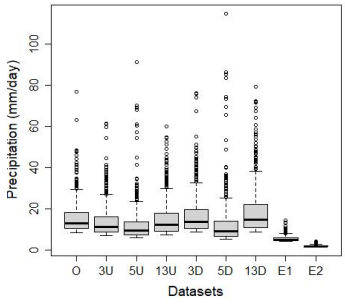

MS 35

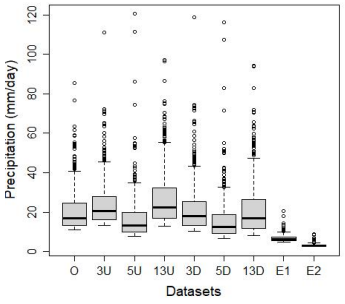

MS 36

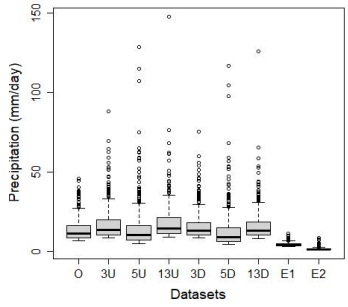

MS 37

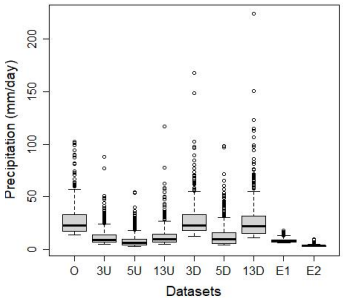

MS 38

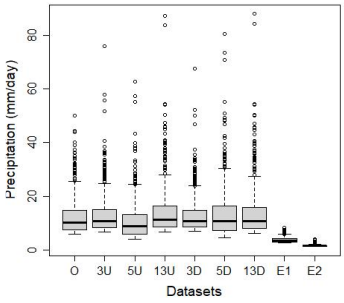

MS 39

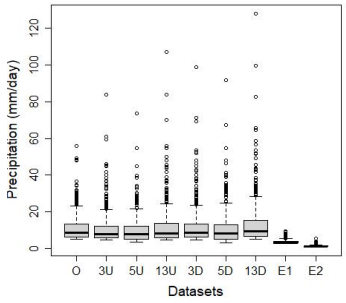

MS 40

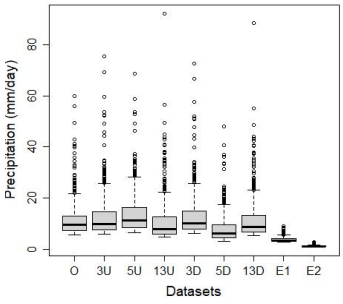

MS 41

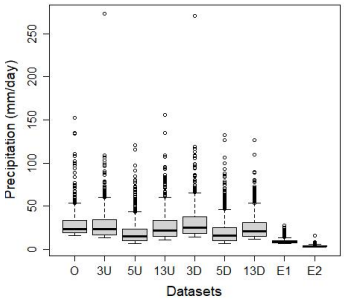

MS 42

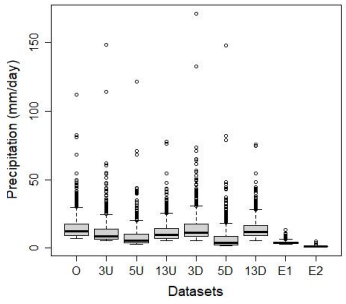

MS 43

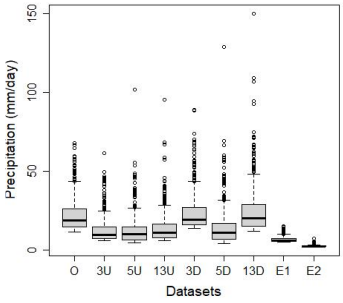

MS 44

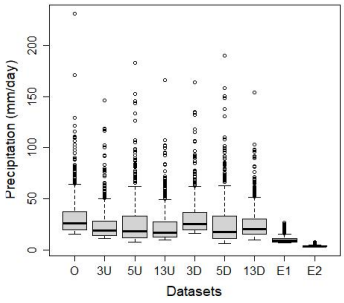

MS 45

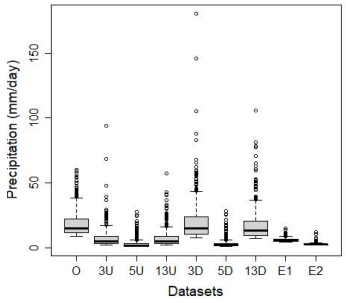

MS 46

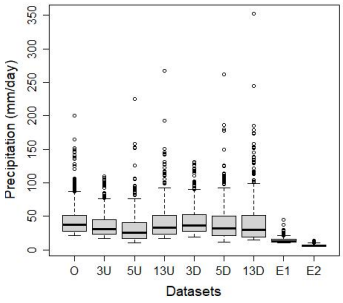

MS 47

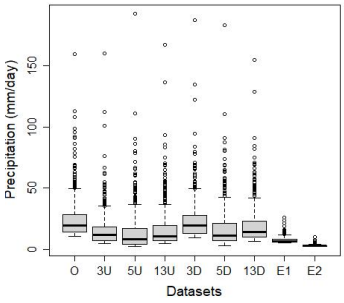

MS 48

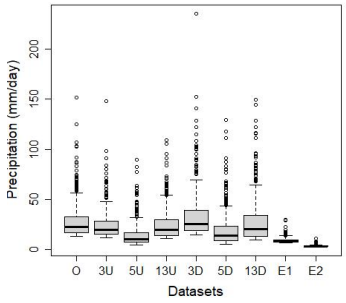

MS 49

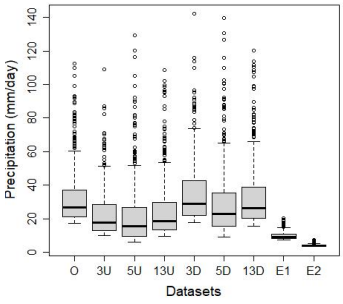

MS 50

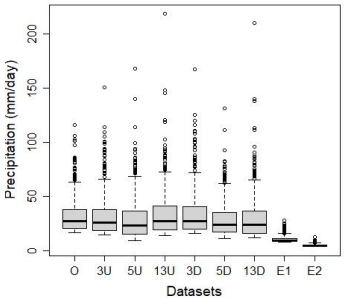

MS 51

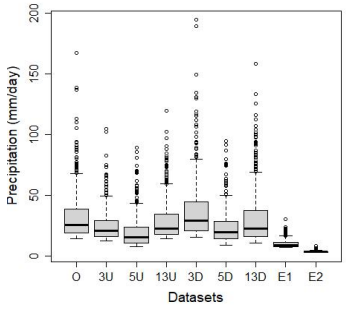

MS 52

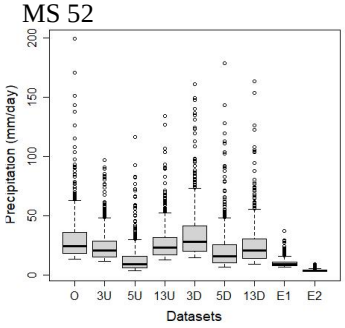
Precipitation (mm/day)
0
50
100
150
200
O
3U
5U
13U
3D
5D
13D
E1
E2
Datasets

MS 53

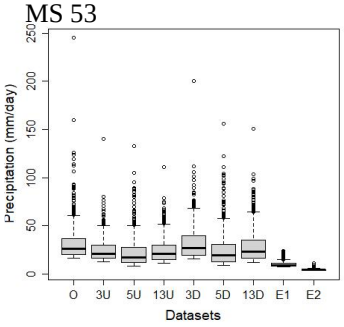
Precipitation (mm/day)
0
50
100
150
200
250
O
3U
5U
13U
3D
5D
13D
E1
E2
Datasets